Eduardo Conde Silva de Sousa

Computational Models for Information Storage in Spiking Neurons

Departamento de Matemática
Faculdade de Ciências da Universidade do Porto
2014

Eduardo Conde Silva de Sousa

Computational Models for Information Storage in Spiking Neurons

Tese submetida à Faculdade de Ciências da Universidade do Porto para obtenção do grau de Doutor em Matemática

Junho de 2014

U.PORTO

FACULDADE DE CIÊNCIAS
UNIVERSIDADE DO PORTO

"Todo hombre puede ser, si se lo propone, escultor de su propio cerebro."

"Every man can, if he so desires, become the sculptor of his own brain."

Santiago Ramón y Cajal

Agradecimentos

Ao longo destes quatro anos, assim como em toda a minha vida, pude contar com a presença contínua de uma série de pessoas que sempre me apoiaram e que sei que sempre me apoiarão naquilo que fizer falta. A todos gostaria de agradecer por me ajudarem a ser aquilo que hoje sou hoje...

Ao Paulo Aguiar, meu orientador e amigo, uma palavra de gratidão pelo tempo dispensado a guiar-me, a ouvir-me, a incentivar-me e ajudar-me em tudo o que precisei!

À Faculdade de Ciências e ao Centro de Matemática da Universidade do Porto, o meu obrigado pelas condições que me foram proporcionadas, sem as quais este trabalho não teria sido possível.

À Fundação para a Ciência e Tecnologia, agradeço o financiamento através da bolsa de doutoramento SFRH / BD / 65633 / 2009, sem a qual não teria tido condições de concluir este projecto.

Aos meus amigos agradeço pelos momentos divertidos, pelas experiências partilhadas ao longo de muitos anos de crescimento juntos!

À minha família, agradeço o apoio e o amor...

Aos meus padrinhos, que sempre me viram como um filho, obrigado...

À minha família de Bragança o meu sincero obrigado pela forma como me receberam de braços abertos, pelo exemplo que são para mim e para os meus filhos, pelos princípios e valores com que se norteiam e que passaram para a geração seguinte. Uma palavra especial para quem me deixa muitas saudades, Vó Lina, obrigado por tudo...

Aos meus pais agradeço por tudo, por aquilo que sou, pelo esforço que sempre me dedicaram, pela confiança ilimitada que sempre depositaram em mim e nas minhas escolhas, pelo carinho, pelo amor que sempre me proporcionaram...

Ao João agradeço por ser o menino lindo e maravilhoso que é. Obrigado meu amor! O papá e a mamã estarão sempre disponíveis para ti, de braços abertos, prontos para tudo!

Ao Xavier que ainda agora aqui chegou e sem saber já enche de alegria as nossas vidas, obrigado. Conta com os pais para tudo o que precisares... estaremos cá sempre de braços abertos, prontos para tudo!

À Nádia, minha mulher, minha melhor amiga, minha mais que tudo, agradeço por tudo, porque muito daquilo que sou hoje o devo a ela, à sua força, aos seus valores, mas principalmente ao seu amor incondicional. Obrigado pela equipa maravilhosa que formamos, pelos nossos filhos lindos, por arranjar forças onde elas não existem quando eu me vou abaixo... Obrigado por tudo!

À Nádia, ao João e ao Xavier...

Resumo

Working Memory refere-se a um sistema de memória de capacidade limitada em que a informação é armazenada de forma rápida e é guardada durante o tempo necessário à sua utilização por outros sistemas. Muitos modelos de *Working Memory* baseiam-se na existência de uma estrutura neuronal que depende de forma directa de aprendizagens prévias. Existem ainda outros modelos em que a plasticidade sináptica de curto prazo é utilizada no armazenamento de informação. Contudo, existem outros mecanismos celulares com propriedades adequadas para o armazenamento de informação. Nesta tese, utilizamos modelos matemáticos/computacionais para estudar um desses mecanismos, a modulação da excitabilidade intrínseca do neurónio.

Começamos o nosso estudo pela avaliação sobre a forma como as correntes iónicas presentes num neurónio podem ser utilizadas para modular a sua excitabilidade e assim armazenar informação. Propomos um modelo neuronal simples, contendo um número reduzido de correntes iónicas que interagem de forma a aumentar ou diminuir a excitabilidade do neurónio em função da sua actividade recente. O neurónio assim modelado pode ser condicionado a responder de modo diferente a um mesmo estímulo e está na base de dois modelos integrados no âmbito das memórias de trabalho (*Working Memory*). As redes neuronais propostas são capazes de armazenar informação de forma rápida (em poucas centenas de milissegundos) e de a suster de forma robusta durante vários segundos (durante o chamado *delay period*).

Uma das redes propostas, mais simples, é formada por uma população de neurónios excitatórios ligados de forma aleatória entre si e duas populações de neurónios inibitórios. Esta rede é capaz de armazenar um padrão de actividade e consegue detectar a repetição do mesmo padrão após o *delay period*. Além disso, consegue decidir se um novo padrão deve apenas ser classificado como diferente do primeiro ou se deve substituí-lo.

Utilizando uma arquitectura de rede diferente, mostramos que é possível armazenar, de forma rápida e duradoura, uma sequência de até 6 padrões de actividade, sem recorrer

a plasticidade sináptica. Verificamos ainda que é possível apagar uma sequência previamente armazenada e gravar uma nova, eventualmente não disjunta da primeira, em cerca de um segundo.

Para além do trabalho anteriormente descrito, foi ainda estabelecida uma parceria com um grupo que trabalha em electrofisiologia (Neural Networks, IBMC – Instituto de Biologia Molecular e Celular, Porto). O objectivo desta colaboração foi o de combinar resultados experimentais com modelos matemáticos de forma a estudar a integração e processamento de sinais sinápticos. No contexto desta colaboração, foram desenvolvidas ferramentas computacionais que permitiram: (i) corrigir computacionalmente anomalias na árvore dendrítica resultantes de problemas na preparação histológica; (ii) inserir e activar sinapses artificiais na árvore dendrítica nos locais especificados pelas espinhas; e (iii) quantificar a distância electrotónica entre cada espinha/sinapse e o soma (região onde o potencial de acção é iniciado), como forma de inferir eficácia sináptica.

Abstract

Working Memory refers to a memory system with limited capacity but where information is quickly stored and sustained while it is used by other brain systems. Many models in working memory are based on the existence of a neural structure directly dependent on previously learned information. There are other models in which short-term synaptic plasticity is used for the storage of information. However, other cellular mechanisms have suitable properties for information storage. In this thesis, we use mathematical/computational models to study one of these mechanisms, the modulation of intrinsic neuronal excitability.

We started our study by assessing how some of the ionic currents can be used to modulate the neuronal excitability and thus to store information. We propose a simple neuronal model with a limited number of ionic currents which interact to increase or decrease the neuronal excitability according to its recent activity. The proposed neuron can give different responses to the same stimulus depending on the level of excitability induced by its ionic currents, and is the basis of two network models on working memory. The proposed neural networks are capable of quickly storing information (within a few hundreds of milliseconds) and of robustly sustain it for several seconds (during the so-called *delay period*).

One of the proposed networks is formed by a population of excitatory neurons randomly connected to each other and two populations of inhibitory neurons. This network is capable of storing a pattern of activity and can detect the repetition of the same pattern after the delay period. Additionally, the network is able to decide whether a new pattern should only be classified as different from the first, or should replace it.

Using a different network architecture, we show that it is possible to quickly store a sequence of up to 6 patterns of activity without using synaptic plasticity. We also show that it is possible to delete a previously stored sequence and store a new one, possibly not disjoint from the first, in about one second.

In addition to the work described above it was also established a collaboration with a group that works in electrophysiology (Neural Networks, IBMC – Institute for Molecular and Cell Biology, Porto). The goal of this collaboration was to combine experimental results with mathematical models in order to study the integration and processing of synaptic signals. As part of this collaboration, computational tools were developed that allowed: (i) to computationally fix dendritic bumps resulting from the histological preparation of some neurons; (ii) to insert and activate artificial synapses in the dendritic tree in the locations specified by the spines; and (iii) to quantify the electrotonic distance between each spine/synapse and the soma (region where the action potential is initiated) as a way of inferring synaptic efficacy.

List of Symbols, Abbreviations and Acronyms

ACh	Acetylcholine
ADP	Afterdepolarization
AHP	Afterhiperpolarization
AMPA	α-amino-3-hydroxy-5-methyl-4-isoxazole propionic acid
AP	Action potential
CaL current	High threshold calcium current
CAN current	Nonspecific cationic current
Ca^{2+}	Calcium
CA1	*Cornu Ammonis* area 1
Cl^{-}	Chloride
GABA	γ-aminobutyric acid
DMS	Delayed match to sample
EC	Entorhinal cortex
GHK	Goldman-Hodgkin-Katz
HH	Hodgkin-Huxley
I_{CaL}	High threshold calcium current
I_{CAN}	Nonspecific cationic current
I_h	Hyperpolarization-activated current
I_K	Potassium current
I_{Kdr}	Delayed rectifier potassium current
I_L	Leakage current
I_{Na}	Transient sodium current
I_{syn}	Synaptic current
$I\&F$	Integrate and Fire

ISI	Interspike interval
K^+	Potassium
LTD	Long-term depression
LTP	Long-term potentiation
Mg^{2+}	Magnesium
MINE	Modulation of intrinsic neuronal excitability
Na^+	Sodium
NMDA	N-methyl-D-aspartate
PFC	Prefrontal cortex
STD	Short-term depression
STDP	Spike timing dependent plasticity
STF	Short-term facilitation
STP	Short-term plasticity
WM	Working memory
3D	Three-dimensional
5-HT	5-hydroxytryptamine (Serotonin)

Contents

1 Introduction

How does the brain works? Such a wide problem can be addressed at different levels, from the gene expression to ion channels, to neurons, to local networks or to the entire human connectome. Depending on the specific problem each neuroscientist intents to solve, there are countless questions to answer before we finally could understand how does the brain processes the huge amount of information needed at every instant of our lives or even how does the brain stores information and retrieve it when necessary or discard it when no longer needed. Does the answer to the previous questions lies in neural connectivity (network), in the neurons themselves or in a combination of both?

1.1. Thesis Goals

In this thesis we focus our attention in one particular mechanism – the modulation of intrinsic neuronal excitability – to give insights into one specific topic inside the whole problem of information storage and recall. How does the brain stores novel information after brief exposures to stimuli? How does the brain holds this information enough time to use it and how it is discarded after that? The problem we face here is a component of the neuroscience field called *working memory*.

Working memory is a system where new information is temporarily stored (and eventually combined with previously known information) during the planning and execution of forthcoming actions (Dudai, 2002). Among its main characteristics one is of major importance, the working memory time scales. Information has to be stored in a few hundreds of milliseconds to account for the presentation of transient stimuli, and kept in the working memory system for at least a few seconds while the task is fulfilled.

Several studies focus on working memory systems (Durstewitz et al., 2000; Barak and Tsodyks, 2014). The novelty presented on this thesis lies in the used methodologies to address the problem and in the mechanisms to store information. We propose conductance-based models where the interplay between different ion currents give to each

neuron the ability to "decide", in function of its past activity, whether the network signals are sufficient to elicit its own activity. This is a mechanism called *modulation of intrinsic neuronal excitability* and is used in this thesis as a possible mechanism to store novel information without synaptic plasticity.

To fulfill the proposed goals, we split the problem into two different subtopics:

(i) How can we store one novel item in a working memory system?
(ii) How can we extend the previous answer to account for the storage of a sequence of items?

Mathematical and computational models were used in order to enlighten the key points of our work. The process of modeling requires the identification of the key features of the system. Deciding which biophysical constraints are essential and which could be relaxed in order to obtain a biologically realistic model that fits the study's goals is a challenge. In top of this, it is necessary to decide the simulation software that suits the mathematical model and the chosen network size required to answer the proposed questions.

In addition to the theoretical study on working memory there was also the goal of applying mathematical/computational methods to ongoing experimental work addressing current problems in neuroscience. With this in mind a collaboration was established with an experimental group working in electrophysiology (Neural Networks, IBMC – Institute for Molecular and Cell Biology, Porto). The collaboration was focused in the functional characterization of neurons from the superficial dorsal horn of the spinal cord. Combining experimental and mathematical/computational methods, the goal was to better understand how a particular class of neurons, 'tonic neurons', integrates and processes information from other neurons. In the scope of this collaboration the following novel contributions were given:

(i) A procedure that places each spine in the appropriate dendrite portion in the fully reconstructed neuronal structure was created;
(ii) A tool was developed to determine the electrotonic distance from each spine to the soma; and
(iii) An algorithm was written to remove tissue shrinkage artifacts.

The above mentioned computational tools: (i) enabled the interconnection between different software packages used in collecting the data and in the simulation of the computational models; and also enabled the establishment of real locations for the synaptic terminals that will be attached to each neuron; (ii) were used to better understand the signal propagation along the neuronal fiber, and to obtain a good predictor of synaptic efficacy; and (iii) allowed the removal of reconstruction artifacts that potentially changes the morphological shape and size of the neuron or the signal propagation along the neurite.

1.2. Overview of the Thesis

The present thesis is divided into nine chapters. After the Introduction (Chapter 1), an overview on mathematical models for neurons (Chapter 2) and synapses (Chapter 3) will be presented, with a special focus on the Hodgkin-Huxley model. Then, a review over learning mechanisms on neurons and/or neuronal populations will be presented Chapter 4 and in Chapter 5 an overview on working memory and on some strategies that have been used in working memory models will be presented.

In Chapter 6, the construction of the single cell model proposed in Articles I and II (presented in Sections 7.1 and 7.2) as well as the choice of the software package used in the model simulations are discussed.

The main results of the thesis are then presented in Chapter 7.

We will conclude with a discussion (in Chapter 8) and with ideas for future work (in Chapter 9).

2 Mathematical Models for Neurons

Mathematical models are an essential tool for the study of several aspects in Biology, Physics, Chemistry among other fields of science. In Neuroscience, computational models are widespread and have been used to study mechanisms ranging from the molecular level, to the network level. In this chapter we focus on mathematical models for single neurons.

Before building a model for some study, a neuroscientist must start by addressing the following question: where is the information encoded? Depending on the study to perform, on the neurons or neuronal network which are the focus of that study, or on the level of detail and accuracy required, two different answers to the previous question are possible. The first possibility is to assume that "the information is encoded in the average firing activity of neurons". In this scenario, a Firing Rate Model should be selected. If on the contrary the information at hand suggests that "every spike counts", then a Spiking Model is required.

Firing rate models are based on the assumption that the most important properties of a neural network could be described by the average firing frequency (number of spikes over a time window). So, it is possible, according to the firing rate paradigm, to discard the precise time of spikes.

On the other hand, *spiking models* can account for the precise timing of action potentials. All the variables of a spiking model represent instantaneous quantities, and so, these models can explain time scales ranging from milliseconds (the time scale of a channel opening or of the duration of an action potential) to seconds or more (time scales resulting from the network collective behavior) while only the larger time scales are considered in firing rate models.

The basic assumptions on firing rate models make them simpler than spiking models enabling the modeler who chooses a firing rate model to perform analytical calculations and to quickly simulate large networks. Furthermore, a spiking model usually have more free parameters, and so, a spiking model is usually harder to fit to experimental data.

Nevertheless, unlike firing rate models, a spiking model can account for some network collective properties such as synchronism or the correlations between spike times of several neurons.

Another argument in favor of spiking models is that in several known neuronal systems, each individual spike encodes information about stimuli (see, for example, studies on the fly visual system (Rieke et al., 1999), the auditory nerve (Anderson et al., 1971) or the locust antennal lobe (Laurent, 1996)).

In addition to the assumptions regarding information encoding, other questions need to be addressed in the process of building an appropriate mathematical model for neuronal dynamics.

(i) Which is the required degree of biophysical realism?
(ii) Is it intended to model action potentials which are close to those of real neurons or is it enough to model the sub-threshold dynamics?
(iii) Is it important to have model parameters with biological correspondence or just to fit the model's membrane potential trace to real data?
(iv) What is the size of the neuronal network required to answer the proposed questions and which are the available resources (both hardware, and software)?

Depending on the answer to these questions a neuroscientist can choose from a plethora of models. In the following sections the most relevant/influential will be highlighted.

2.1. Integrate and Fire

Integrate and fire models constitute a family of neural models which was first introduced in 1907 by Lapicque (Lapicque, 1907; Brunel and van Rossum, 2007).

According to the original integrate and fire model a neuron temporal dynamic can be described by a capacitive current with a threshold parameter (V_{th}) and reset mechanism. The time evolution of the membrane potential follows the equation:

$$C_m \frac{dV}{dt} = I(t), \qquad \text{if} \qquad V \geq V_{th} : V \leftarrow V_{res} \tag{2.1}$$

where $I(t)$ is the total membrane current density, V is the membrane potential, C_m is the membrane capacitance per unit of area, and t is time. Whenever the membrane potential reaches the threshold V_{th} a spike is fired (it is assumed but not explicitly modeled) and V is reset to V_{res}.

The original integrate and fire model has evolved to one of the most used neuronal models, the *leaky integrate and fire*.

In the original integrate and fire model, whenever a current increases the membrane potential to a sub-threshold level, the neuron retains that information forever until it fires again. In the leaky integrate and fire model another term is added to the main equation to solve this problem:

$$C_m \frac{dV}{dt} = I(t) - \frac{V(t) - V_{rest}}{R_m}, \qquad \text{if} \qquad V \geq V_{th} : V \leftarrow V_{res} \tag{2.2}$$

where $I_m = (V(t) - V_{rest})/R_m$ is a resistive current following the Ohm's law, and V_{rest} is the resting potential.

Multiplying all the terms in equation (2.2) by R_m and denoting by $\tau_m = C_m \times R_m$, equation (2.2) can be rewritten as:

$$\tau_m \frac{dV}{dt} = R_m I(t) - V(t) + V_{rest}, \qquad \text{if} \qquad V \geq V_{th} : V \leftarrow V_{res} \tag{2.3}$$

Given its simplicity – it has only one state variable – the leaky integrate and fire model is widely used. With this model it is possible to perform analytical calculations and run fast simulations although it is not a good choice if some biophysical detail is required (Izhikevich, 2004). Unlike real neurons in the cortex, the leaky integrate and fire model cannot account for features like bursting, resonance, or spike time adaptation.

Over the years, other variants of the integrate and fire model have been developed to address some of these neuronal features. Among others, it is possible to highlight the *Integrate and Fire or Burst* model (Smith et al., 2000), the *Adaptive Exponential Integrate and Fire* model (Brette and Gerstner, 2005), the *Resonate and Fire* model (Izhikevich, 2001), or the *Quadratic Integrate and Fire* model (Latham et al., 2000).

Integrate and Fire neurons are suited for models where the use of large networks is necessary. If performing analytical calculations is more important than biophysical realism the choice should be the leaky integrate and fire model. On the other hand, if some features of the real neurons are a requirement, one of other integrate and fire models can be used since these models are still computationally efficient and can be tuned with parameters with biophysical meaning.

2.2. Hodgkin-Huxley

Much of the work in the last decades on Computational Neuroscience arises from the extraordinary contribution of Alan Lloyd Hodgkin and Andrew Huxley in a series of articles (Hodgkin and Huxley, 1952b,c,d; Hodgkin et al., 1952) culminating in the publication of one of the most important articles in the Neuroscience field (Hodgkin and Huxley, 1952a).

2.2.1. Back to 1952

Hodgkin and Huxley knew that electrical current flowing through a patch of the neuron's membrane is driven by ions. The authors studied the squid giant axon and hypothesize that this current is the result of the combined interaction of two specific ionic currents, sodium (Na^+), and potassium (K^+); and a generic current named leak current which serves as an approximation of the combined effect of other existing currents, mostly chloride (Cl^-).

Changes in the membrane potential arises from the flow of some of these ions through the neuron's membrane. Ions can cross the neuron's membrane through large transmembrane protein molecules called ion channels. According to the Hodgkin-Huxley model, there are channels selective to sodium ions and channels selective to potassium ions. For an ion being able to cross the corresponding ion channel, it is necessary that the channel is opened. The open and the closed states of each selective ion channel are determined by voltage dependent gating particles (gates). For the Na^+ channels there are two types of gates, those that *activate* the channel and those that *inactivate* the channel, while for K^+ channels there are only activation particles (see Figure 2.1).

Denoting by m the probability of an activation gate being open and by h the probability of an inactivation gate being open, and assuming that every two gates are independent, the probability an ion channel being open is:

$$p = m^a \times h^b \tag{2.4}$$

where a and b are, respectively, the number of activation and inactivation gates.

Given a gating variable, it is possible to describe through a kinetic scheme the transition between the open and the closed states. Denoting by α the transition rate constant from the closed state to the open state and β the reverse transition rate constant (in the

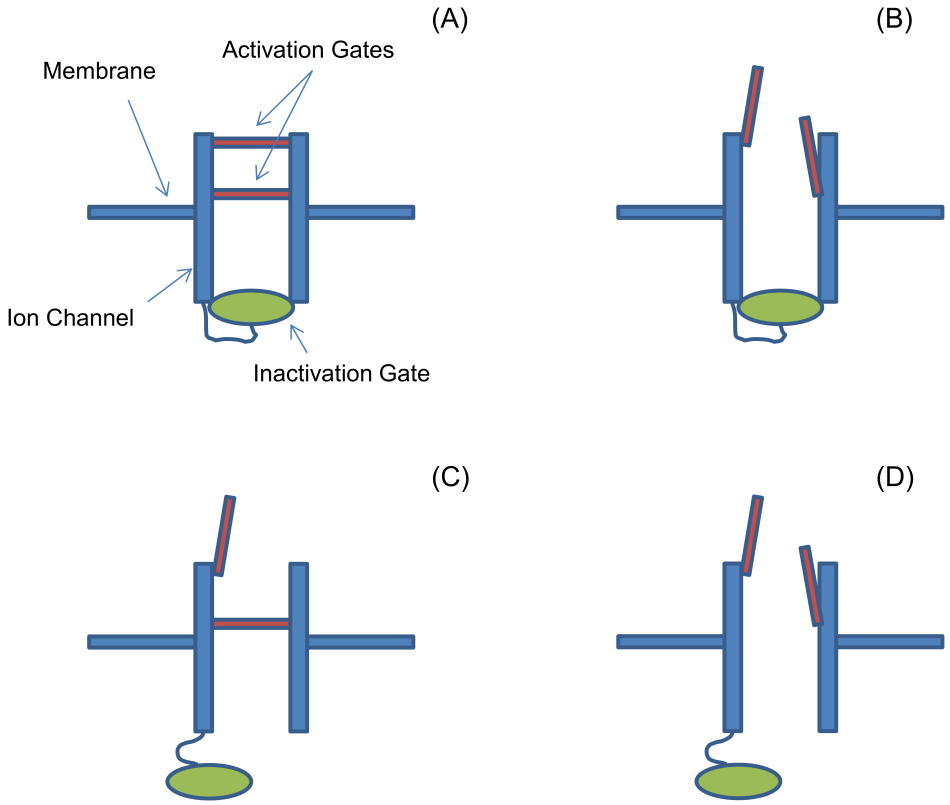

FIGURE 2.1. Hypothetic scheme of a channel with three gates, two activation gates and one inactivation gate. (A) to (C) Ions cannot cross the channel because in (A) the channel is deactivated and inactivated, in (B) the channel is inactivated, and in (C) the channel is deactivated. (D) Ions can cross the channel – the channel is open.

Hodgkin-Huxley model both transition rates are voltage dependent), the probability of finding a transition from the closed state to the open state, over a short period of time, is the product of the opening rate constant by the probability of finding a closed gate. On the other hand, the probability of finding a transition from the open state to the closed state, over a short period of time, is the product of the closing rate constant by the probability of finding an opened gate. Thus, denoting by m the probability of a gate being open and by $\alpha(V)$ and $\beta(V)$ the opening and closing transition rates:

$$\frac{dm}{dt} = \alpha_m(V)(1-m) - \beta_m(V)m \tag{2.5}$$

Hodgkin and Huxley proposed that the total membrane current can be divided into capacitive current and ionic current:

$$I = C_m \frac{dV}{dt} + I_{ion} \tag{2.6}$$

where I is the total membrane current density, and I_{ion} is the total ionic current density, all in $\mu A/cm^2$, V is the displacement of the membrane potential from its resting value, in mV, C_m is the membrane capacitance per unit of area, in $\mu F/cm^2$, and t is time, in ms.

Considering that, in their model, $I_{ion} = I_{Na} + I_K + I_L$, and denoting by I_{app} the applied current, the time evolution of the membrane potential is described by the equation:

$$C_m \frac{dV}{dt} = I_{app} - I_{Na} - I_K - I_L \tag{2.7}$$

To fit experimental data, Hodgkin and Huxley concluded that the sodium channels have three activation gates and one inactivation gate while the potassium channels have four activation gates. As so, the full set of Hodgkin and Huxley (HH) equations is:

$$C_m \frac{dV}{dt} = I_{app} - \overbrace{\bar{g}_{Na} m^3 h (V - V_{Na})}^{I_{Na}} - \overbrace{\bar{g}_K n^4 (V - V_K)}^{I_K} - \overbrace{g_L (V - V_L)}^{I_L} \tag{2.8a}$$

$$\frac{dn}{dt} = \alpha_n(V)(1 - n) - \beta_n(V) n \tag{2.8b}$$

$$\frac{dm}{dt} = \alpha_m(V)(1 - m) - \beta_m(V) m \tag{2.8c}$$

$$\frac{dh}{dt} = \alpha_h(V)(1 - h) - \beta_h(V) h \tag{2.8d}$$

where the opening and closing transition rates, in units of $1/ms$, are defined as function of V by:

$$\alpha_n(V) = 0.01 \frac{10 - V}{\exp\left(\frac{10 - V}{10}\right) - 1} \tag{2.9a}$$

$$\beta_n(V) = 1.125 \exp\left(\frac{-V}{80}\right) \tag{2.9b}$$

$$\alpha_m(V) = 0.1 \frac{25 - V}{\exp\left(\frac{25 - V}{10}\right) - 1} \tag{2.9c}$$

$$\beta_m(V) = 4 \exp\left(\frac{-V}{18}\right) \tag{2.9d}$$

$$\alpha_h(V) = 0.07 \exp\left(\frac{-V}{20}\right) \qquad (2.9e) \qquad \beta_h(V) = \frac{1}{\exp\left(\frac{30-V}{10}\right)+1} \qquad (2.9f)$$

The values of the constants are:

$$\begin{aligned} C_m &= 1\ \mu F/cm^2; \\ \bar{g}_{Na} &= 120\ mS/cm^2; \qquad V_{Na} = 120\ mV; \\ \bar{g}_K &= 36\ mS/cm^2; \qquad V_K = -12\ mV; \\ g_L &= 0.3\ mS/cm^2; \qquad V_L = 10.6\ mV. \end{aligned}$$

For a sake of convenience, Hodgkin and Huxley shifted the membrane potential by 65 mV to achieve a resting potential of 0 mV. Although nowadays, most of the computational models following the Hodgkin-Huxley formalism does not incorporate this shift, for historical reasons we followed the original equations during this section.

2.2.2. The Action Potential in the Hodgkin-Huxley Model

Considering, for $x \in \{n, m, h\}$:

$$x_\infty(V) = \frac{\alpha_x(V)}{\alpha_x(V) + \beta_x(V)} \qquad (2.10)$$

and

$$\tau_x(V) = \frac{1}{\alpha_x(V) + \beta_x(V)}, \qquad (2.11)$$

equations (2.8b) to (2.8d) can then be rewritten as:

$$\frac{dx}{dt} = \frac{x_\infty(V) - x}{\tau_x(V)} \qquad (2.12)$$

where x_∞ represents voltage-sensitive steady-state activation (or inactivation) levels which gives the asymptotic value of x when the potential is fixed, and τ_x is the time constant with which x converges to x_∞ (a smaller time constant corresponds to a faster convergence of x to x_∞). As can be seen in Figure 2.2, both m_∞ and n_∞ increase with voltage since they correspond to activation variables, while h_∞, which correspond to Na^+ inactivation

variable, decrease with voltage. When looking at the voltage-dependent time constants, it is possible to notice that τ_m is smaller than τ_h or τ_n.

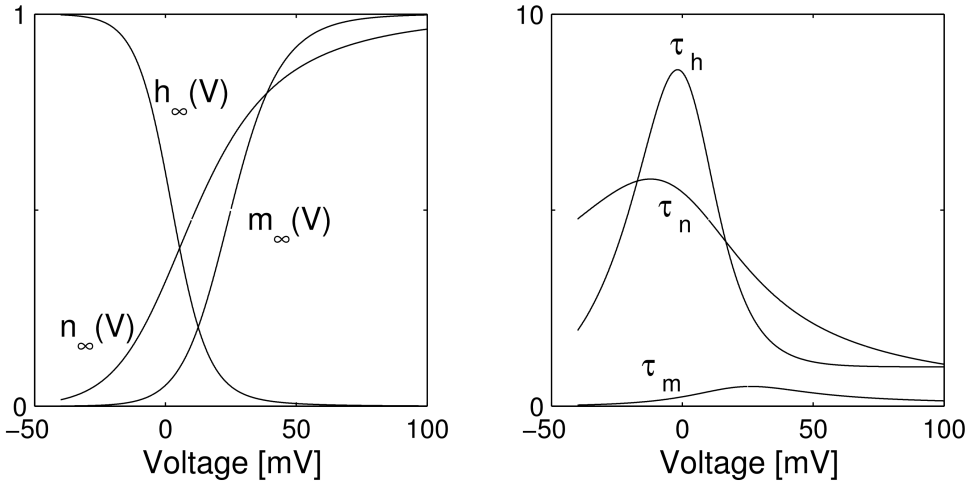

FIGURE 2.2. Voltage-dependent functions of the Hodgkin-Huxley model. On the left panel the steady-state of activation and inactivation levels and on the right panel the time constants at which the gating variables approaches the steady-state levels.

When at rest, with $V \approx 0\ mV$, the activation variable of Na^+ is close to zero, meaning that there is a small amount of Na^+ ions crossing the membrane. If some event produces a small depolarization of the membrane, a small amount of ions flow through ion channels and so, the membrane recovers to its equilibrium. Although, if some event (sufficiently) depolarizes the membrane, m_∞ rises, and, since τ_m is small, so do m, causing the Na^+ channels to be the first to open which leads to an influx of Na^+ and depolarizing the membrane even more. This positive feedback loop triggers an action potential (AP) or spike (see Figure 2.3). During the rising of V, the activation variable of K^+ and the inactivation variable of Na^+ (which are slower) starts approaching to the corresponding steady-states and then two phenomena occurs, h approaches 0 which inactivates the sodium current and roughly at the same time n rises which activates the outward potassium current.

The interplay of the activation and inactivation variables results in three different stages of the action potential. The first, when the sodium channels are opened, results in the rise of the membrane potential. The second occurs when the sodium channels

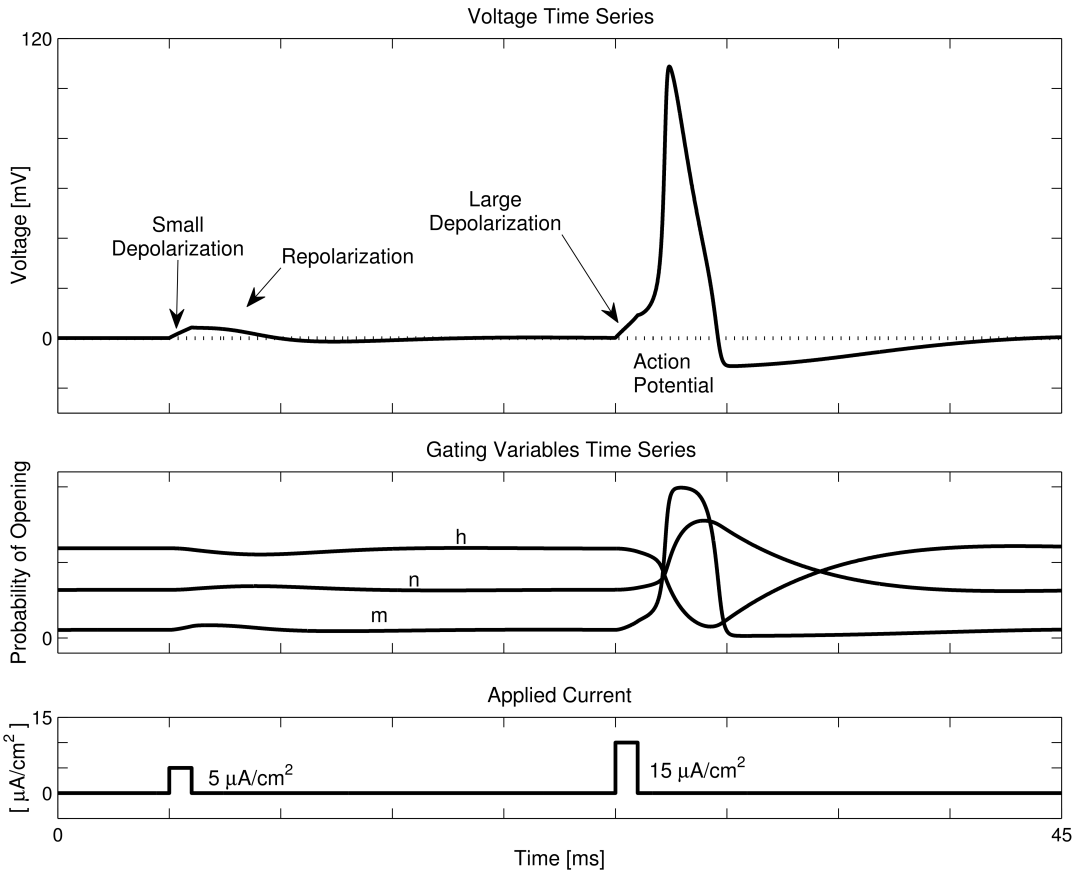

FIGURE 2.3. The Action Potential in the Hodgkin-Huxley Model. Two currents of 1 ms were applied to an HH neuron. The first with amplitude $5\mu S/cm^2$ and the second with amplitude $15\mu S/cm^2$. With the first current, only a small depolarization was induced. After a few milliseconds the neuron recovered its equilibrium. With the second current, a large depolarization was induced and the sodium channels were opened leading to a positive feedback loop which increased even more the membrane potential giving rise to an action potential. (Top) Temporal evolution of the membrane potential. (Middle) Temporal evolution of gating variables. (Bottom) Current applied to the neuron.

close due to the drop in the value of the inactivation variable h. This period is known as the *absolute refractory period*, and during this interval, a second action potential is impossible to be initiated. The third stage is known as the *relative refractory period*. Since the potassium activation variable is slower, at the moment when the membrane potential reaches the equilibrium potential, the potassium channels are still opened and

so, the membrane potential continues to drop towards the potassium reversal potential giving rise to a hyperpolarization which hinders a future spike.

2.2.3. Conductance-based models

The Hodgkin-Huxley model was built for modeling the squid giant axon. It is therefore not intended for modeling the mammalian cortex neurons or other neurons studied in numerous species. Nevertheless, changes in the parameters of the original model has allowed, over the past decades, to successfully model a wide variety of neurons of countless neuronal systems. With the evolution of the available technology it was possible to study and model other ionic currents and the Hodgkin-Huxley equations were often used as a starting point for new models, being the basis for what are now known as the *conductance-based models*.

Conductance-based models (based on the Hodgkin-Huxley formalism) are suited to model single neurons or small networks because they require a large computational effort per single neuron. On the other hand, all the parameters have biophysical meaning and are measurable. In conductance-based models there is a strong link between the laboratory results and the model parameters and therefore they are often used in studies aiming to answer questions at the cellular level, such as how the interplay between different ionic currents or even variations in channels density can support the existence of features such as bursting, resonance, spike time adaptation, bistability, among others.

2.3. FitzHugh-Nagumo

Nearly a decade after the work of Hodgkin and Huxley (1952a), Richard FitzHugh (FitzHugh, 1961) suggests a simplification of the Hodgkin-Huxley model through the *Bonhoeffer-van der Pol* model. At about the same time, an electric circuit analog for a similar model was constructed by Jin-Ichi Nagumo and collegues (Nagumo et al., 1962). The model, known since then by *FitzHugh-Nagumo Model* is a two-dimensional reduction of the Hodgkin-Huxley model wich results from the mixing of the Hodgkin-Huxley fast variables V and m into the variable v resembling the membrane potential, and the mixing of the slow gating variables n and h into the recovery variable w. The time evolution of the system is described by the equations:

$$\frac{dv}{dt} = v - \frac{v^3}{3} - w + I \tag{2.13a}$$

$$\frac{dw}{dt} = 0.08\,(v + 0.7 - 0.8w) \tag{2.13b}$$

where I is the magnitude of stimulus current.

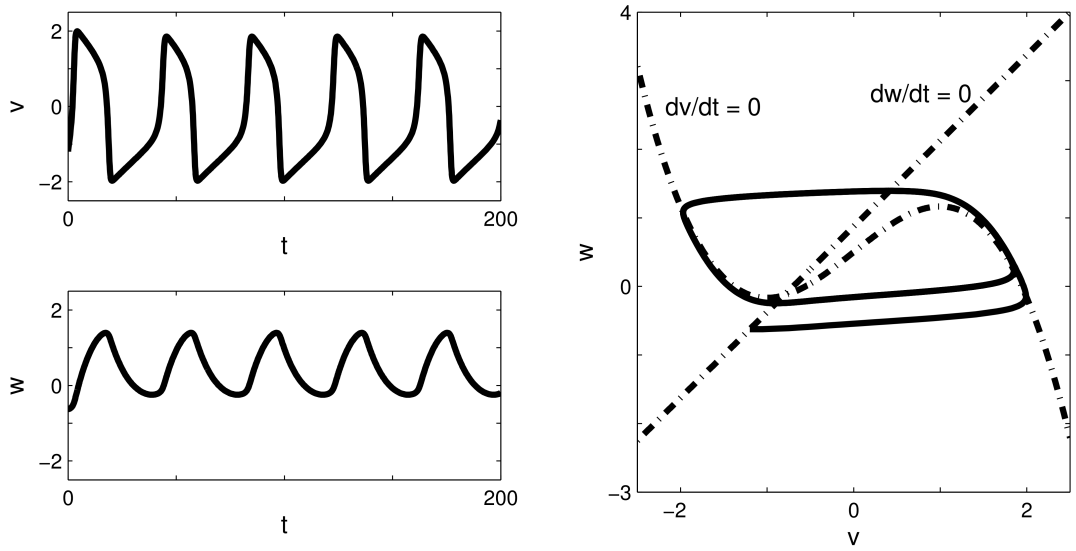

FIGURE 2.4. FitzHugh-Nagumo dynamics after injection of a constant current $I = 0.4$. (Left) Time evolution of the state variables v (on top) and w (on bottom); (Right) Phase portrait.

The behavior of this simpler model is qualitatively similar to the four-dimension model proposed by Hodgkin and Huxley (1952a). In Figure 2.4 the temporal dynamics of the model's variables are depicted for the case where $I = 0.4$. The reduction in dimensionality permits the visualization of the entire solution at once while in the Hodgkin-Huxley model only projections of the four-dimensional space can be observed.

Despite being simpler, the FitzHugh-Nagumo model preserves some features of the Hodgkin-Huxley model such as the absence of threshold or the rebound spikes (action potentials triggered by hyperpolarization currents) among others (for more information see Izhikevich and FitzHugh, 2006). The dimension of the model, when compared with conductance-based models, allows simulation of large networks in feasible time. Nevertheless, the parameters of the FitzHugh-Nagumo model have no direct biophysical meaning,

and a neuron modeled with these equations cannot reproduce some features of real neurons such as bursting (Izhikevich, 2004).

2.4. Morris-Lecar

Another two-dimensional reduction of the Hodgkin-Huxley model was proposed in 1981 by Cathy Morris and Harold Lecar. The *Morris-Lecar model* (Morris and Lecar, 1981) considers two ionic currents: an instantaneously responding calcium (Ca^{2+}) current responsible for the excitation, and a potassium current responsible for the recovery. The time evolution of the membrane potential is described by:

$$C_m \frac{dV}{dt} = -\bar{g}_{Ca} m_\infty (V)(V - V_{Ca}) - \bar{g}_K W (V - V_K) - g_L (V - V_L) + I_{app} \tag{2.14a}$$

$$\frac{dW}{dt} = \frac{W_\infty (V) - W}{\tau_W (V)} \tag{2.14b}$$

$$m_\infty = 0.5 \left(1 + tanh\left(\frac{V - V_1}{V_2}\right)\right) \tag{2.14c}$$

$$W_\infty = 0.5 \left(1 + tanh\left(\frac{V - V_3}{V_4}\right)\right) \tag{2.14d}$$

$$\tau_W = \frac{\phi}{cosh\left(\frac{V - V_3}{2V_4}\right)} \tag{2.14e}$$

where V is the membrane potential, in mV, W is the recovery variable (mimicking the Hodgkin-Huxley K^+ current gating variable), I_{app} is the applied current density, in $\mu A/cm^2$, $C_m = 20\ \mu F/cm^2$ is the membrane capacitance per unit of area, $V_{Ca} = 120\ mV$, $V_K = -84\ mV$, and $V_L = -60\ mV$ are, respectively, the calcium, the potassium and the leakage reversal potentials, $\bar{g}_{Ca}$, $\bar{g}_K$, and g_L are, respectively, the calcium, the potassium and the leakage maximal conductances, in mS/cm^2, ϕ is a temperature/time scaling parameter, and t is time, in ms.

Parameters ϕ, $\bar{g}_{Ca}$, $\bar{g}_K$, g_L, V_1, V_2, V_3, and V_4 can be chosen to fit data. Different sets of parameters originate different qualitative responses to applied currents. For example,

Sterratt et al. (2011, Chapter 8) shows that depending on the choice of the parameters, a Morris-Lecar neuron can be classified as Type I[1] or as Type II[2].

The Morris-Lecar model, as well as some other models resulting from adaptations of the original equations, have become widely used in computational neuroscience. While being as simple as the FitzHugh-Nagumo model, it has parameters with biological meaning. However it is only able to reproduce tonic bursting through the addition of at least one more equation, which leaves it with a degree of complexity similar to the Hodgkin-Huxley model (Izhikevich, 2004).

2.5. Izhikevich

Using bifurcation methods, Izhikevich (2003) built a model that was capable of producing a wide variety of firing patterns resembling those of real neurons but at the same time that was computationally efficient. Izhikevich proposed a two-dimensional model with four free parameters:

$$\frac{dv}{dt} = 0.04v^2 + 5v + 140 - u + I \tag{2.15a}$$

$$\frac{du}{dt} = a\,(bv - u) \tag{2.15b}$$

with a reset mechanism:

$$\text{if } v > 30\ mV, \text{ then } \begin{cases} v \leftarrow c \\ u \leftarrow u + d \end{cases} \tag{2.16}$$

where a, b, c, and d are dimensionless parameters. The variable v represents the membrane potential and u is a recovery variable mimicking the activation of K^+ and inactivation of Na^+ currents.

As can be seen in Figure 2.5, depending on the choice of the parameters, an Izhikevich neuron can exhibit completely different firing patterns. This two-dimensional model is simple and therefore computationally efficient, allowing faster simulations of large neural networks. As the FitzHugh-Nagumo model, the Izhikevich model includes parameters that cannot be measured experimentally. In addition, such as in the Integrate and Fire

[1] Type I neurons: neurons that can fire at arbitrary low firing frequencies

[2] Type II neurons: neurons that cannot fire at arbitrary low firing frequencies

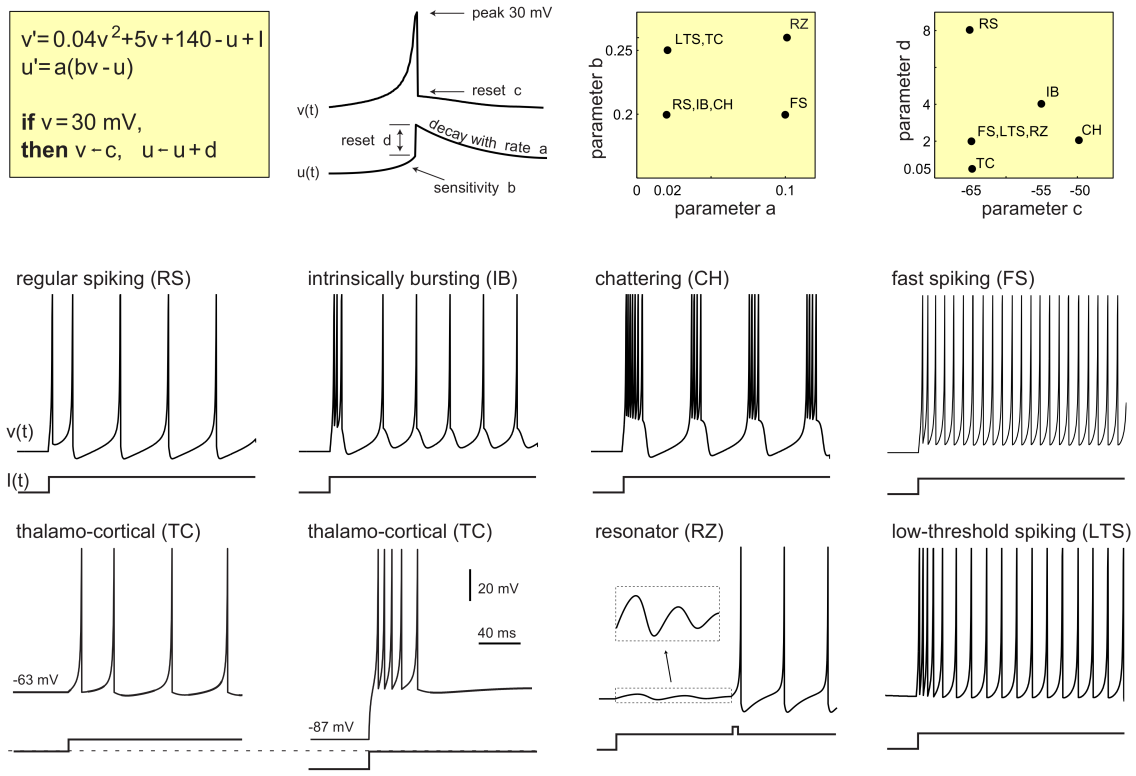

FIGURE 2.5. Different firing patterns as a result of the choice of the model's four parameters. (Electronic version of the figure and reproduction permissions are freely available at www.izhikevich.com.)

models, the action potentials are not explicitly modeled, but rather replaced by a reset mechanism.

2.6. Modeling the Neuronal Morphology

So far, we focused only on how to model a small portion of membrane which is assumed to be isopotential; in other words, we focused on modeling point-wise neurons. However, in real neurons, the current longitudinally flows through the intracellular medium and shapes the response to a given input signal. Depending on the questions that the model is intended to address, it may be necessary to take into account some spatial characteristics of neurons such as morphological dimensions, spatial distribution of the dendritic branches, distribution of ion channels throughout the dendritic tree, or the spatial distribution of synapses.

2.6.1. The Cable Equation

Membrane potential can vary considerably along the neuron. Even in a small patch of dendrite, these differences can be observed. In response to these differences ions tend to flow longitudinally along the neurite. Long and narrow stretches of neurite provide higher resistance to the ion flow, while in short and thick stretches the resistance is lower. The longitudinal resistance, R_L, of a segment of neurite (modeled as a cylindrical compartment of length l and radius a) is proportional to l and inversely proportional to the cylinder's cross-sectional area (πa^2), and so, longitudinal resistance is given by $R_L = r_L \frac{l}{\pi a^2}$, where r_L represents the intracellular resistivity (in units of Ohm$\times$length).

Consider, as in Figure 2.6, a cylindrical portion of membrane with radius a and infinitesimal length Δx.

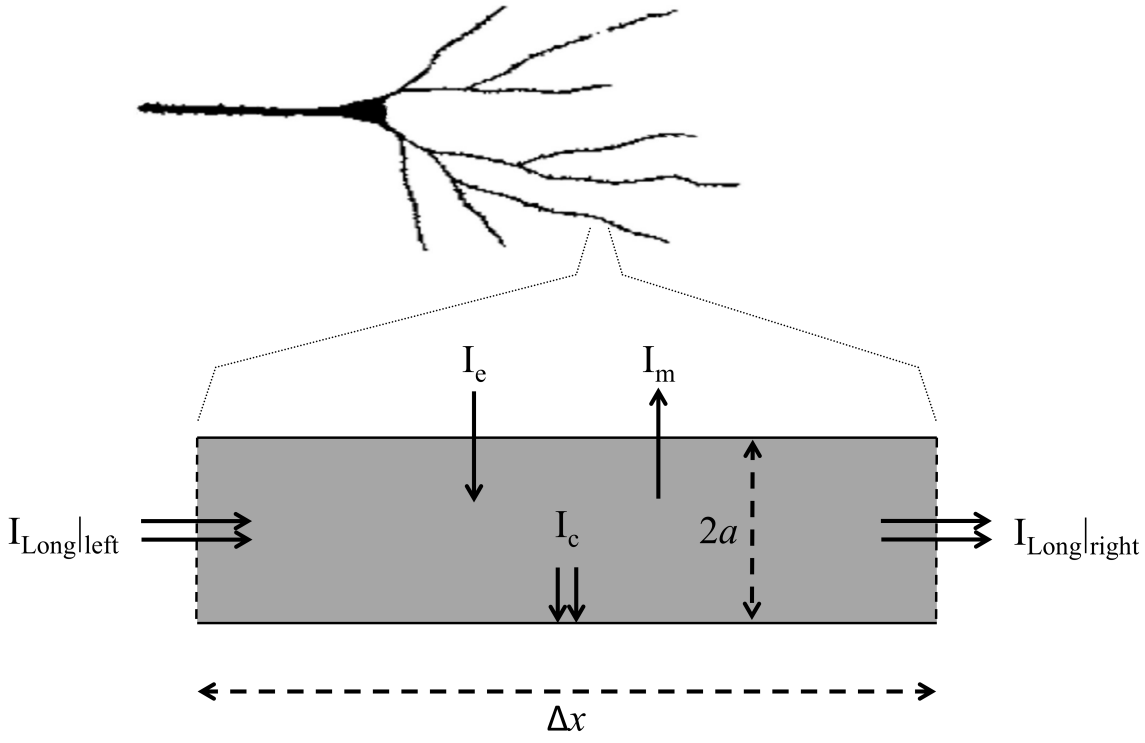

FIGURE 2.6. Cylindrical segment of length Δx and radius a used to represent a small patch of neurite. I_e, I_m, I_c, $I_{Long}|_{left}$, and $I_{Long}|_{right}$ are the currents that can change the membrane potential. Figure adapted from Dayan and Abbott (2005).

To determine the membrane potential as a function of time and space it is necessary to take into account all of the currents that can change the membrane potential: the electrode current, $I_e = 2\pi\, a\, \Delta x\, i_e$, the resistive current, $I_m = 2\pi\, a\, \Delta x\, i_m$, the capacitive current, $I_c = 2\pi\, a\, \Delta x\, c_m \frac{\partial V}{\partial t}$, and the longitudinal current.

Defining as positive, resistive currents when they are outward, electrode currents when they are inward, and longitudinal currents when they flow in the direction of increasing distance to the soma (increasing x), and using the *Ohm's law*, it results that:

$$\Delta V = -\frac{r_L \Delta x}{\pi\, a^2} I_{Long} \tag{2.17}$$

where $\Delta V = V(x + \Delta x) - V(x)$ and I_{Long} is the longitudinal current.

Considering $\Delta x \to 0$, then:

$$I_{Long} = -\frac{\pi\, a^2}{r_L} \frac{\partial V}{\partial x} \tag{2.18}$$

Using the charge conservation principle, and taking the longitudinal current as the the difference between the current entering on the left side and the current leaving on the right side, it is possible to derive the *Cable Equation*:

$$2\pi\, a\, \Delta x\, c_m \frac{\partial V}{\partial t} = \left(-\frac{\pi\, a^2}{r_L} \frac{\partial V}{\partial x}\right) |_{left} - \left(-\frac{\pi\, a^2}{r_L} \frac{\partial V}{\partial x}\right) |_{right} - 2\pi\, a\, \Delta x\ (i_m - i_e) \tag{2.19}$$

Dividing both sides by $2\pi\, a\, \Delta x$, equation (2.19) can be rewritten as:

$$c_m \frac{\partial V}{\partial t} = \frac{1}{2\pi\, a\, \Delta x} \left[\left(\frac{\pi\, a^2}{r_L} \frac{\partial V}{\partial x}\right) |_{right} - \left(\frac{\pi\, a^2}{r_L} \frac{\partial V}{\partial x}\right) |_{left}\right] - i_m + i_e \tag{2.20}$$

Noting that, when $\Delta x \to 0$:

$$\frac{1}{\Delta x} \left[\left(\frac{\pi\, a^2}{r_L} \frac{\partial V}{\partial x}\right) |_{right} - \left(\frac{\pi\, a^2}{r_L} \frac{\partial V}{\partial x}\right) |_{left}\right] \to \frac{\partial}{\partial x} \left(\frac{\pi\, a^2}{r_L} \frac{\partial V}{\partial x}\right) \tag{2.21}$$

the cable equation for a cylindrical compartment is:

$$c_m \frac{\partial V}{\partial t} = \frac{1}{2\, a\, r_L} \frac{\partial}{\partial x} \left(a^2 \frac{\partial V}{\partial x}\right) - i_m + i_e \tag{2.22}$$

To derive equation (2.22), r_L was moved outside the derivative under the assumption that the intracellular resistivity is independent of position.

If the radius a is assumed to be constant, then equation (2.22) can be rewritten as:

$$c_m \frac{\partial V}{\partial t} = \frac{a}{2r_L} \frac{\partial^2 V}{\partial x^2} - i_m + i_e \tag{2.23}$$

Other simplifications are often made on the cable equation. If the membrane potential stays close to the resting potential, a linear approximation can be considered. If no network currents flows across the membrane, the resistive current per unit of area, i_m, can be approximated by:

$$i_m = \frac{V - V_{rest}}{r_m} \tag{2.24}$$

where V_{rest} is the resting potential, and r_m is the membrane resistance per unit of area.

Considering a variable changing defined by $v = V - V_{rest}$, and multiplying all terms in the cable equation by r_m, we obtain:

$$r_m c_m \frac{\partial v}{\partial t} = \frac{a\, r_m}{2r_L} \frac{\partial^2 v}{\partial x^2} - \frac{v}{r_m}\, r_m + i_e\, r_m \tag{2.25}$$

or:

$$\tau_m \frac{\partial v}{\partial t} = \lambda^2 \frac{\partial^2 v}{\partial x^2} - v + i_e\, r_m \tag{2.26}$$

where

$$\tau_m = r_m c_m \tag{2.27}$$

is the *time constant* which defines the time scale with which the membrane responds to perturbations in the injected current, and

$$\lambda = \sqrt{\frac{a\, r_m}{2r_L}} \tag{2.28}$$

is the *length constant* which defines the spatial range of influence of a local perturbation in membrane potential.

Finally, it is necessary to take into account what happens to the membrane potential at the end of each segment, that is, it is necessary to specify the boundary conditions. At the end of each segment, the neurite can branch or terminate.

If multiple segments joint at one point (called "node"), $V\,(x,t)$ must be continuous, that is, the membrane potential must be equal either if it is computed at the end of one segment either if it is computed at the beginning of the adjacent one. In addition, the

charge conservation principle requires that the sum of all longitudinal currents at one node must be zero (that is, the current which leaves one segment has to split to all other segments joining that node).

For terminating segments several boundary conditions can be considered. One possibility is the *killed end* condition in which it is assumed that the neurite has been cut. Thus, the membrane potential at the end of the neurite equates the extracellular potential. Another possibility is the *leaky end* condition in which the longitudinal current is equal to the current flowing through the end of the cable. Another reasonable condition which can be considered is the *sealed end* boundary condition in which it is assumed that no current flows out through the end of the cable.

Although an analytical solution of the cable equation is useful to study simple cases, due to the wide range of questions that can depend on complex neuronal morphologies the cable equation is often solved numerically.

2.6.2. Multi-compartment Models

The Cable Equation allows the modeling of the neuronal morphology, nevertheless, the analytical solution of the cable equation is only possible for simple cases. If a complex neuronal structure has to be conserved by the model only spatial discretizations are feasible. To model a neuron's three-dimensional (3D) structure, the dendritic (and/or axonal) tree should be divided into small segments (compartments) where variations in membrane potential across them are negligible. Furthermore, for sufficiently small compartments, it is reasonable to assume spatial uniformity in all its properties. Thus, differences in voltage, dendritic diameters or ion channel densities, among others, are assumed to occur only between compartments.

Each compartment is represented by a single geometric object (the most common examples are cylinders or spheres), which facilitates the computation of surface area or cross-sectional areas. Then, each compartment j will have its own membrane potential, V_j, which will represent the membrane potential of all points in the compartment, and its own ion channels. The time evolution of the compartment membrane potential will follow the equation:

$$c_m \frac{dV_j}{dt} = -i_m^j + \frac{I_e^j}{A_j} + g_{j,j+1}\left(V_{j+1} - V_j\right) + g_{j,j-1}\left(V_{j-1} - V_j\right) \tag{2.29}$$

where I_e^j is the total electrode current impinging on compartment j, A_j is its surface area, i_m^j is the membrane current per unit of area of compartment j, and V_{j+1} and V_{j-1} are the membrane potentials of the neighbor compartments. Equation (2.29) should be updated if compartment j is a terminal segment (in which case only one neighbor exists and so the last two terms in the right side of the equation must be replaced by just one) or if compartment j branches in two (in such case three terms must replace the last two).

The factor $g_{j,i}$ represents the coupling conductance from compartment i to compartment j. To compute the value of $g_{j,i}$, the Ohm's law should be used. Suppose that compartment j is modeled as a cylinder of length L_j and radius a_j and compartment i is modeled as a cylinder of length L_i and radius a_i. Then the resistance between compartments i and j is the sum of the resistance from the middle of the cylinder i to the junction point and the resistance from the junction point to the middle of compartment j, that is, $r_L \frac{L_i}{2\,\pi\,a_i^2} + r_L \frac{L_j}{2\,\pi\,a_j^2}$. By inverting this expression and dividing the result by the total surface area of compartment j, $2\pi a_j L_j$ we obtain

$$g_{j,i} = \frac{a_i^2\, a_j^2}{r_L\, L_j \left(L_j\, a_j^2 + L_i\, a_i^2\right)} \tag{2.30}$$

A crucial problem the modeler faces when start building a multi-compartment model is to decide how closely the neuronal structure must be captured. If on one hand a larger number of compartments increases the precision of the model, on the other hand it also increases its complexity and thus the simulation time. The number of compartments used to describe a neuron can vary from thousands, in very spatially accurate models, to a few, in some models, to just one, in models where the spatial structure can be neglected (see Figure 2.7).

2.6.3. Electrical Flow Through Complex Morphologies

Solutions of equation (2.26) depends on both time and position, however, if a constant current is injected into the neuron, equation (2.26) will became time-independent and so, can be rewritten as:

$$\lambda^2 \frac{\partial^2 v}{\partial x^2} = v - i_e\, r_m \tag{2.31}$$

For a small region around the current injection site (for simplicity, we can assume $x = 0$), with length Δx, the injected current per unit of area is $i_e = \frac{I_e}{2\,\pi\,a\,\Delta x}$, where I_e is

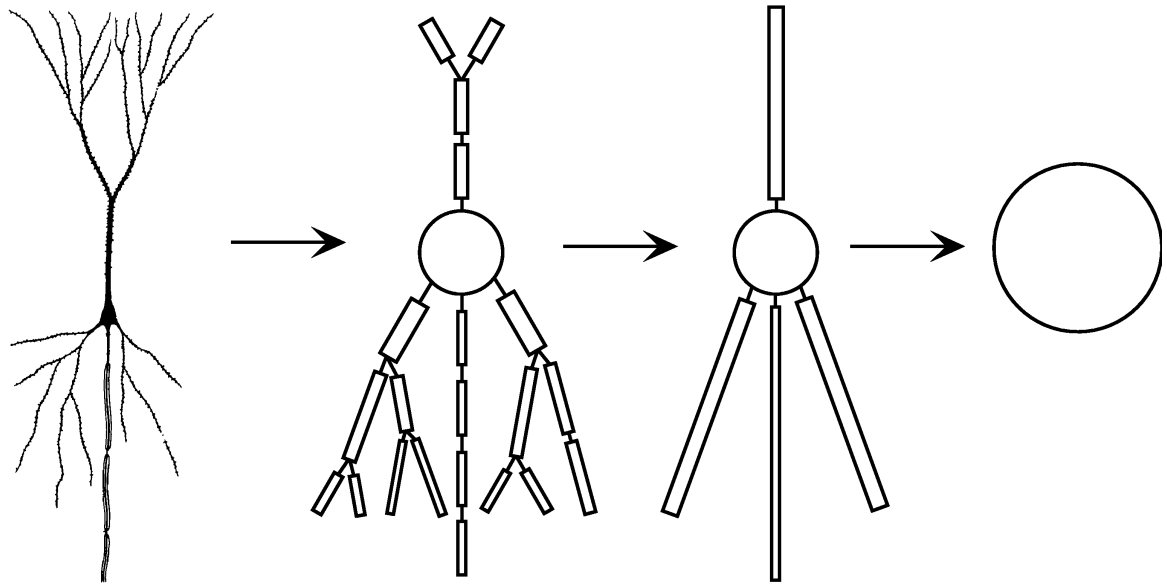

FIGURE 2.7. Modeling the neuronal morphology. The same neuron can be represented by a variable number of compartments. A balance between spatial accuracy and complexity of the model must be carefully taken into consideration. Figure adapted from Dayan and Abbott (2005).

the total current injected. Everywhere else $i_e = 0$. Solving equation (2.31) for an infinite cable an considering a small enough Δx, the membrane potential along the (infinite) cable is given by:

$$v(x) = \frac{I_e R_\lambda}{2} \exp\left(-\frac{|x|}{\lambda}\right) \tag{2.32}$$

where $R_\lambda = \frac{r_L \lambda}{\pi a^2}$ (for more details see, for example, Dayan and Abbott 2005, Chapter 6).

From equation (2.32), it is possible to define the voltage attenuation between two points x_1 and x_2 as:

$$A(x_1, x_2) = \frac{v(x_2)}{v(x_1)} \tag{2.33}$$

It is, however, important to notice that the voltage attenuation is not a suitable quantity to geometrically describe a neuron since it is not additive, that is, considering three points along a cable such that $x_1 < x_2 < x_3$, $A(x_1, x_3) \neq A(x_1, x_2) + A(x_2, x_3)$. Nevertheless, $A(x_1, x_3) = A(x_1, x_2) \times A(x_2, x_3)$, and so, the logarithm of the attenuation is additive. Therefore, for an infinite cylindrical cable, it is possible to define the electrotonic

distance as $X = \log(A)$, which is directly proportional to physical distance x: $X = \frac{x}{\lambda}$ (Zador et al., 1991; Brown et al., 1992).

However, real neuron dendrites and/or axons are neither infinite nor cylindrical, preventing the utilization of this measure to describe some important properties of neurons. In real neurons, the attenuation is strongly affected by irregular variations of diameters and lengths in dendritic branches.

In order to overcome these difficulties, Carnevale and Johnston (1982) studied the *two-port theory*. Between their results, three are of major importance:

(i) Signal attenuation depends on the direction of the propagation. Consider two points x_1 and x_2 of the same neuron and assume that voltage is spreading from x_1 to x_2. Denote by $A^V_{x_1,x_2} = \frac{v(x_2)}{v(x_1)}$ the voltage attenuation between x_1 and x_2. Lets now consider the reverse situation, that is, voltage is spreading from x_2 to x_1, and consider $A^V_{x_2,x_1} = \frac{v(x_1)}{v(x_2)}$. Generally, $A^V_{x_1,x_2} \neq A^V_{x_2,x_1}$.

(ii) Current attenuation in one direction is identical to voltage attenuation in the opposite direction. Define I_{x_1} as the current injected at x_1 and I_{x_2} as the current recorded at x_2 under voltage clamp conditions. Denoting the current attenuation between x_1 and x_2 by $A^I_{x_1,x_2} = \frac{I_{x_2}}{I_{x_1}}$, the authors show that $A^I_{x_1,x_2} = A^V_{x_2,x_1}$, and similarly that $A^I_{x_2,x_1} = A^V_{x_1,x_2}$

(iii) Charge and DC current attenuation in the same direction are identical.

Combining (i), (ii) and (iii), it results that, knowing the voltage attenuation between two points in both directions is enough to fully describe the spread of the electrical signals between them.

3 Mathematical Models for Synapses

Neurons are cells whose activity is strongly linked to the activity of other cells of the neural network. Neural signals are transmitted from a neuron to the next via synapses, specialized regions where the axon of a neuron grows close to the dendrite (or the soma) of another neuron.

3.1. The Biology of Synapses

The most studied synapses in the cortex are the chemical synapses (see Figure 3.1A). In a chemical synapse, when a action potential reaches the axon terminal of the presynaptic neuron, the electrical activity is converted into the release of neurotransmitter molecules (like glutamate or γ-aminobutyric acid) into a small space called the *synaptic cleft*. The neurotransmitters in the synaptic cleft then bind with receptors on the postsynaptic cell and cause the activation of the receptor molecules.

If the activated receptors are *ionotropic*, some ion channels will open allowing the flow of ions and causing a postsynaptic potential, a local variation in the membrane potential of the postsynaptic neuron which then spreads to the rest of the neuron (see Section 2.6).

If the activated receptors are *metabotropic*, an intracellular chemical cascade is initiated at the postsynaptic cell, starting in the activation of a small chemical called "G-protein" which then activates a secondary messenger. Then, the secondary messengers may act in two different forms:

- in some cases, the secondary messenger travel along the cell until bind and open ion channels;
- in other cases, the secondary messenger travel along the cell and activate other molecules somewhere else.

Due to these differences, ionotropic receptors acts faster than metabotropic receptors. Secondary messengers act slower than the opening of ion channels but typically leads to long-lasting changes in neuron behavior.

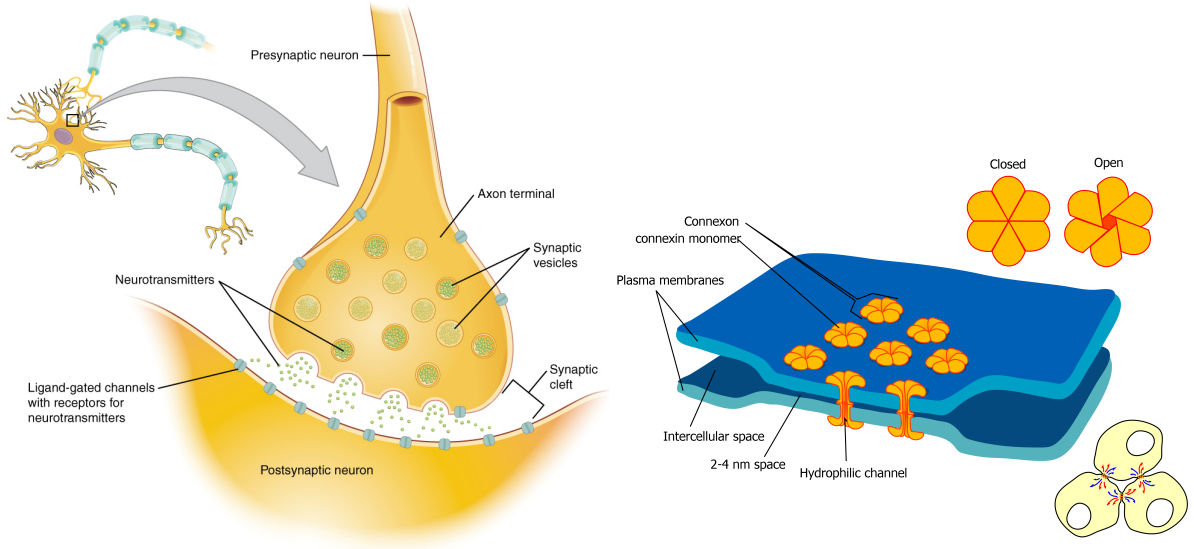

(A) Chemical synapse. (B) Electrical synapse.

FIGURE 3.1. Schematic of two types of synapses. Images from the public domain, downloaded from (A) http://upload.wikimedia.org/wikipedia/commons/3/37/1225_Chemical_Synapse.jpg; and (B) http://upload.wikimedia.org/wikipedia/commons/b/b7/Gap_cell_junction-en.svg.

Another kind of synapses are the *electrical synapses* also known as *gap junctions* (Figure 3.1B). These synapses are electrical connections between two neurons which developed so close that they share some protein channels, called connexons, which enable the transfer of ions and other small molecules between both neurons and consequently allow the exchange of membrane voltage between them.

3.2. Modeling Synapses

Before modeling a synapse it is necessary to identify the scientific question that the model is intended to address and establish a desirable degree of biological accuracy. In order to study networks of neurons it is usual to use simple synaptic models such as those that model only the synaptic conductance waveform or those which consider simple kinetic schemes, while to explore intrinsic mechanisms of the synapse, complex stochastic models including vesicle recycling and release are often used.

3.2.1. Modeling the Conductance Waveform

When the synapse is placed just as a tool to study the behavior of a neuronal network, the most common approach is to model solely the postsynaptic response. If the postsynaptic response is electrical, the focus is often placed in capture the synaptic conductance waveform.

If, at time t_{spike} a signal is sent from a presynaptic neuron to a postsynaptic neuron, the electrical current that influences the membrane potential of the postsynaptic neuron is described, for $t > t_{spike}$, by:

$$I_{syn}(t) = g_{syn}(t)\left(V(t) - E_{syn}\right) \tag{3.1}$$

where g_{syn} is the synaptic conductance, $V(t)$ is the postsynaptic membrane potential and E_{syn} is the synaptic reversal potential. Depending on the neurotransmitter molecule and, consequently, on the ion channel that the receptors open, the synapse may be *excitatory* or *inhibitory*. Glutamate is a neurotransmitter which activates two different kinds of receptors, AMPA/kainate, which are very fast, and NMDA, which are slower. In both cases, the membrane will be excited after the binding. For these excitatory synapses, typical values of E_{syn} are close to 0 mV. Inhibitory synapses are mainly activated by γ-aminobutyric acid (GABA), which is the principal inhibithory neurotransmitter in the cortex. There are two receptors for GABA, $\mathrm{GABA_A}$ and $\mathrm{GABA_B}$ and typical values of E_{syn} for inhibitory synapses are lower than -65 mV.

Depicted in Figure 3.2 are the most used waveforms to model the time evolution of g_{syn}. The conductance waveform can be modeled, for example, by a single exponential function (equation (3.2a)), by an alpha function (equation (3.2b)), or by a dual exponential function (equation (3.2c)):

$$g_{syn}(t) = \bar{g}_{syn} \exp\left(-\frac{t - t_{spike}}{\tau}\right) \tag{3.2a}$$

$$g_{syn}(t) = \bar{g}_{syn} \frac{t - t_{spike}}{\tau} \exp\left(-\frac{t - t_{spike}}{\tau}\right) \tag{3.2b}$$

$$g_{syn}(t) = \bar{g}_{syn} \frac{\tau_{rise}\,\tau_{decay}}{\tau_{decay} - \tau_{rise}} \left(\exp\left(-\frac{t - t_{spike}}{\tau_{decay}}\right) - \exp\left(-\frac{t - t_{spike}}{\tau_{rise}}\right)\right) \tag{3.2c}$$

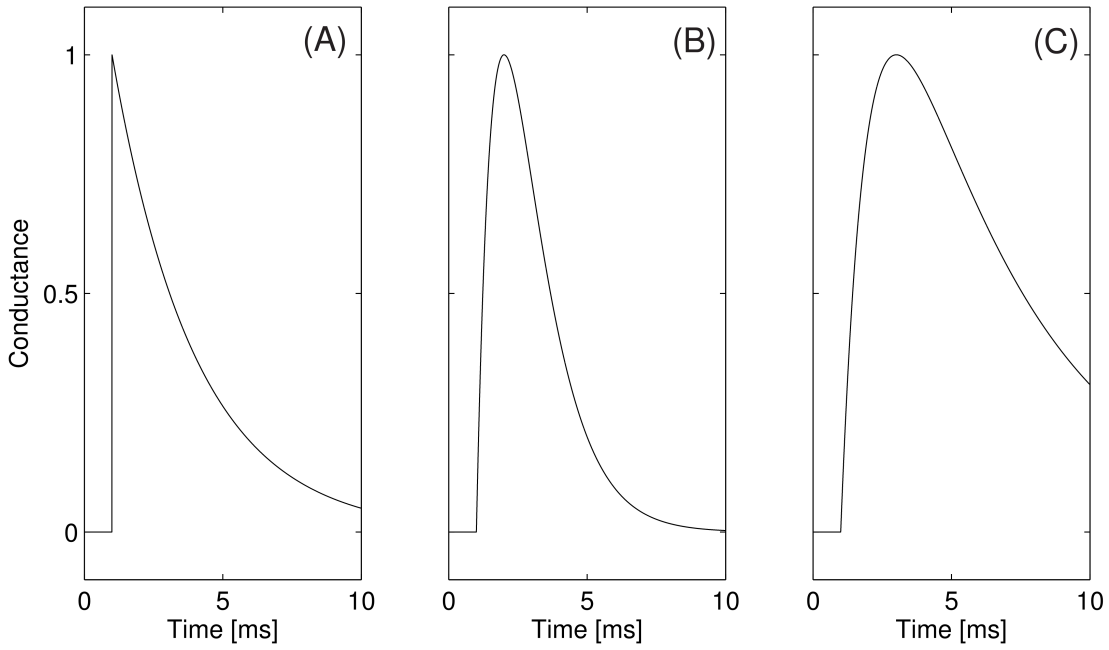

FIGURE 3.2. Synaptic conductance waveforms in response to a single presynaptic action potential arriving at time $t_{spike} = 1ms$. (A) single exponential function with decay $\tau = 3\ ms$; (B) alpha function with time constant $\tau = 1\ ms$; and (C) dual exponential function with $t_{rise} = 1\ ms$ and $t_{decay} = 5\ ms$. Conductances scaled to a maximum of 1. Figure adapted from Sterratt et al. (2011).

When instead of the response to an action potential is necessary to model the response to a series of presynaptic action potentials, equation (3.1) is still used and g_{syn} is obtained by adding the corresponding waveforms. For example, if a dual exponential function is used to model the synaptic conductance waveform, then the time evolution of g_{syn} after the arrival of the n^{th} action potential, follows the equation:

$$g_{syn}(t) = \sum_{i=1}^{n} \bar{g}_{syn} \frac{\tau_{rise}\,\tau_{decay}}{\tau_{decay} - \tau_{rise}} \left(\exp\left(-\frac{t - t_i}{\tau_{decay}} \right) - \exp\left(-\frac{t - t_i}{\tau_{rise}} \right) \right) \tag{3.3}$$

where t_i is the time of the arrival of the i^{th} action potential.

Equations (3.2a) to (3.2c) are good approximations of conductance waveforms that are independent of the postsynaptic neuron. Nevertheless, there are synapses which are dependent of the membrane potential of the postsynaptic neuron and/or of the concentration of certain ions. For example, NMDA receptors are voltage-sensitive and are also

influenced by the extracellular concentration of magnesium (Jahr and Stevens, 1990). To take into account these dependencies, a factor representing the magnesium block should be considered (Zador et al., 1990):

$$g_{syn}(t) = \bar{g}_{syn} \frac{\exp\left(-\frac{t-t_{spike}}{\tau_{decay}}\right) - \exp\left(-\frac{t-t_{spike}}{\tau_{rise}}\right)}{1 + \mu\left[Mg^{2+}\right]\exp\left(-\gamma V\right)} \tag{3.4}$$

where $[Mg^{2+}]$ represents the extracellular concentration of magnesium, V is the postsynaptic voltage and the μ and γ are factors to set the magnesium and the voltage dependencies, respectively. With typical values for the parameters, the peak of g_{syn} will be higher if the postsynaptic neuron's membrane is depolarized than if it is at rest.

3.2.2. Kinetic Schemes

Modeling only the conductance waveform, despite being efficient, does not include some features of synaptic transmission. Whenever an action potential reaches the axon terminal, neurotransmitters are released and bind with receptors causing a postsynaptic potential. If multiple action potentials occur in a small time window, it is expected that some receptors become saturated and that some are still open. Some receptors could also exhibit desensitisation, which is a period, after transmitter-binding, where the receptor cannot be reopened. As such, it is unlikely that the subsequent action potentials contribute to the postsynaptic potential as much as the first. *Kinetic schemes* has been successfully used to address this problem (Destexhe et al., 1994b, 1998).

The simplest kinetic model is the two-state scheme. According to this scheme, receptors can be closed or open. Variables C and O represents the closed and the open sates, respectively, of the receptors:

$$\mathrm{C} \underset{\beta}{\overset{\alpha[T]}{\rightleftharpoons}} \mathrm{O}$$

where $\alpha[T]$ is the forward rate constant, which is dependent of the transmitter concentration in the synaptic cleft, $[T]$, and β is the backward rate constant. The dynamics of the states are described by:

$$\begin{aligned} \frac{dO}{dt} &= \alpha[T]\,C - \beta O \\ C &= 1 - O \end{aligned} \tag{3.5}$$

The synaptic conductance is defined as:

$$g_{syn}(t) = \bar{g}_{syn} O(t) \tag{3.6}$$

More detailed kinetic schemes can be considered to model synapses, for example, the six-gate kinetic scheme:

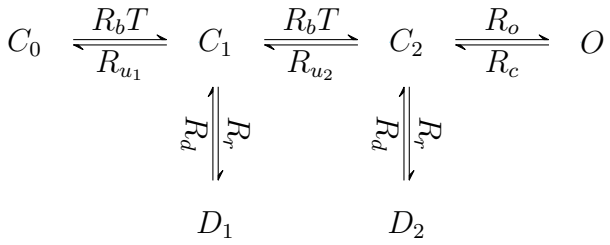

was proposed by Patneau and Mayer (1991) to model the AMPA/kainate receptors. According to this model, C_0 is the unbound state, which can bind to one molecule of transmitter, originating the singly bound form C_1, which can bind with another molecule of transmitter to form C_2, which can then open. Both C_1 and C_2 can desensitize to forms D_1 and D_2 before opening.

The dynamics of the states are described by:

$$\begin{aligned}
\frac{dC_0}{dt} &= R_{u1}\, C1 - R_b T\, C_0 \\
\frac{dC_1}{dt} &= R_b T\, C_0 + R_{u2}\, C2 + R_r\, D_1 - (R_{u1} + R_b T + R_d)\, C_1 \\
\frac{dC_2}{dt} &= R_b T\, C_1 + R_c\, O + R_r\, D_2 - (R_{u2} + R_o + R_d)\, C_2 \\
\frac{dD_1}{dt} &= R_d\, C_1 - R_r\, D_1 \\
\frac{dD_2}{dt} &= R_d\, C_2 - R_r\, D_2 \\
O &= 1 - (C_0 + C_1 + C_2 + D_1 + D_2)
\end{aligned} \tag{3.7}$$

Other kinetic schemes were proposed to model NMDA, $GABA_A$, or $GABA_B$ synapses.

3.2.3. Gap Junctions

Many neurons communicate with each other through protein channels that are shared by the membranes of both. These channels allow the flow of ions and other small molecules resulting in an exchange of voltage between both neurons. Unlike chemical synapses,

which become activated only when an action potential arrives at the axon terminal, gap junctions allow a continuous communication between both neurons because they act as resistors between two compartments.

The simpler gap junction model assumes a symmetric permeability between neurons. Thus, the current flowing throug a gap junction is modeled as:

$$I_{gap}(t) = g_{gap}(V_{post}(t) - V_{pre}(t))$$

where g_{gap} is the conductance and V_{post} and V_{pre} are the membrane potential of the post- and presynaptic neurons, respectively.

4 Neural Plasticity and Learning

Memory is the process of storing past experiences in the brain. Different brain systems are involved in memory storage, some specialized in long-term storage, and others suited for short-term memories. Several models have been proposed to support the memory storage, distinguishing themselves either by the time scales under study either by the mechanisms involved.

4.1. Long-Term Synaptic Plasticity

Over the past decades, numerous studies have proposed that long-term memory storage is done through changes in the connectivity of neural systems (Bliss and Lomo, 1973; Abbott and Nelson, 2000; Kandel, 2001). The strengthening or weakening of the effectiveness with which a presynaptic action potential modifies the membrane potential of the postsynaptic neuron was successfully used to explain the appearance of cell assemblies whose activity is correlated. At the origin of these studies is the *Hebbian learning rule*. Donald Olding Hebb (Hebb, 1949) postulated that "when an axon of cell A is near enough to excite a cell B and repeatedly and persistently takes part in firing it, some growth process or metabolic change takes place in one or both cells such that A's efficiency, as one of the cells firing B, is increased". In other words, Hebb postulated that if the activity of neuron A repeatedly or persistently contributes to the activity of neuron B then the synapse between A and B should be strengthened. Over the years, the original postulate of Donald Hebb has been modified to account for weakening of the synaptic efficacy when the activation of A repeatably fails the activation of B.

Spike Timing Dependent Plasticity (STDP) is a form of Hebbian learning rule that depends on the correlations between the pre- and the postsynaptic action potentials (see Figure 4.1). If the presynaptic neuron repeatedly fires a few milliseconds before the postsynaptic neuron then there is a process known as *Long-Term Potentiation* (LTP) resulting in the strengthening of the synapse. If, on the contrary, the postsynaptic neuron

repeatedly fires before the presynaptic neuron *Long-Term Depression* (LTD) weakens the synapse (Sjöström and Gerstner, 2010).

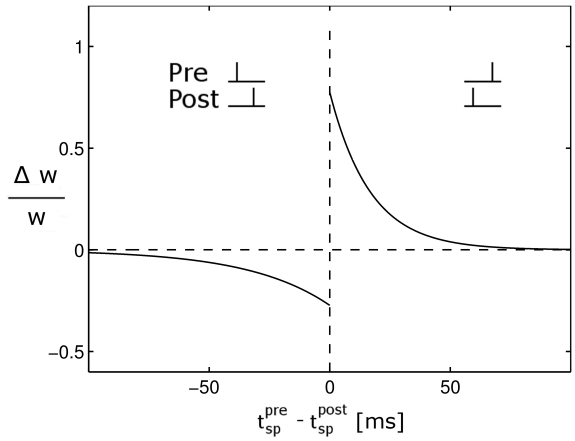

FIGURE 4.1. Spike Timing Dependent Plasticity. Depending on the precise time difference between a pre- and a postsynaptic spike $\left(t_{sp}^{pre} - t_{sp}^{post}\right)$, the synaptic weight (w) can be either strengthened or weakened. Figure adapted from Bi and Poo (2001) representing two exponential curves fitting the total amount of change in synaptic weight after 60 pairs of correlated spiking between hippocampal glutamatergic neurons in culture.

Other theories in synaptic plasticity suggests that the postsynaptic action potential is not necessary to induce LTP or LTD of a synapse, only a certain level of depolarization in the postsynaptic membrane is needed (Artola et al., 1990; Sjöström et al., 2004).

4.2. Short-Term Synaptic Plasticity

In addition to the long-term synaptic plasticity (LTP and LTD) involved in the formation of long-lasting memories, there are short-term synaptic mechanisms which affect the transmission of signals between neurons and have been used to support the storage of short-term memories (Mongillo et al., 2008; Rolls et al., 2013). *Short-Term Plasticity* (STP) (Stevens and Wang, 1995; Fuhrmann et al., 2002; Zucker and Regehr, 2002) accounts for temporary synaptic efficacy changes resulting from its recent history of activity. Two processes are at the origin of the STP. By one hand, the limited amount of neurotransmitters in the axon terminal along with its depletion during synaptic signaling causes, in a high-frequency train of action potentials, a decrease in the number neurotransmitters available for releasing leading to Short-Term Depression (STD). On the other

hand, after each action potential, there is a calcium influx into the axon terminal which increases the fraction of neurotransmitters released, leading to Short-Term Facilitation (STF) (Tsodyks and Wu, 2013).

4.3. Non-Synaptic Plasticity

Although widespread on neuroscience literature, synaptic plasticity is not the only mechanism available in the nervous system to store information. Some patterns of neuronal activity may lead to changes in excitability, input resistance, spike threshold or afterhyperpolarization (Sahley et al., 1994; Marder et al., 1996; Schreurs et al., 1998; Burrell et al., 2001; Mozzachiodi and Byrne, 2010). These changes can be used as non-synaptic mechanisms to store information, or, in some cases, can be used as addition to synaptic mechanisms to facilitate the memory storage (Mozzachiodi and Byrne, 2010).

Changes in excitability can be achieved by the modulation of some voltage- and/or calcium-dependent conductances (Ganguly et al., 2000; Egorov et al., 2002; Xu et al., 2005; Campanac et al., 2008). Some of these changes were reported along with LTP or LTD and so, can be viewed as additional mechanisms involved in learning. For example, Fan et al. (2005) reported that subthreshold synaptic stimulation paired with back-propagating APs at theta frequency results on both LTP and decrease in somatic excitability in CA1 pyramidal neurons. According to the authors, the decrease in somatic excitability is a consequence of an enhancement of the hyperpolarization-activated current I_h which decreases the membrane input resistance and reduces the ability to elicit APs. Similarly, Xu et al. (2005) reported that a LTP-induced shift in the activation curve of the Na^+ current can increase the neuronal excitability and decrease the firing threshold. Studies such as those mentioned above indicate that changes in synaptic efficacy (LTP and/or LTD) can coexist with changes at the cellular level and may serve, in some cases, to facilitate learning (Mozzachiodi and Byrne, 2010), or in other cases, as homeostatic mechanisms for activity regulation (Campanac et al., 2008).

Other changes in neuronal intrinsic excitability can account for memory formation by itself. Neurons can have a large variety of ion channels that allow them to display a wide range of patterns of activity. Some neurons, exhibit plateau properties and have the ability to store information about their past inputs by switching from one pattern of activity to another as a consequence of a transient stimulus (Marder et al., 1996).

For example, Egorov and colleagues (Egorov et al., 2002) argue that persistent activity at single cellular level can be achieved by activity-dependent interplay between Ca^{2+} and Ca^{2+}-dependent cationic currents, and thus, they proposed that the modulation of these currents may be a suitable mechanism for the storage of short-term memories (see Chapter 5).

Other ion currents can also be used to store information. Some ion currents have slow kinetics that can progressively modulate the neuronal excitability and thus can underlie short-term memory formation. For example, the $Kv1.3$ potassium channels slowly inactivate and slowly de-inactivate (Marom and Abbott, 1994) enhancing the neuron's response to a depolarizing current pulse subsequent to a long depolarization. Turrigiano et al. (1996) show that a neuron with $Kv1.3$ potassium channels can respond differently to the same input current depending on its previous activity history, and therefore, this current can give the neuron the ability to store information about events occurred up to several seconds before.

5 Working Memory

Working memory (WM) refers to a memory system of lower capacity but with fast storage and manipulation, involved in complex cognitive process such as learning, language comprehension, planning or decision-making (Miller et al., 1960; Baddeley and Hitch, 2010; Dudai, 2002). In a working memory system, the information is stored only as long as necessary and then is discarded enabling the system to store new information. Prefrontal cortex (PFC) and entorhinal cortex (EC) are two regions known to be involved in the processing of working memory tasks (Durstewitz et al., 2000; Durstewitz, 2003; Baddeley, 2003; Hahn et al., 2012; Suh et al., 2011). Studies show that when a cue stimulus initiate a working memory task, the activity of some neurons – those coding the stimulus – rises from low to high firing rates and remains at high levels even after the removal of the stimulus (Durstewitz et al., 2000). If the same stimulus is presented a second time the firing rate of the same group of neurons rises again, while the presentation of a different stimulus activates a different constellation of neurons (Funahashi et al., 1989; Funahashi and Kubota, 1994).

The working memory performance has been tested using *delay tasks*. A delay task consists in the presentation to a subject (animal or human) of a transient stimulus that has to be stored for a few seconds during the *delay period*. After this period the subject must recall the information and perform some task dependent on the information encoded. Different experimental protocols can be used in delay tasks. One of the oldest protocols consists in the presentation of a stimulus A, followed by the presentation of one or several distractor stimuli (none of them repeated) before the presentation of the match stimulus A. The subject is rewarded if it signals the match stimulus A (Miller et al., 1991). A different protocol was proposed by Miller and Desimone (1994), the so-called ABBA protocol, in which the presentation of a cue stimulus A, is followed by a set of distractors among which at least one, B, is presented twice before the match stimulus A is presented again. The subject must retain the first stimulus (A) and should signal its repetition

without signaling the repetition of the distractor stimulus B. These and other protocols indicates that the information can be stored quickly and in a flexible fashion. In addition, certain studies demonstrate the possibility of storing several items simultaneously (see for example Miller, 1956).

5.1. Working Memory Models

Mathematical models have been used to explain the mechanisms underlying a working memory system. Some models focus on the storage of one item while others focus on the storage of multiple items or even sequences of items. There are models focusing on the storage of new information while others propose mechanisms that support the activity at high rates in constellations of neurons coding previously known information. In addition to the differences in the objectives, there are important differences in the mechanisms considered. Some models rely on single cell mechanisms while others argue that the neuronal network plays the key role.

5.1.1. Recurrent Attractor Networks

Most WM models based on network mechanisms involve memories that were previously engraved in the brain through long-term learning mechanisms (Durstewitz et al., 2000; Barak and Tsodyks, 2014). Neuronal assemblies with correlated patterns of activity tend to emerge from progressive but slow changes in synaptic efficacies (Hebb, 1949; Hopfield, 1982; Amit and Brunel, 1997). Such modifications occur through long-term potentiation (LTP) and long-term depression (LTD) which requires several seconds to be effective (Lee et al., 1980; Klintsova and Greenough, 1999). Given the time scales in which a WM system should perform, models based on LTP or LTD are only capable of eliciting previously stored memories and sustaining those memories during the delay period (Durstewitz et al., 2000).

5.1.1.1. *Single-item Models*

Under the attractor networks paradigm, after the learning period, the network becomes divided into subpopulations of neurons. The activity at high firing rates during the delay period in one of the subpopulations of neurons while other neurons fire spontaneously at low firing rates is possible due to a balance between strong excitations inside each cell assembly and week excitations between neurons in different assemblies (Wang,

2001). If the ratio between the excitation strengths inside each subpopulation of neurons and the excitation strengths between neurons in different subpopulations is too small, the recurrent excitation is not strong enough to support the persistent activity during the delay period. Above a critical threshold for that ratio, if a stimulus generate a transient activity peak in one subpopulation, the rising firing frequencies will generate enough recurrent excitation which in turn will rise even more the firing rates constituting a positive feedback that supports the persistent activity during the delay period. The firing rates can then be stabilized by a negative feedback from inhibitory interneurons (Brunel and Wang, 2001). The balance between recurrent excitation and inhibition in addition to supporting the persistent activity in a subpopulation of neurons while other neurons remain in spontaneous activity, also increases the robustness against distractors (Brunel and Wang, 2001) and the interspike variability (Tsodyks and Sejnowski, 1995; van Vreeswijk and Sompolinsky, 1996; Vogels and Abbott, 2009). Finally, it is noteworthy that if the ratio between the excitation strengths inside each subpopulation of neurons and the excitation strengths between neurons in different subpopulations is too large, the system is unable of supporting spontaneous activity in other neurons during the delay period and therefore that ratio must range within an appropriate interval to allow the sustaining of the persistent activity in the active subpopulation at the same time that allows the spontaneous activity in the remaining neurons (Brunel and Wang, 2001; Wang, 2001).

5.1.1.2. *Multi-item Models*

Attractor network models can also address the problem of sustaining the activity in more than one constellation of neurons selective to previously learned memories. Amit and colleagues (Amit et al., 2003), using a network similar to the one proposed by Brunel and Wang (2001), showed that more than one item can be hold in a WM system during the delay period. Rolls and co-workers (Rolls et al., 2013), by incorporating more biological detail through short-term facilitation, showed that it is possible to increase the number of items that can be simultaneously active during the delay period.

A conceptually different way of sustaining more than one item in a working memory system is to separate items over time. Instead of having more than one constellation of active neurons at the same time, the active constellations can fire in different phases. For example, Mongillo and colleagues (Mongillo et al., 2008) use the short-term synaptic

plasticity to sustain the activity in more than one item. When a second item is presented, the activity of the first is temporarily suppressed, and after the storage of the second item both constellations start firing out of phase.

Separation of items over time can also constitute a mechanism underlying WM systems for sequences of items. Under a recurrent attractor network paradigm, the storage of the order of a sequence of items can be the result of the strengthening of the associations between successive items (Henson, 1998; Botvinick and Plaut, 2006) where the activity of one is elicited by the activity in the preceding item or items of the sequence (Elman, 1990; Murdock, 1995).

5.1.2. Networks with Continuous Attractors

Some information is, presumably, discrete by nature, while other should be coded under a continuum space. For example, there is a discrete set of letters, words, or numerical digits so a WM system which is meant to hold this kind of information can be modeled as a recurrent discrete attractor network. On the other hand, information like spatial position or head direction is better represented by a continuous variable and so a WM system which is intended to store this information must be able to account for it.

Experiments suggests that some neurons are selective to the location of visual cues, and the activity of the neuronal population can be described as a function of stimulus position (Funahashi et al., 1989). To support this behavior, specific networks combining local recurrent excitation with broader feedback inhibition were introduced (Amari, 1977; Camperi and Wang, 1998; Wang, 1999) enabling the system to respond to a given stimulus by displaying a bell-shaped pattern of activity, or "bump attractor", where the peak of the bump encodes information about the angle of the stimulus (Wang, 2001). Bump attractor models have been successfully used for storing continuous variables such as angles, however some features of cortical neurons that can be detrimental to the maintenance of the information have been neglected. For example, spike-frequency adaptation is ubiquitous in cortical neurons but most of the spatial working memory models cannot accommodate the degree of cellular adaptation imposed by these currents (Compte et al., 2000; Wang et al., 2004). The spike-frequency adaptation originates a continuous movement (traveling wave) in the region of activity along the network causing information loss (Hansel and Sompolinsky, 1998; Laing and Longtin, 2001). Laing and Longtin (2001) proposed that

an increase in the noisy input from external sources can stop the continuous movement of the bump but at the same time enhances its random drift.

5.1.3. Single Cell Based Mechanisms

To account for novel information storage, single cell mechanisms may be considered. Mechanisms activated by Acetylcholine (ACh) support the persistent activity without recurrent excitation (Hasselmo and Stern, 2006). The interplay between ion currents at single cellular level was introduced to account for the storage of one item. Egorov and colleagues (Egorov et al., 2002) showed that single neurons respond to stimuli with graded changes in their firing frequencies. Furthermore, the firing frequency is stable during the delay period and can be modulated in a stimuli-dependent manner.

Fransén and co-workers (Fransén et al., 2002) proposed a multi-compartment model where a calcium and a calcium-sensitive nonspecific cation currents synergistically interact to support the selective maintenance of spiking activity in some neurons in the entorhinal cortex. Network models were then used to study the behavior of these neurons when performing delay tasks. The authors showed that considering a specific connectivity, along with tuned maximal synaptic conductances can reproduce experimental results such as match enhancement, match suppression, non-match enhancement and non-match suppression.

To account for the storage of more than one novel item, namely for a sequences of novel items, single cellular mechanisms were combined with the *theta* and *gamma* rhythms of the brain (Koene and Hasselmo, 2007, 2008; Lisman and Idiart, 1995). These studies are based in the fact that, in the presence of some neuromodulators like ACh or serotonin (5-HT), some neuron exhibit an afterdepolarization (ADP) that results in a transient increase in excitability. Altought too brief to account for the duration of a short-term memory, this ADP is long enough to interact with the *theta* and *gamma* rhythms of the brain to support the single-cell persistent activity.

6 Building the Model

"Things should be made as simple as possible, but not any simpler."
Albert Einstein

Any mathematical model has a limited capability of mimicking the biophysical world. A balance between the available scientific knowledge and the simplicity of the model compared to the questions to be asked should be carefully taken into account.

Given the questions to address in this thesis, a mathematically simpler but more abstract model should be discarded in favor of biological plausibility. At the same time, there was a high necessity to keep the model simple enough to be possible to perform the required network simulations in small periods of time.

As so, the Hodgkin-Huxley formalism was used to describe neuronal dynamics producing biophysically accurate neuronal conductances.

Since in the questions at hand there was no *a priori* indication for a contribution of neuronal topology, the complex neuronal tree was collapsed into a point-wise neuron.

Several ion currents are known to be present in PFC pyramidal cells. Each new current added to the model will increment the biophysical accuracy but at the same time will increase the computational effort required to simulate large networks. Therefore, building a model with a reduced number of ion currents was a requirement. The transient sodium, the delay rectifier potassium and the leak currents, similar to those proposed by Hodgkin and Huxley (1952a), were the first currents selected to the model, because in the PFC neurons they are the basis for the action potential generation. Afterwards, the aim was to find the minimum set of ion currents that produces the intended model dynamics. Two currents were then chosen to complete the model, the high threshold calcium current, and the calcium activated nonspecific cation current. With these two currents the neuron is able to preserve part of its firing history, enabling the modulation of its excitability without any form of synaptic plasticity.

In order to use accurate models which were previously validated by the scientific community, all the ion currents used in this thesis were taken from the ModelDB database (Hines et al., 2004).

To perform the numerical simulations, several simulation languages were available, from MATLAB to Python, BRIAN, GENESIS, NEST, NEURON, or even C++. Given the foreseen complexities of simulations, a language with a big community of users in the neuroscience field and which *a priori* would guarantee numerical stability, accuracy and efficiency was a requirement. Among the available options, the NEURON Simulation Environment (Hines and Carnevale, 1997) was selected to perform all neuronal simulations. NEURON is an efficient environment for simulating conductance-based models of individual neurons or networks. It is one of the most used languages in the computational neuroscience field and specific communities are available to support users. Appropriate numerical methods are implemented and lastly, but certainly not least, NEURON's capability to run in parallel hardware such as multiprocessor personal computers, workstation clusters, or massively parallel supercomputers, enables significant gains in simulation times with almost linear speedup of simulation speed as the number of processors increases (Migliore et al., 2006).

7 Results

This chapter will be divided into 3 topics:

(i) Working memory models for completely new information coded in one pattern of activity,

(ii) Working memory models for sequence learning,

(iii) Computational tools for assessing synaptic integration.

The work developed under the scope of (i) was presented to the scientific community in:

(1) *Poster presentation*

Conde-Sousa E., Aguiar P., Storing information in membrane conductances dynamics – working memory without synaptic plasticity, 1st Champalimaud Neuroscience Symposium, Lisbon, Portugal, September 18th – September 21st, 2011.

(2) *Papers in national scientific periodicals*

Conde-Sousa E., Aguiar P., Detailed mathematical models in neurobiology: Storing information in membrane conductances dynamics, CIM Bulletin, 2012, 31, 19 - 26.

http://www.cim.pt/files/publications/b31.pdf

(3) *Papers in international scientific periodicals*

Conde-Sousa E., Aguiar P., Synergy between different membrane currents as a mechanism for one-shot short-term memory, *submitted*.

The work developed under the scope of (ii) was presented to the scientific community in:

(1) *Poster presentation*

Conde-Sousa E., Aguiar P., A working memory model capable of storing sequences of patterns without using synaptic plasticity, 2nd Champalimaud Neuroscience Symposium, Lisbon, Portugal, September 30th – October 3rd, 2012.

(2) *Papers in international scientific periodicals*

Conde-Sousa E., Aguiar P., A working memory model for serial order that stores information in the intrinsic excitability properties of neurons, Journal of Computational Neuroscience, Volume 35, Issue 2, October 2013, pp 187-199
http://link.springer.com/article/10.1007/s10827-013-0447-7

(3) *Poster presentation*

Conde-Sousa E., Aguiar P., Conversion from spatial patterns of activity to sequences of neuronal activations using gate interneurons, 22nd Annual Computational Neuroscience Meeting: CNS*2013, Paris, France, July 13th – July 18th, 2013.
Published in:
BMC Neuroscience 2013, 14(Suppl 1):P3
http://www.biomedcentral.com/1471-2202/14/S1/P3

The work developed under the scope of (iii) is part of a larger project and, at the time of the submission of this thesis, the manuscript is still in preparation for submission in peer-reviewed international journal.

7.1. Synergy Between Different Membrane Currents as a Mechanism for One-Shot Short-Term Memory

Conde-Sousa E., Aguiar P., *submitted*.

Synergy between different membrane currents as a mechanism for one-shot short-term memory

Eduardo Conde-Sousa[1,2] • **Paulo Aguiar**[1,3]

Abstract

Recordings in behaving animals show that during working memory tasks some neurons keep their firing activity at high levels without any external cue. Working memory has two important characteristics: it provides a short-term memory buffer which keeps relevant information while it is being used, and information can be encoded and preserved after very short exposures to the stimuli. Here we present a model which avoids the canonical approach of relying on synaptic plasticity to store information. Instead, we use a spiking network model with high biophysical detail to show that a one-shot short-term memory system can be achieved in neurons through the synergy between different membrane currents. Our model exhibits properties which are in close agreement with experimental results in working memory, namely: (i) it works in time windows compatible with the notion of "one-shot learning" (hundreds of milliseconds), (ii) it is robust to noise, (iii) it is resistant to distractors, (iv) it can be reset with mild inhibition, (v) it exhibits the match-enhancement effect, and (vi) the memory is self-sustained while its information is being used.

Keywords

Working memory • Intrinsic excitability • Membrane current properties • Short-term memory • One-shot learning

7.1.1. Introduction

Memory storage and recall is one of the most studied fields in neuroscience. Models addressing these questions vary considerably in neuronal complexity, network complexity

[1] FCUP – Faculdade de Ciências da Universidade do Porto

[2] CMUP – Centro de Matemática da Universidade do Porto

[3] IBMC – Instituto de Biologia Molecular e Celular

and biophysical plausibility in the mechanisms considered. The vast majority of models regarding memory formation use the same main idea: memories are stored in the brain as a consequence of modification in synaptic efficacies (Bliss and Lomo, 1973; Kandel, 2001). However this plasticity paradigm is not sufficient to explain adequately all processes of information storage. Experiments show that some memory systems, such as working memory (WM), are capable of correctly storing information after very short exposures to the stimuli (on the time scale of a few hundreds of milliseconds). From the cognitive level, the working memory system provides the ability to temporarily store information on a time scale of several seconds and after a single exposure to the stimulus (Baddeley, 2003). This is incompatible with the mechanisms associated with synaptic long-term potentiation (LTP) or long-term depression (LTD), which require time scales of many seconds. While there are synaptic mechanisms working on shorter time scales (short-term synaptic plasticity), they are unreliable for robust one-shot storage as they typically involve the modulation of the probability of synaptic activation/release. Most WM models do rely however on LTP and LTD (Brunel and Wang, 2001; Rolls et al., 2013), or short-term synaptic plasticity (STP) (Mongillo et al., 2008) to explain the dynamics of the system (but see Versace and Zorzi 2010).

Here we take a different approach and present a biophysically detailed spiking model for WM which uses the dynamics of intrinsic membrane currents to store information (Marder et al., 1996; Durstewitz et al., 2000; Mozzachiodi and Byrne, 2010). Excitability of neurons can be modified according to the recent activity history as a consequence of the synergistic action of ionic currents. It has already been shown that these modifications can give rise to changes that can be used to temporarily store patterns of activity (Durstewitz et al., 2000; Fransén et al., 2002, 2006). Some models use this mechanism as a source for producing cellular bistability which is then used to store information (Lisman and Idiart, 1995; Fall and Rinzel, 2006; Koene and Hasselmo, 2007). However, in some bistable models, resetting the memory system requires abnormal levels of inhibition for prolonged times (Fransén et al., 2002).

Another class of models use modulation of intrinsic neuronal excitability (MINE) to store temporal information – that is, store information about time, instead of storing spatial activity patterns in the neuronal population. The MINE mechanism has been

shown to be able to support learning and storing time delays (Durstewitz, 2003) or the serial order between patterns of activity (Conde-Sousa and Aguiar, 2013).

In this work, the goal is to establish a working memory model which is:

(i) capable of storing information in exposure time windows of few hundreds of milliseconds being compatible with the one-shot learning paradigm;
(ii) robust to noise – neurons not belonging to the ensemble coding the information fire stochastically at low firing frequencies;
(iii) resistant to distractors – during the delay period the active constellation is robust to an attempt to store another constellation;
(iv) capable of showing match enhancement – when the sample stimulus is again presented the firing rate of the associated neurons rises;
(v) capable of self-sustaining the stored information while it is being used/replayed;

The novelty in the approach taken here is centered in combining in a single model the following properties: uses MINE to store new information; does not require synaptic plasticity nor bistability at the cellular level; does not impose strong constraints in the network architecture; uses membrane conductances to describe neuronal dynamics; establishes a one-shot short-term memory system. The ability to store new information is important as some WM models focus on the mechanisms for selecting, and sustaining, the activity of cell assemblies coding previously stored information (Brunel and Wang, 2001; Rolls et al., 2013).

7.1.2. Materials and methods

Neuronal dynamics were modeled using the Hodgkin-Huxley formalism (Hodgkin and Huxley, 1952a). This type of spiking models provides a high level of biophysical detail on the description of the membrane dynamics including the spike generating mechanism. While the computational power of networks using spiking models is extremely high they are also costly to simulate. To balance the biophysical plausibility with the simulation cost, single compartment neurons were considered. Simulations were carried out in the NEURON simulation environment (Hines and Carnevale, 1997) taking advantage of NEURON's capability to run in parallel hardware.

7.1.2.1. *Single cell dynamics*

All neurons are modeled as single cylindrical compartment with length $L = 18\ \mu m$ and diameter $d = \frac{1000}{L \times \pi}\ \mu m$ to obtain a total surface area of the compartment of 1000 μm^2.

The main class of neurons is the principal neurons (P), responsible for receiving and transmitting information from/to other brain areas. Two other neuronal classes are considered to provide inhibition to the principal class: (i) activity control inhibitory interneurons ($\mathrm{I_c}$), responsible for controlling the network activity level; and (ii) activity resetting inhibitory interneurons ($\mathrm{I_r}$), responsible for resetting the activity of the system.

Together with leakage current (I_L) and synaptic currents (I_{syn}), all neurons have two standard ion currents: the transient sodium (I_{Na}) and the delayed rectifier potassium (I_{Kdr}) currents. The principal neurons have however two additional ion currents: a high threshold calcium current (I_{CaL}) which is activated by membrane depolarization, and a nonspecific cationic current (I_{CAN}) whose activation increases when the intracellular calcium concentration rises. These two currents act synergistically to prolong membrane excitability states. While in this work we focus on this pair of membrane currents (which are widely present in many neuronal classes), other currents with the ability to prolong neuronal excitability could be used (e.g. persistent sodium current), while maintaining the same qualitative results of this model.

The time evolution of the membrane potential is described by the equation:

$$C_m \dot{V} = -I_L - I_{ion} - I_{syn}$$

where $C_m = 1\ \mu F/cm^2$ is the membrane capacitance; V represents the membrane potential; $I_L = g_L\,(V - E_L)$ is the leakage current, g_L is the leakage conductance and E_L is the reversal potential for the leakage current; I_{ion} is the sum of all the ionic currents on each neuron; and I_{syn} is the sum of all synaptic currents impinging on the neuron. For principal neurons $I_{ion} = I_{Na} + I_{Kdr} + I_{CaL} + I_{CAN}$, and for interneurons $I_{ion} = I_{Na} + I_{Kdr}$. The equations describing the dynamics for each of the individual currents (I_{Na}, I_{Kdr}, I_{CaL} and I_{CAN}), as well as the intracellular calcium dynamics that interacts with I_{CaL} and I_{CAN}, were taken from Conde-Sousa and Aguiar (2013) which in turn were taken from SenseLab(Crasto et al., 2007). A temperature of 22° Celsius was assumed in all simulations.

TABLE 7.1. Synaptic reversal potential and conductance profile parameters.

Synapse	$E_X\,[mV]$	$\tau_{rise}\,[ms]$	$\tau_{decay}\,[ms]$
AMPA	0	1	10
$GABA_A$	-75	1	15
$GABA_B$	-85	10	200

Synaptic currents

Three different types of synapses are considered (AMPA, $GABA_A$ and $GABA_B$). A dual exponential function with parameters τ_{rise} and τ_{decay} (Table 7.1) is used to model each synaptic conductance profile. The total synaptic current is then modeled as the sum all input synaptic currents to each neuron.

Membrane currents

Membrane ionic currents and correspondent gating variables are described elsewhere (see Conde-Sousa and Aguiar, 2013, and references therein) with one difference: the time constant of the activation variable of the calcium activated nonspecific cation (CAN) current is increased by twofold. This change allows the model to be more robust to noise while it preserves the ability to store information in small time windows. Used parameters are shown in Table 7.2.

7.1.2.2. *Network architecture*

One of the main objectives of this work is to provide evidence that MINE properties are sufficient to store completely new information in time windows according to the one-shot learning paradigm. As such, any combination of neurons may be co-activated, forming a pattern of activity, for a period of time compatible with the working memory system. This constellation of co-active neurons must remain stable without recruiting new neurons to the pattern (which would contribute to disrupt the information stored). To ensure that no combination is more probable to occur than others, given an ordered pair of principal neurons A and B, the probability of existing one synapse linking A to B is fixed. When this number, which represents the connectivity rate of the model, is 1.0, all principal neurons establish connections with all principal neurons (full connectivity).

TABLE 7.2. Parameters for membrane currents. The notation $\overline{g}_X$ refers to the maximal conductance of current X, whereas E_X refers to the reversal potential, and $\overline{p}_{CaL}$ is the Ca^{2+} membrane permeability. The reversal potential for calcium is calculated according to the Goldman-Hodgkin-Katz (GHK) equation, since the intracellular calcium concentration (cai) is not constant.

Ion Current	Parameters	P	I_c	I_r
I_L	$E_L\,[mV]$	-65	-65	-65
	$g_L\,[mS/cm^2]$	4×10^{-5}	10×10^{-5}	2×10^{-5}
I_{Na}	$E_{Na}\,[mV]$	50	50	50
	$\overline{g}_{Na}\,[mS/cm^2]$	80	80	80
	$V_{traub}\,[mV]$	-60	-60	-60
I_{Kdr}	$E_{Kdr}\,[mV]$	-70	-70	-70
	$\overline{g}_{Kdr}\,[mS/cm^2]$	20	20	20
	$V_{traub}\,[mV]$	-60	-60	-60
I_{CaL}	$E_{Ca}\,[mV]$	GHK	–	–
	$\overline{p}_{Ca}\,[cm/s]$	3×10^{-5}	–	–
I_{CAN}	$E_{CAN}\,[mV]$	0	–	–
	$\overline{g}_{CAN}\,[mS/cm^2]$	1×10^{-2}	–	–

A model composed only by excitatory neurons following the described dynamics is already capable of producing key features of a WM system based on MIME properties. However inhibition can play a central role in activity level control adding to the model a noise filtering and ensuring that the system can reset and be ready to store new information when the previous is no longer needed. In order to reduce computational cost,

TABLE 7.3. Synaptic mean peak conductances, in μS, between the three population classes in the network. k_1 and k_2 are normalization factors given by: $k_1 = (PS - 1) \times CR$ and $k_2 = PS$, where PS represents the number of principal neurons engaged in the codification of one pattern of activity, and CR is the connectivity rate.

		postsynaptic neuron		
		P	I_c	I_r
presynaptic neuron	P	$\frac{3.5\times10^{-5}}{k_1}$	$\frac{1.0\times10^{-4}}{k_2}$	$\frac{2.7\times10^{-5}}{k_2}$
	I_c	13×10^{-3}	-	-
	I_r	5×10^{-4}	-	-

the model is composed only by two global inhibitory interneurons, one of each functional class, establishing bidirectional connections with all the principal neurons.

The average synaptic peak conductances (efficacies) for connections between neurons in each classes are summarized in Table 7.3. To introduce variability in the synapses, each individual synaptic peak conductance is drawn from a uniform distribution with mean value taken from Table 7.3 and with a variability of $\pm 2.5\%$.

The synaptic conduction delays for all synapses are fixed at 1 ms.

Noise is provided to all principal neurons in the network and is introduced in the form of stochastic activations following a Poisson process. The average interspike interval is set to 2000 ms (0.5 Hz), in agreement with experimental data regarding cortical neurons.

7.1.3. Results

With this model, we intend to show that MINE properties are sufficient to produce several features of working memory, namely, the fast storage, the activity during the delay period, the resistance to noise and distractors, and the emergence of match enhancement. In order to fully exhibit the model features more clearly, the results are separated into topics. First, the intrinsic characteristics of principal neurons are presented. Secondly, the emergence of the working memory system is analyzed using two different tests: the network collective behavior during a delayed match-to-sample task, and subsequently the response of the model to the presentation of a distractor stimulus. We conclude

this section with the study of constraints regarding the information resetting and/or replacement, model scaling and robustness in parameter space.

7.1.3.1. *Principal neurons firing properties*

It is known that CAN current acts together with calcium current shaping the dynamics in neurons in prefrontal cortex (PFC) and in the entorhinal cortex (EC) (Bal and McCormick, 1993; Haj-Dahmane and Andrade, 1999; Klink and Alonso, 1997) two regions with identified roles in working memory tasks (Durstewitz et al., 2000; Baddeley, 2003; Hahn et al., 2012; Suh et al., 2011).

The activation of the CAN current is mediated by the intracellular calcium concentration (*cai*) and its reversal potential is close to 0 mV. These two characteristics combined result in the emergence of an after depolarization (ADP). Whenever an action potential (AP) is triggered, there is a rise in *cai* driven by the calcium current, which in turn contributes to the activation of the CAN current. Since this current has slow dynamics, its activation takes place after the inactivation of the Na^{2+} and the deactivation of K^{+} channels, and leads to a depolarization of the membrane. Depending on the density of the calcium and the nonspecific cationic channels, one neuron with these currents may present different features. If these two currents are sufficiently strong, then the ADP is high enough to promote a new AP. If not, the membrane depolarizes only at subthreshold levels. Neurons with larger densities of the CAN current tend to be bistable even when isolated from the network. An important element to acknowledge is that, with the parameterization used in our model, each neuron is not bistable.

Although not bistable, the principal neurons presented here have the capability to distinguish between spurious and consistent excitations, having qualitative different responses to stimuli of different durations.

After a long period close to resting potential the CAN current is deactivated and produces a negligible effect in the neuron behavior. When some external source excite the neuron above the threshold, an AP is produced and with each AP there is an entrance of calcium into the cell leading to a rise in *cai*. This increase in *cai* leads to a partial activation of the CAN current which in turn results in a subthreshold ADP. If the external stimulus is short enough, the membrane will return to the resting potential after a few hundreds of milliseconds. If, on the other hand, the stimulus is consistent and sufficiently

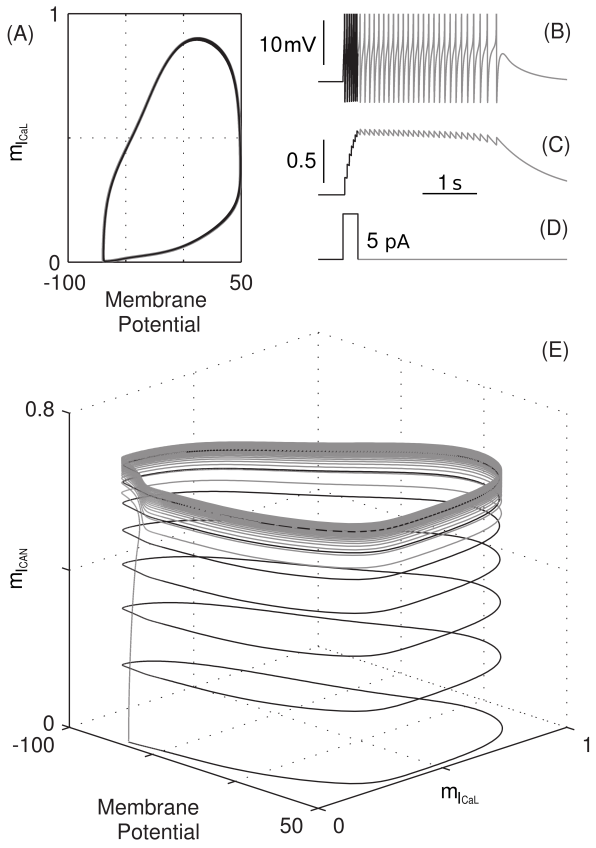

FIGURE 7.1. Short duration current injection analysis. A current of 5 pA was injected during 300 ms. (A) Phase plane with membrane potential (in mV), and $m_{I_{CaL}}$, calcium current activation variable. (B-D) Time evolution of (B) membrane potential, (C) CAN current activation variable ($m_{I_{CAN}}$), and (D) injected current. (E) Phase space with membrane potential, calcium current activation variable ($m_{I_{CaL}}$), and CAN current activation variable ($m_{I_{CAN}}$). Action potentials are truncated at -50 mV. Two important stages are color-coded: the first, in black, corresponds to the early stage where the current injection takes place; the second, in gray, corresponds to the period where the neuron (self-)sustains the activity for a while returning afterwards to the equilibrium point due to stability loss.

long to trigger a series of APs at firing rates above 8 Hz, the interspike interval (ISI) is shorter than the recovery time of the CAN current activation variable ($m_{I_{CAN}}$), and so, after each AP $m_{I_{CAN}}$ will be higher than it was after the previous one. This difference between ISI and $m_{I_{CAN}}$ recovery time leads to a more pronounced ADP after each new

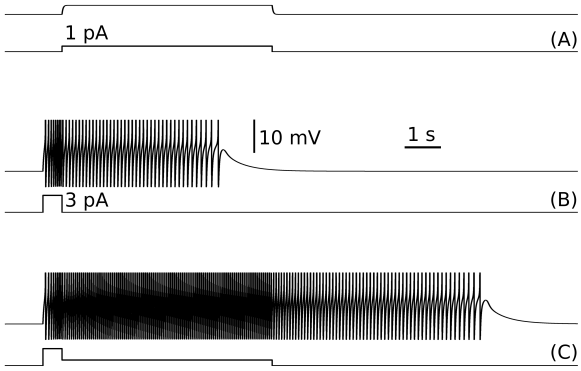

FIGURE 7.2. Sustaining neuronal activity. Three current steps where presented to an isolated principal neuron. (A) A current of 1 pA with a duration of 5.5 seconds depolarizes the membrane but at a subthreshold level; (B) A current of 3 pA with a duration of 0.5 seconds elicits 8 APs. After the stimulation period the neuron holds the activity for roughly 4 seconds; (C) Applying sequentially currents such as those of (B) and (A), the activity is maintained while the small amplitude current is present. Upon termination of the small (residual) current, the neuronal spiking activity vanishes after approximately 5 seconds. Each panel is composed by two traces: upper traces are membrane potentials (APs are truncated at $-50\ mV$); lower traces are the input step currents.

AP. If the number and frequency of APs are high enough, the ADP will, eventually, be above threshold. The depolarization induced by the CAN current will then be capable of reactivating the sodium current leading to a new AP, and starting the cycle again. This mechanism is transiently maintained without the need for an external current.

In Figure 7.1, it is possible to visualize the dynamics of the described behavior. With the generation of each AP there is a cycle in which the membrane potential rises, followed by the activation of the calcium current ($m_{I_{CaL}}$ rises), which results in an increment of cai and the consequent augmentation of $m_{I_{CAN}}$. After each AP, $m_{I_{CaL}}$ and the membrane potential return to near the equilibrium values (panel (A) of Figure 7.1) but $m_{I_{CAN}}$ stays higher than before due to the slower dynamics of the CAN current (panel (E) of Figure 7.1). If $m_{I_{CAN}}$ goes beyond a threshold value the ADP induced by the CAN current is sufficient to reactivate the sodium current leading to a new AP. After the external

excitation vanishes (gray traces in Figure 7.1) the activity is self-sustained for a period of several seconds but inevitably, and spontaneously, converges to the resting state.

As a result of the presence of CAN current in the neuron, a residual current which is not sufficient to excite by itself a neuron at rest is able to hold the activity in a neuron which was previously excited. In other words, the amplitude of an external current required to sustain the activity is much smaller than the one that is required to activate a neuron in the first place (see Figure 7.2).

7.1.3.2. *Encoding information*

We assume that when sensory/perceptual information is presented, specific groups of neurons in other brain regions are excited (Figure 7.3). The information requiring temporary storage is then provided to the spiking neuronal population engaged in the WM system. Each principal neuron in the WM network receives 100 AMPA connections from outside neurons (parameters in Table 7.1). Each of the presynaptic neurons fired for about 300 ms at a firing rate of roughly 20 Hz. The information is then stored as a pattern of activity where encoding neurons sustain the high spiking activity through recurrent excitation while all other principal neurons in the network remain at residual low activity. In order to simulate the arrival of the external information, each neuron receives stochastic synaptic activations following a Poisson process with a firing rate of $100 \times 20 = 2000$ Hz during 300 ms. Whenever it is mentioned that a neuron was *consistently excited*, it is being assumed an excitatory stimulation as described (100 neurons firing at 20 Hz for 300 ms). Notice that 300 ms is well within the temporal constraints associated with the notion of "one-shot learning".

7.1.3.3. *Network behavior in delayed match-to-sample tasks*

The first goal of the model is to show that it is possible to store information in exposure time windows of few hundreds of milliseconds ("one-shot" learning paradigm) in a noise robust manner (neurons outside the activity pattern fire stochastically at low firing rates) using only MINE properties (without synaptic modifications). Another goal is to provide evidence that these mechanisms could be used to identify if there is a match between the test cue and the sample stimulus.

In order to test if the model is able to accomplish these purposes, the following simulation protocol was implemented:

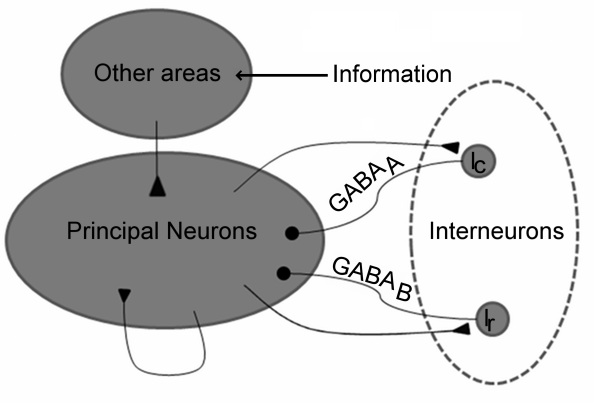

FIGURE 7.3. Enconding information. The information arrives to the WM spiking network model via other brain areas. All excitatory connections are AMPA synapses while inhibitory connections can be either GABA_A or GABA_B synapses.

(i) A pre-cue time interval of 1.5 seconds is considered.

(ii) After this period, occurs the stimulus presentation. Each of the first 200 principal neurons (those coding the information) is excited for 300 ms at roughly 20 Hz from 100 neurons from other brain region (see Section 7.1.3.2).

(iii) After the external stimulus is removed the neurons in the activity pattern must retain the activity without external stimulation, during the delay period (approximately 5.2 seconds).

(iv) After the delay period a match stimulus is presented. The first group is again excited. The excitation follows the same protocol as the sample stimulus.

As a consequence of the behavior described in Figure 7.2, it is possible to excite and sustain the excitation in any subgroup of principal neurons, of a fixed size, without a previous learning period. Consider a randomly connected network where all principal neurons receive equivalent recurrent excitation from the network (more details in Section 7.1.3.6). If an external current excite a group of them consistently, these neurons, as a group, will change their intrinsic excitability, sustaining the activity for a period of a few seconds. If the synaptic efficacies are balanced in accordance with the number of neurons and connectivity rate (Table 7.3) these neurons will receive enough synaptic current to prolong indefinitely their activity. On the other hand, all other neurons in the network,

which receives roughly the same synaptic current with the same parameters, will only partially depolarize, since these neurons don't have enough activation of the CAN current. In Figure 7.4 (left panels) it is possible to observe the collective behavior of a network of 2000 principal neurons with a connectivity rate of 0.2. These numbers means that each principal neuron receives, on average, $0.2 \times (2000 - 1) \approx 400$ excitatory synapses from other principal neurons. After being excited by 100 neurons from other areas (at 20 Hz during 300 ms), each of the first 200 principal neurons (10% of the population) sustains the activity with firing rates close to 17 Hz while other neurons in the network keeps its firing rates at lower levels (0.5 Hz).

Notice that when a cue stimulus matches the sample stimulus, the firing activity of the active group rises and a match enhancement is revealed.

7.1.3.4. *Resistance to distractors*

The model behavior regarding the presence of distractor stimuli, is assessed using tests where, after a delay period, a confounding pattern of activity is added to the sustained pattern. As distractor it is considered a stimulus that, if applied to a set of neurons when the network is in a spontaneous activity mode, would be considered a sample stimulus. The excitation of the distractor follows the same protocol described in Section 7.1.3.2.

The WM model can be considered robust to distractors if the activation of a new constellation while the spiking network is already holding some information, does not disrupt the currently held information.

In the presence of a distractor, the activity control interneuron (I_c) fires, preventing the storage of the new pattern, without resetting the activity in the previous constellation (first 10 seconds of simulation in right panels of Figure 7.4). Observing the average firing rate of neurons in the first constellation, it is possible to notice a non-match suppression during this period.

7.1.3.5. *Resetting the network*

According to the chosen network architecture, the model resets in one of three situations: (i) when, for some reason, the network is over-excited, leading to the activation of the activity resetting inhibitory interneuron (I_r); (ii) when the working memory's objective is achieved and an external afferent signal activate the resetting mechanism (see the last five seconds of simulation in panel A1 of Figure 7.4); or (iii) if the network needs to

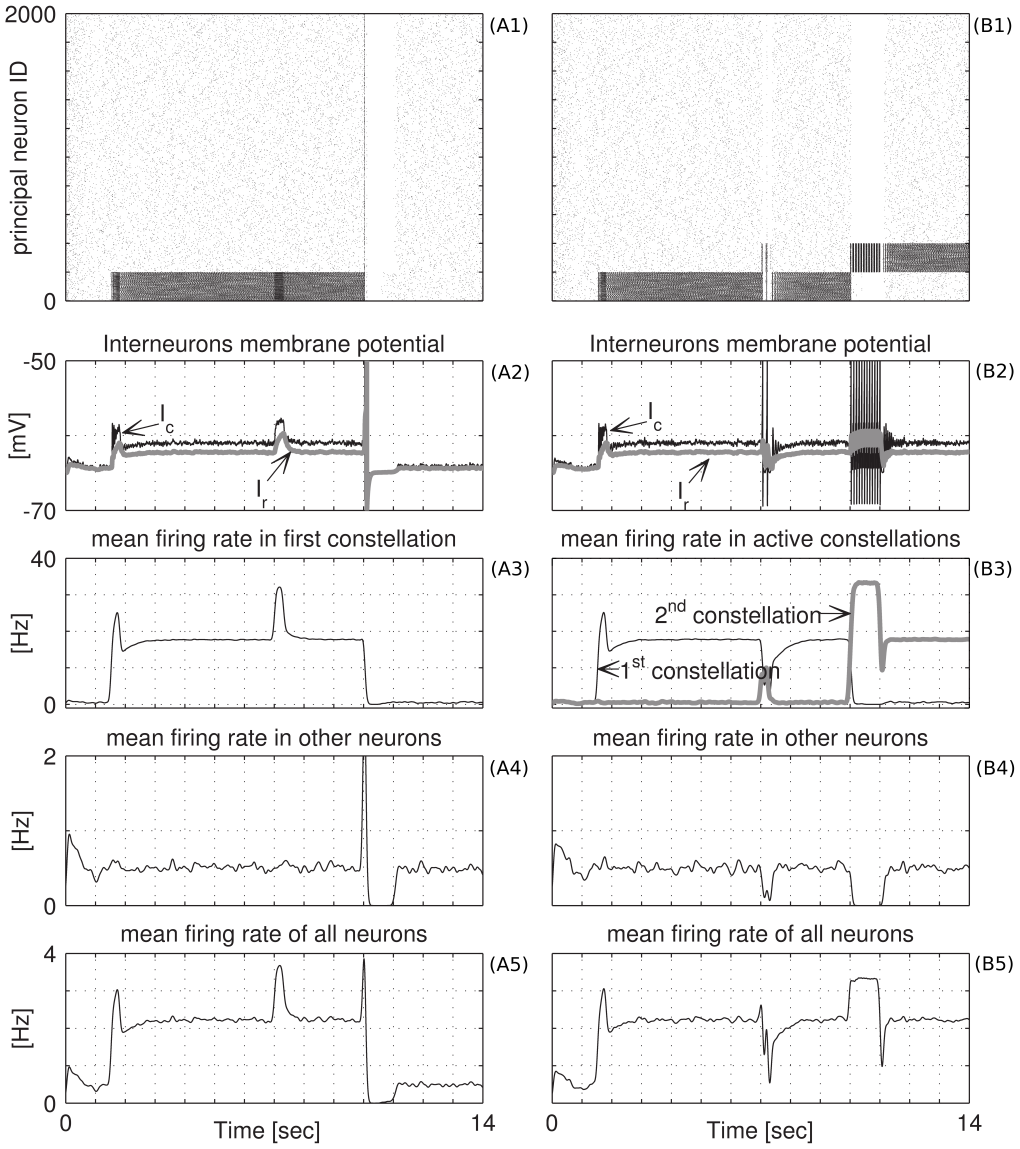

FIGURE 7.4. Working memory dynamics. The network comprises 2000 principal neurons with a connectivity rate of 0.2. (A1 to A5) Delayed match to sample. (B1 to B5) Resistance to distractors. (A1 and B1) raster plot of the principal neuron population. (A2 and B2) Interneurons membrane potential. (A3 and B3) Mean firing rates in active constellations (neurons subjected to external stimulation). (A4 and B4) Mean firing rates in other neurons. (A5 and B5) Mean firing rate in all neurons in the network. Firing rates were calculated using a non causal Gaussian kernel with a time scale of $\sigma = 50\ ms$.

replace the stored information by other (see the last five seconds of simulation in panel B1 of Figure 7.4).

In the first two scenarios the activity is reset by I_r which hyperpolarizes the membrane of all principal neurons for a period of a few hundreds of milliseconds. The nonexistence of APs during this period leads to the deactivation of the CAN current bringing the active neurons to a resting state (there are, nevertheless, stochastic activations during this period).

In the third case, the reset is due to the hyper-excitation of the activity control inhibitory interneuron I_c. In order to replace information, the activity induced to a new constellation must be amplified. Instead of being excited during 300 ms for 100 neurons at firing rates of 20 Hz, these neurons are excited at 120 Hz for a period of 1 second. Notice that the presynaptic neurons responsible for this excitation are the same and thus the synaptic efficacies are the same. The change in the external excitation occurs only at the firing rates and duration levels, but remains at biologically plausible values.

The increase in the network activity is insufficient to activate I_r, but originates continuous spikes of I_c which instead of vanishing all the activity in the network only prevents the activity which is not induced by the outside perceptual/sensory configuration, allowing the new pattern to be stored while interrupting the previous activity pattern.

7.1.3.6. *Model scaling and robustness in parameter space*

As described, to ensure that all principal neurons can equally participate in coding external information, principal neurons need to receive similar synaptic currents form the network. One way to ensure that all principal neurons receive similar synaptic currents is to connect all principal neurons to each other, and considering synapses with the same parameters - a full recurrent connectivity scenario, with identical synapses. However this is biologically implausible. But if the neuronal network population size is sufficiently large, even if the connectivity rate is smaller than one (with all neurons receiving synapses from only fraction of its neighbors), the synaptic input variability can still be controlled and kept within low values. In order to achieve the proper functional behavior of the model (given the presented parameterization) it is required that the sum of all synaptic inputs each principal neuron receives, from neurons in the active constellation, varies between 2.4×10^{-5} and 4.6×10^{-5} μS.

With a total synaptic current below 2.4×10^{-5} μS the model would reset when a distractor arrives. On the other hand, with a total synaptic current above 4.6×10^{-5} μS the activity control interneuron would not be strong enough to prevent the co-activation of both groups of neurons. Both patterns of activity would merge, leading to an over-excitation which finally would result in the activation of the resetting interneuron eliminating all activity in the spiking network. This is a core constraint setting of the memory system performance.

Consider a model with N_P principal neurons, with pattern size M and connectivity rate γ. For simplicity we will assume that $M = 10\%N_P$. It is expected that each principal neuron receives $\gamma \times M$ synapses from neurons in the active constellation and $\gamma \times (N_P - M)$ synapses from neurons firing at low rates. For neurons belonging to the active constellation the correct value is $\gamma \times (M - 1)$, but as M grows this difference becomes irrelevant. Although for small values of N_P the variability introduced with the randomly chosen connections could disrupt the proper behavior of the model, as this number increases, the variability will become less relevant (see Figure 7.5).

Consider $w = \frac{2.4+4.6}{2} \times 10^{-5}$ μS, the mean point of the interval $[2.4 \times 10^{-5}, 4.6 \times 10^{-5}]$. Since $\frac{w-2.4\times10^{-5}}{w} = \frac{4.6\times10^{-5}-w}{w} \approx 0.31$, if the synaptic peak conductance for connections between principal neurons is $\frac{w}{\gamma\times(M-1)}$, to ensure that all neurons in the network will receive a total synaptic current within the acceptable boundaries, we just need choose N_P large enough according to γ (see Fig 7.5).

Therefore, a functional and robust working memory system is possible considering a biophysical realistic number of neurons and connectivity rates.

Besides the synaptic efficacy for connections between principal neurons there is a wide range of parameters that could be considered with different values and yet preserve the model's biological realism. Changes in parameters such as the membrane time constant or the CAN current activation variable time constant would alter significantly the time integration of new signals and resistance of the model to distractors. For example, if there was a reduction by one half of the CAN current activation variable time constant, the storage of new information would be much faster, but on the other hand the amount of time the model could hold the information, when subjected to inhibition, would also decrease. Other changes at the level of ion channels densities could have strong effects in the model

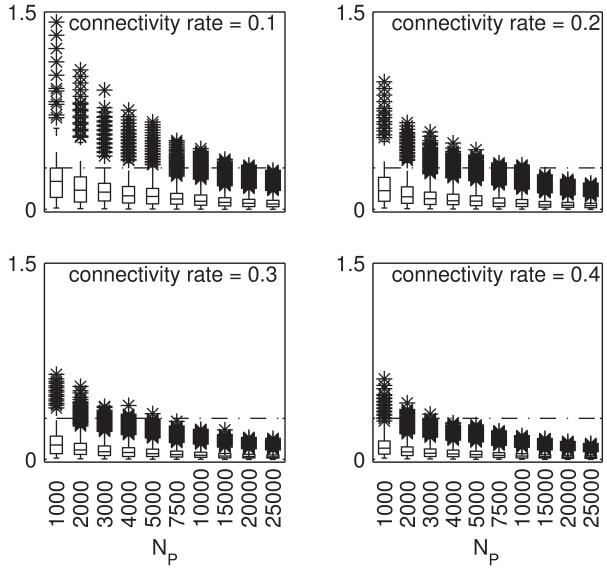

FIGURE 7.5. Larger population sizes produce more robust working memory systems. Each of the box-and-whisker diagrams represents the percentage of variation between the number of active presynaptic principal neurons that each principal neuron receives and its expected value. The four panels correspond to connectivity rates of 0.1, 0.2, 0.3, and 0.4. Each box-and-whisker results from 100 samples in a network where the number of principal neurons varied from 500 to 25000. The dashed line marks the upper limit of variation which allows the model to maintain its proper behavior.

behavior if made in isolation. For example, a significant reduction in CAN current's maximum conductance would eliminate the principal neuron capability of sustaining, alone, its activity for a short period of time. However, if this change is compensated by a proper increase in maximum permeability of calcium current, the single neuron behavior would remain qualitatively equal. We therefore argue, for these cases, that the model is globally stable if one considers that all parameters are regulated by homeostatic mechanisms (Grashow et al., 2010; Prinz et al., 2004).

Another parameter that is critical in some models of short-term or working memory is the type of excitatory synapse considered (AMPA *vs* NMDA) (Durstewitz et al., 2000). In this work, we have considered AMPA synapses, characterized by its fast dynamics (short time constants), but similar results could be achieved if NMDA synapses would have been

used, despite their larger time constants (10 to 20 fold higher) and the magnesium block mechanism which limits the synaptic current in hyperpolarized neurons.

7.1.4. Concluding remarks

In this work the synergy between different membrane currents is used to effectively support the temporary storage of new information after stimuli exposures of a few hundreds of milliseconds. This is accomplished without enforcing bistability at the level of the neuronal dynamics and without synaptic plasticity.

Considering only four ionic currents, we introduced a spiking model that, despite its simplicity, is biologically plausible, matches experimental data and shows that one-shot short-term memories can be achieved in network models without prior learning (strongly connected cell assemblies) or short-term synaptic plasticity. The working memory model presented here is in accordance with well established experimental results. Namely it (i) is capable of storing information in a few hundreds of milliseconds; (ii) is robust to noise; (iii) is resistant to distractor stimuli; (iv) shows match enhancement; and (v) preserves memory content while the information is being used (replayed).

In order to capture the essential biophysical realism and at the same time to be able to perform simulations with a large network in feasible time, in the present work we consider some simplifications: (i) a reduced number (four) of ion currents were considered; (ii) the neuronal morphology was collapsed into single compartment neurons; and (iii) all the inhibition of the model was carried out by two global inhibitory interneurons. These simplifications allowed us to reduce the computational complexity without affecting the general principles of the model.

The calcium and calcium activated currents used in the presented model, and ubiquitous in the nervous system, can be found in other models (Bal and McCormick, 1993; Haj-Dahmane and Andrade, 1999; Klink and Alonso, 1997). In some models they are the basis for the generation of plateau potentials or sustained activity (Fransén et al., 2002; Aguiar et al., 2010; Conde-Sousa and Aguiar, 2013). These currents, in combination with others, are also used to support the existence of bursts or rhythmic behaviors (Traub et al., 1991; McCormick and Huguenard, 1992; Destexhe et al., 1994a; Amini et al., 1999).

Some models explore the use of the combination of calcium and depolarizing calcium activated currents to store information. Koene and colleagues (2007) presented a simplified integrate and fire (I&F) model with two additional currents, one responsible for an after hyperpolarization (mimicking the refractory period) and other responsible for an after depolarization (resembling the effect of an calcium activated depolarizing current). The authors take advantages of the neuronal features to temporarily store a sequence of patterns of activity, but the sustaining activity requires the precise interplay between the neuron properties and the currents resulting from the *theta* and the *gamma* rhythms, without which the activity could not be self-sustained.

Durstewitz (2003) also explores a similar combination of currents in an I&F model. Unlike Koene and colleagues' model, Durstewitz explicitly modeled the intracellular calcium concentration providing the model specific features that allow it to distinguish between short (spurious) excitations and prolonged (consistent) excitations. Despite some similarities with our proposed model, these two models are different in both objectives and underlying mechanisms. The model presented by Durstewitz aims to explain the increase in firing frequency (climbing activity) that some prefrontal cortex neurons exhibit in working memory tasks where it is possible to anticipate the occurrence of a certain event after a delay period. Therefore, this model requires learning that enables neurons to adapt the climbing slope so that the activity peak matches the expected time for the event. In our model we show that the interplay between different ion currents could supports the modulation of the intrinsic excitability of neurons which allows the network to store completely new information in time windows of a few hundreds of milliseconds.

The neuronal model presented here shares the neuronal dynamics with gate interneurons from the model of Conde-Sousa and Aguiar (2013), however both models are different in their goals and network architectures. The model proposed in Conde-Sousa and Aguiar (2013) is focused on storing the order between patterns of neuronal activity within a sequence. To achieve this, the model requires an architecture with rigid constraints providing control of the flow of activations in the network. These constraints are not necessary for the model proposed here, which is focused on storing a single activity pattern instead of order between patterns. However, it is relevant to notice that both models can complement each other in the sense that the present model can provide the memory buffer supporting the mechanism of sequence reactivation.

Acknowledgments

Research funded by the European Regional Development Fund through the programme COMPETE and by the Portuguese Government through the FCT - Fundação para a Ciência e a Tecnologia under the project PEst-C/MAT/UI0144/2011. Eduardo Conde-Sousa was supported by the grant SFRH/BD/65633/2009 from FCT, co-financed by European Social Fund under the program POPH of the National Strategic Reference Framework.

7.2. A Working Memory Model for Serial Order that Stores Information in the Intrinsic Excitability Properties of Neurons

Conde-Sousa E., Aguiar P., Journal of Computational Neuroscience, Volume 35, Issue 2, October 2013, pp 187-199

A working memory model for serial order that stores information in the intrinsic excitability properties of neurons

Eduardo Conde-Sousa[1,2] • **Paulo Aguiar**[1,2]

Abstract

Models for temporary information storage in neuronal populations are dominated by mechanisms directly dependent on synaptic plasticity. There are nevertheless other mechanisms available that are well suited for creating short-term memories. Here we present a model for working memory which relies on the modulation of the intrinsic excitability properties of neurons, instead of synaptic plasticity, to retain novel information for periods of seconds to minutes. We show that it is possible to effectively use this mechanism to store the serial order in a sequence of patterns of activity. For this we introduce a functional class of neurons, named gate interneurons, which can store information in their membrane dynamics and can literally act as gates routing the flow of activations in the principal neurons population. The presented model exhibits properties which are in close agreement with experimental results in working memory. Namely, the recall process plays an important role in stabilizing and prolonging the memory trace. This means that the stored information is correctly maintained as long as it is being used. Moreover, the working memory model is adequate for storing completely new information, in time windows compatible with the notion of "one-shot" learning (hundreds of milliseconds).

Keywords

Working memory • Serial order • Intrinsic excitability modulation • Delay period • Match enhancement • Short-term memory

[1] FCUP – Faculdade de Ciências da Universidade do Porto

[2] CMUP – Centro de Matemática da Universidade do Porto

7.2.1. Introduction

Findings by Eric Kandel, Tim Bliss and Terje Lomo (Bliss and Lomo, 1973; Kandel, 2001), have led to the widely held view that memories are stored as modifications of synaptic strength. Since this outstanding work, many mathematical models have successfully used synaptic plasticity, in various forms, as the basis for mechanisms related to learning, memory and development in neural circuits (Abbott and Nelson, 2000). But synaptic plasticity is not, by far, the only adaptive processes available on the nervous system with the suitable properties for memory formation. Parallel studies have demonstrated information storage based on non-synaptic processes, with the modulation of membrane conductances being one of the most important among them (Mozzachiodi and Byrne, 2010). A combination of experimental and theoretical studies has shown that neurons with complex temporal dynamics can provide short-term memory properties supported only by their intrinsic neuronal mechanisms (Marder et al., 1996). In other words, the modulation of membrane conductances, giving rise to changes in neuronal excitability, can be used to temporarily store information.

The ideas of membrane conductances modulation as a mechanism for information storage have naturally perfused to the mathematical models of working memory (Durstewitz et al., 2000; Fall and Rinzel, 2006; Fransén et al., 2002, 2006). Working memory (WM) is a well-established type of distributed short-term memory (Baddeley, 2003) which, among other things, has the capability of being activated with a single exposure to the information pattern. Specific features associated with the short-term modulation of intrinsic excitability, most notably the time-scales, are in accordance with the requirements of a working memory system. The few theoretical studies addressing this connection analyze a specific set of biologically plausible membrane currents that can act synergistically to prolong excitability states, and focus on the behavior of single neurons or small networks of neurons (Fall and Rinzel, 2006; Fransén et al., 2002, 2006).

Here we present a working memory model which uses modulation of intrinsic neuronal excitability (MINE) for temporarily storing multiple novel activity patterns and the serial order between them. Previous models for sequence learning/recall relied mostly on recurrent networks and required specific synaptic plasticity rules (Botvinick and Plaut, 2006; White et al., 2004). The network architectures have taken advantage of auto-associative recurrent networks (Gibson and Robinson, 1992), networks with transmission delays (Herz

et al., 1991) or modular functional units (Dehaene et al., 1987). Nevertheless, ubiquitous to these networks for sequence learning is the use of synapses to store the information. Our model shows that MINE properties can effectively support the temporary storage of completely new information, on time scales which are compatible with WM. Furthermore, MINE can produce memory formation mechanisms which are simultaneously robust to noise and capable of storing information in exposure time windows of less than 100 milliseconds (compatible with "one-shot" learning). All synapses in our model are static, in the sense that they do not exhibit any form of plasticity.

A key element in the model we propose is the existence of a specific class of excitatory interneurons which we call "gate" interneurons. These gate interneurons are able to store information regarding the patterns of activity, and their order, in their membranes intrinsic excitability. While sharing the use of a calcium activated nonspecific cation current (I_{CAN}) and the absence of synaptic plasticity, the dynamics of the proposed model and the existence of the gate interneurons distinguishes it from previous models capable of one-shot short-term buffering (Lisman and Idiart, 1995; Jensen et al., 1996; Koene and Hasselmo, 2007, 2008).

7.2.2. Material and methods

The dynamics of the neurons were mathematically described using conductance based models following the Hodgkin-Huxley formalism (Hodgkin and Huxley, 1952a), in order to achieve a significant biophysical detail. All simulations were carried out in the NEURON simulation environment (Hines and Carnevale, 1997). The model implementation was written to take advantage of NEURON's capability to run in parallel hardware. A dual quad-core Xeon 5355 (2.66 GHz) workstation with 32 GB RAM was used for the numerical simulations. The model implementation in NEURON is available through ModelDB (Crasto et al., 2007) under accession number 147461.

7.2.2.1. *Single cell models*

Neuronal morphology is not relevant for the WM model we propose here and, as such, point-wise neurons are considered. In terms of NEURON implementation, each neuron is however modeled by a single cylindrical compartment (single segment) with length $L = 20\ \mu m$ and diameter $diam = 20\ \mu m$. The total surface area of the compartment is

1.257 μm^2. This value can be taken into account to convert area dependent quantities to absolute values and vice-versa.

Three classes of neurons are considered: i) principal neurons (P) responsible for receiving and transmitting information to other brain areas; ii) inhibitory interneurons (I) responsible for controlling the network activity level; and iii) excitatory gate interneurons (G) responsible for storing pattern information and pattern order through MINE mechanisms. Together with leakage current and synaptic currents, all neuron classes have two standard ion currents: the transient sodium and the delayed rectifier potassium currents. The gate interneurons have however two additional ion currents: a high threshold calcium current I_{CaL} which is activated by strong membrane potential depolarization, and a nonspecific cation current I_{CAN} which activation increases when the intracellular calcium concentration rises.

The time evolution of the membrane potential is described by the equation:

$$C_m \dot{V} = -I_L - I_{ion} - I_{syn}$$

where $C_m = 1\ \mu F/cm^2$ is the membrane capacitance; V represents the membrane potential; $I_L = g_L \times (V - E_L)$ is the leakage current, g_L is the maximal leak conductance and E_L is the reversal potential for the leakage current; I_{ion} is the sum of all the ionic currents on each neuron; and I_{syn} is the sum of all synaptic currents impinging on the neuron.

For inhibitory interneurons and principal neurons $I_{ion} = I_{Na} + I_{Kdr}$, and for gate interneurons $I_{ion} = I_{Na} + I_{Kdr} + I_{CaL} + I_{CAN}$.

A temperature of 22º C was assumed in all simulations and all the ionic current dynamics were taken from SenseLab (Crasto et al., 2007).

Synaptic current

The synaptic current is modeled as the sum of all input synaptic currents to each neuron. The model uses three different types of synapses: NMDA, AMPA and $GABA_B$. In all types, the synaptic conductance profile is modeled by a dual exponential function with parameters τ_{rise} and τ_{decay} (Table 7.4). In NMDA synapses the conductance is further multiplied by a factor representing the magnesium block (Jahr and Stevens, 1990). From the total NMDA synaptic current impinging on the gate interneurons, a fraction of 10% is

TABLE 7.4. Synaptic reversal potential and conductance profile parameters.

Synapse	$E_X\,[mV]$	$\tau_{rise}\,[ms]$	$\tau_{decay}\,[ms]$
AMPA	0	0.1	5
NMDA	0	5	70
$GABA_B$	-85	10	200

in the form of calcium current (Burnashev et al., 1995) which contributes to modifications in the intracellular calcium concentration.

Inhibition relies on $GABA_B$ synapses with a slow time course in the order of 200 ms, a value in accordance with experimental data (Otis et al., 1993). This slow time course, as soon will become clear, is important to promote competition between individual patterns in the stored sequence: the slow time course ensures that each pattern in the sequence is not erroneously reactivated. The time scale of the of the $GABA_B$ inhibition sets an upper bound for the duration of the entire sequence recall and has a direct impact on the maximum number of patterns which can be stored in a sequence. A value of 200 ms is chosen to enable the storage of sequences with 5 – 6 patterns.

Sodium and potassium currents

The transient sodium I_{Na} and the delayed rectifier potassium I_{kdr} currents are modeled according to the canonical Hodgkin-Huxley kinetics with modifications proposed by Traub and Miles (1991) to model hippocampal pyramidal cells (parameters in Table 7.5).

$$I_{Na} = \overline{g}_{Na} \times m^3 \times h \times (V - E_{Na})$$

$$I_{Kdr} = \overline{g}_{Kdr} \times n^4 \times (V - E_{Kdr})$$

The kinetic equations for gating variables are given by

$$\dot{x} = -\frac{x - x_\infty(V)}{\tau_x(V)}$$

where

$$x_\infty = \frac{\alpha_x}{\alpha_x + \beta_x}$$

and

$$\tau_x = \frac{1}{\alpha_x + \beta_x}$$

for $x \in \{m, n, h\}$. The activation and inactivation gate functions are:

$$\alpha_m = \frac{0.32 \times (13 - (V - V_{traub}))}{\exp\left(\frac{13-(V-V_{traub})}{4}\right) - 1}$$
$$\beta_m = \frac{0.28 \times ((V - V_{traub}) - 40)}{\exp\left(\frac{(V-V_{traub})-40}{5}\right) - 1}$$
$$\alpha_h = 0.128 \times \exp\left(\frac{12 - (V - V_{traub})}{18}\right)$$
$$\beta_h = \frac{4}{1 + \exp\left(\frac{35-(V-V_{traub})}{5}\right)}$$
$$\alpha_n = \frac{0.032 \times (15 - (V - V_{traub}))}{\exp\left(\frac{15-(V-V_{traub})}{5}\right) - 1}$$
$$\beta_n = 0.5 \times \exp\left(\frac{10 - (V - V_{traub})}{40}\right)$$

High-threshold calcium current

The high-threshold calcium current I_{CaL} is modeled according to the equation (McCormick and Huguenard, 1992):

$$I_{CaL} = \overline{p}_{CaL} \times m^2 \times GHK\left(V, cai, cao\right)$$

where $\overline{p}_{CaL}$ is the Ca^{2+} membrane permeability, *cai* and *cao* are, respectively, the intracellular and extracellular calcium concentration, and *GHK* is the Goldman-Hodgkin-Katz equation. The kinetic equation for activation variable is:

$$\dot{m} = -\frac{m - m_\infty\left(V\right)}{\tau_m\left(V\right)}$$

where

$$m_\infty = \frac{1}{1 + \exp\left(\frac{V+10}{-10}\right)}$$

and

$$\tau_m = \frac{1}{\alpha_m + \beta_m}$$
$$\alpha_m = \frac{1.6}{1 + \exp\left(-0.072 \times (V - 5)\right)}$$
$$\beta_m = 0.02 \times \frac{1.31 - V}{1 - \exp\left(\frac{V - 1.31}{5.36}\right)}$$

Calcium dependent nonspecific cation current

The calcium dependent nonspecific cation current I_{CAN} is taken from (Bal and McCormick, 1993) with modifications introduced in (Destexhe et al., 1994a) and is described by the equation:

$$I_{CAN} = \overline{g}_{CAN} \times m^2 \times (V - E_{CAN})$$

For our version of the model we modified the middle point of activation function to $0.5 \times 10^{-3}\ mM$ (parameters in Table 7.5). The introduction of these specific calcium and calcium-dependent currents follows the results from modeling studies that have demonstrated the effectiveness of these currents in producing temporary modulations in neuronal activity (Aguiar et al., 2010; Fall and Rinzel, 2006).

Intracellular calcium dynamics

The intracellular calcium concentration (cai) is modeled taking into account the calcium entry due to current I_{CaL} and NMDA synapses, and a fast removal process which is due to buffering and active pumps (Destexhe et al., 1993). We use $depth = 0.1\ \mu m$, $cai_\tau = 1\ ms$, $cai_\infty = 5 \times 10^{-5}\ mM$.

7.2.2.2. *Network architecture*

The network connectivity plays an important role in the WM model for serial order. The three neuronal populations are connected according to the following architecture: i) inhibitory interneurons establish bidirectional connections with the nearest principal neuron; ii) gate interneurons are arranged in clusters also establishing bidirectional connections with a principal neuron; iii) principal neurons also send long-range connections to gate interneurons outside the local cluster. This architecture configuration places the

TABLE 7.5. Parameters for ion currents. The notation $\bar{g}_X$ refers to the maximal conductance of current X, whereas E_X refers to the reversal potential and $\overline{p}_{CaL}$ is the calcium membrane permeability. The reversal potential for calcium is calculated according to the Goldman-Hodgkin-Katz (GHK) equation, since the intracellular calcium concentration (cai) is not constant.

Ion Current	Parameters	Principal Neurons	Inhibitory Interneurons	Gate Interneurons
I_L	$E_L\,[mV]$	-65	-65	-65
	$g_L\,[mS/cm^2]$	4.5×10^{-2}	4.5×10^{-2}	3.9×10^{-2}
I_{Na}	$E_{Na}\,[mV]$	50	50	50
	$\overline{g}_{Na}\,[mS/cm^2]$	100	80	80
	$V_{traub}\,[mV]$	-50	-50	-60
I_{Kdr}	$E_{Kdr}\,[mV]$	-70	-70	-70
	$\overline{g}_{Kdr}\,[mS/cm^2]$	20	20	20
	$V_{traub}\,[mV]$	-50	-50	-60
I_{CaL}	$E_{Ca}\,[mV]$	—	—	GHK
	$\overline{p}_{Ca}\,[cm/s]$	—	—	3×10^{-5}
I_{CAN}	$E_{CAN}\,[mV]$	—	—	0
	$\overline{g}_{CAN}\,[mS/cm^2]$	—	—	0.01

gate interneurons in a pivotal position regarding the flow of information in the principal population. An example of a small network with 3 principal neurons is shown in Figure 7.6A, and a schematic representation of the network architecture is presented in Figure 7.6B.

The synaptic peak conductances (efficacies) for each type of connection in the network are summarized in Table 7.6. Some synaptic efficacies have to be scaled according to the

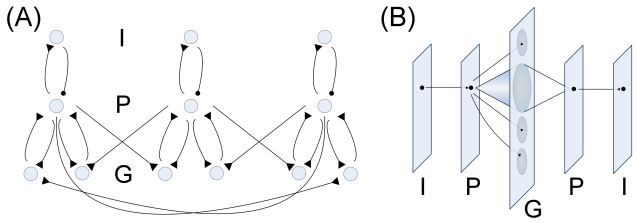

FIGURE 7.6. Network architecture. (A) Model consisting of 3 principal neurons (center), defining 3 clusters with one inhibitory interneuron (top) attached to each principal neuron, and 6 gate interneurons divided in groups of two (bottom). (B) Schematic feed-forward representation of the topographic connections between each population: each interneuron connects to a principal neuron which in turn establish a large number of local connections with the gates local cluster and, in addition, sends isolated long-range connections to gates outside the local cluster; each gates cluster sends convergent connections back to the principal neuron which closes the circuit with the local interneuron. Notice that in the schematic representation, the two P layers correspond to the same population P (the same for the I layers).

pattern size, more precisely to the expected number of active gates associated with each principal neuron. In excitatory synapses with both NMDA and AMPA receptors, the relative contribution of both synaptic currents is subject to the following constraint: at $-72\ mV$ the postsynaptic response amplitude of both AMPA and NMDA currents is the same (Alonso et al., 1990). To introduce variability in the synapses, each individual synaptic peak conductance is drawn from a uniform distribution with mean value taken from Table 7.6 and with a variability of $\pm 2.5\%$. The synaptic peak conductances of the connections from gate interneurons to principal neurons are normalized according to the network size. The normalization factor K reflects the expected number of active gate interneurons connected to each principal neuron. The synaptic conduction delays for all synapses are fixed at 1 ms.

7.2.3. Results

For clarity purposes, the results are separated into topics. First the intrinsic properties of the gate interneurons are presented together with their role in the working memory

TABLE 7.6. Synaptic mean peak conductances, in μS, between the three population classes in the network. G^{in} represents the gate interneurons inside the principal neuron cluster, while G^{out} represents the gate interneurons outside the cluster. The presented excitatory synaptic peak conductances results from the combined sum of NMDA and AMPA conductances. The AMPA peak conductance corresponds to a fraction of 0.16 of the total conductances and the NMDA peak conductance to the remaining fraction of 0.84, in accordance to Alonso et al. (1990) (see text).

		postsynaptic neuron			
		I	P	G^{in}	G^{out}
presynaptic neuron	I	—	1.2×10^{-3}	—	—
	P	1.5×10^{-3}	—	1.3×10^{-4}	5.0×10^{-4}
	G	—	$1.1 \times 10^{-3} \times K$	—	—

model. Secondly the network behavior is addressed, where the emergence of the working memory system is analyzed. Constraints regarding the required properties for efficient storage and recall are also discussed, followed by information on the robustness of the qualitative behavior of the model to changes in parameter space. Finally, issues regarding scaling are addressed and a modified version of the short-term memory model for serial order, with less storage capacity but better scaling properties, is presented.

7.2.3.1. *Gate interneuron firing properties*

Calcium activated nonspecific cation (CAN) currents play an important role in the dynamics of neurons in the prefrontal cortex and in the entorhinal cortex (Bal and McCormick, 1993; Haj-Dahmane and Andrade, 1999; Klink and Alonso, 1997), two regions involved in working memory and sequence learning mechanisms (Baddeley, 2003; Hahn et al., 2012; Suh et al., 2011). In our model, the presence of calcium dependent cation current with slow dynamics allows gate interneurons to have quantitatively different responses to currents of different duration. When the neuron is at its resting potential for a long period, the CAN current is negligible. With the first action potential (AP), elicited by an external current, there is an inward current of calcium due to I_{CaL}, increasing the intracellular calcium concentration (cai). This leads to a partial activation of the CAN

current which in turn originates a subthreshold afterdepolarization (ADP). If the external current leads to more than one spike at a firing rate above 11 Hz, the interspike interval is smaller than the recovery time of the I_{CAN} activation variable ($m_{I_{CAN}}$). This implies that at the end of each spike, the variable $m_{I_{CAN}}$ is higher than it was at the end of the previous spike. If the number of spikes caused by the external current is small, the CAN current will be only partially activated leading to a small membrane depolarization (see Figure 7.7A1, B1 and Figure 7.8A2). However, if there is a sufficient number of spikes in a short period of time (if $m_{I_{CAN}}$ goes beyond 0.71), the activation of the CAN current will generate a depolarization capable of reactivating the sodium current leading to a new AP, and starting the cycle again. This mechanism is transiently maintained without the need for an external current (Figure 7.7A2, B2). This dynamics can be further assessed in phase space. The generation of an action potential is associated with a cycle in the membrane potential (sodium activation followed by sodium inactivation and potassium activation) and a rise in intracellular calcium concentration (cai). As a result of the combined effect of these factors there is an increase in I_{CAN} activation. The trajectories in phase space have three main regions (Figure 7.7B1, B2): i) an initial stage with current injection where each spike produces a cycle in membrane potential and in cai, followed by a progressive increase in the I_{CAN} activation variable; ii) if the stimulation is sufficient (Figure 7.7A2, B2) the synergistic action of the membrane currents is able to sustain membrane activity in the absence of external stimulation for a period of a few seconds; iii) the last region reflects the loss of stability which results from the progressive deactivation of I_{CAN}.

It is important to notice that this is not cellular bistability: the period of self-sustained spiking is finite and the neuron inevitably, and spontaneously, converges to the resting state in the absence of additional stimulation. This behavior is instead associated with the generation of plateau potentials and may be seen as a transiently stable depolarized state.

The partial activation of the CAN current produced by short stimulations produces an additional behavior: the amplitude of the external current needed to prolong the generation of a sequence of APs is smaller than the amplitude needed to generate the initial APs. This happens because after each new AP, the accumulating CAN current depolarizes the membrane and less external current is required for reaching threshold. So if

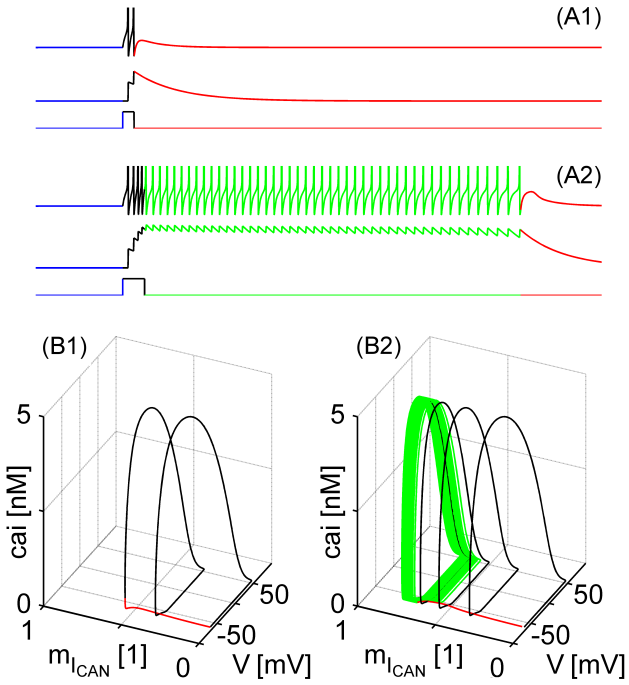

FIGURE 7.7. Phase space analysis. A current of 4 pA is injected into a gate interneuron for two different durations: (A1 and B1) 130 ms and (A2 and B2) 250 ms. On panels A1 and A2 the three traces are (from top to bottom): membrane potential, CAN current and injected current. Action potentials are truncated at -45 mV. Panels B1 and B2 show 3D phase plots corresponding to the two different current injections. The 3D phase plots show the evolution of the variables for membrane potential, CAN current activation variable and intracellular calcium concentration. If enough stimulation is provided (A2 and B2) the synergistic action of the membrane currents is able to sustain membrane activity in the absence of external stimulation, for a period of roughly 4 s.

two currents are introduced sequentially into the neuron, it is possible for the second to be weaker than the first in order to give rise to prolonged activity of elicited APs (Figure 7.8). On the other hand, if the same two currents are injected on the reverse order, the first (smaller) current only weakly depolarizes the membrane, leading to negligible activation of the CAN current, providing almost no contribution to the membrane responses upon the arrival of the second current. This asymmetry plays an important role in our model for serial order since a neuron with this property can respond differently to whether the weak

stimulation arrives first or not. Consider two currents of 250 ms duration and amplitudes of 1 pA (representing weak synaptic connections) and 3 pA (representing strong synaptic connections). In panels A2 and B2 of Figure 7.7 it can be seen that if these two currents impinge on neuron at the same time (4 pA current injection for 250 ms) the neuron undergoes a state transition that allows it to sustain the activity for roughly 4 seconds without the aid of any external current. On the other hand, if these two signals impinge on the neuron sequentially, two qualitatively different responses are produced. If the weaker current arrives first (Figure 7.8, top panels), during the corresponding excitation period the membrane only depolarizes slightly which leads to negligible entrance of calcium which in turn leads to negligible activation of the CAN current. Therefore, when the stronger current arrives, a reduced number of APs are elicited and the neuron is unable to sustain the activity after the end of the excitation. However, if the signals arrive in the reverse order (Figure 7.8, bottom panels), a different response takes place. With the strongest current first, the neuron fires 3 APs which is not enough to sustain the activity by itself. However, the CAN current is partially activated and causes a depolarization close to the threshold level. When the second (weaker) current arrive, with the help of depolarization induced by the CAN current, a few more APs are elicited allowing the neuron to sustain the activity for some seconds after the end of the external excitation.

7.2.3.2. *Network model*

With the asymmetry property previously described it is possible for the gate interneurons to encode a sequence without requiring any synaptic efficacy change over time and trials. Consider a small circuit with direct connections between two principal neurons A and B. A key element in this model is to replace these direct connections with gate interneurons, with their ability to self-sustain activity, as mediators in the connections between principal neurons (Figure 7.9). With the appropriate network architecture, it is possible to differentiate between AB serial activation and BA serial activation. If during a learning phase neuron A is activated followed by neuron B, only gate interneuron AB will be excited to the level of self-sustaining its activity for some seconds. It is important to notice that this framework can be extended to the case where A and B represent not independent isolated neurons but rather synchronous ensembles of neurons.

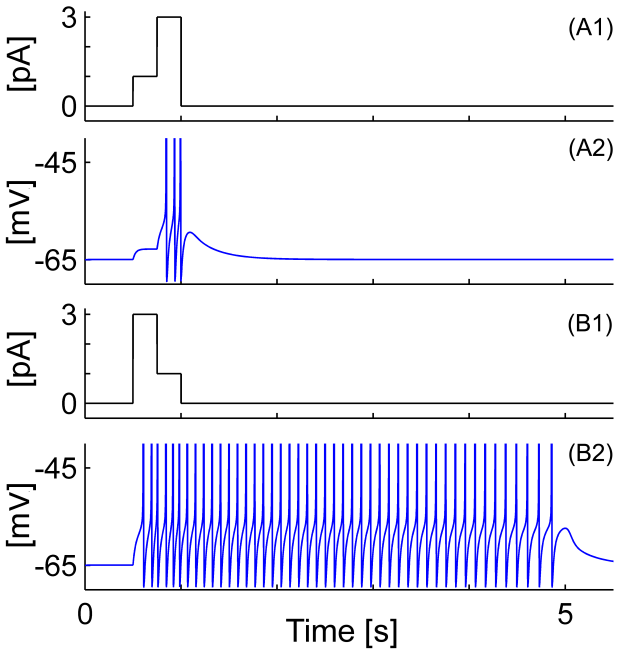

FIGURE 7.8. Relevance of the input stimuli order for the temporary storage mechanism. Two currents with 250 ms duration are injected sequentially into the neuron, one of 1 pA and another of 3 pA. Depending on the order of the injected currents (A1, B1), the neuron responds very differently (A2, B2 respectively). Action potentials are truncated at -40 mV.

These properties of the model are first explored for a small scale network consisting of 3 independent principal neurons, 3 inhibitory interneurons and 6 gate interneurons, as illustrated in Figure 7.6A. Synapses are static and described by the parameters presented in Tables 7.4 and 7.6. The simulation protocol mimics an external stimulation where two of the principal neurons are activated sequentially (P_1 and P_2), leaving the remaining principal neuron without external stimulation. The behavior of the network model is shown in Figure 7.10.

An external stimulus, originated from another brain region, generates four APs at a firing rate of 17 Hz in neuron P_1. After the end of the excitation period of P_1, and with a delay close to 60 ms, P_2 is subject to a similar external stimulation. The sequence of firing $P_1 \rightarrow P_2$ changes the activity state of specific gate interneurons. The interneuron responsible for coding the sequence $P_1 \rightarrow P_2$ (G_{12}) receives a strong synaptic current from P_1 and after the end of this current a weaker current from P_2 arrives, leading to a consistent excitation and consequently to a self-sustained activity for a period of a few

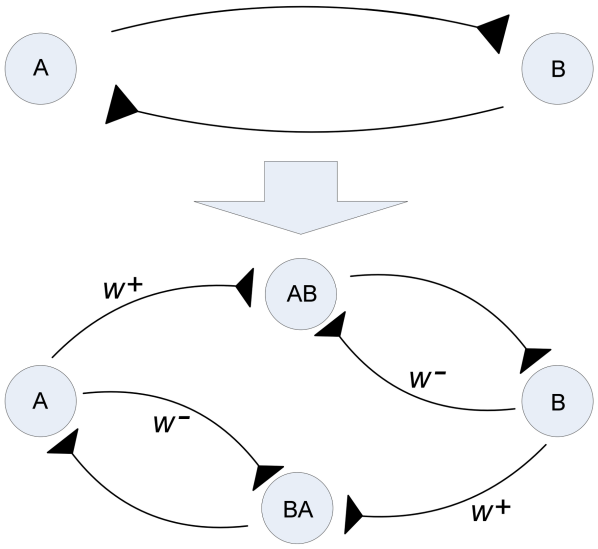

FIGURE 7.9. By allowing gate interneurons (AB and BA) to mediate the connections between principal neurons (A and B) it becomes possible, without any temporal modification in the synaptic efficacies, to store the serial order in the activation of the principal neurons. All synapses are static: strong synapses are represented by w^+ and weak synapses by w^-.

seconds. On the other hand, the gate interneuron responsible for coding the sequence $P_2 \rightarrow P_1$ (G_{21}) receives the same two currents but in reverse order, so it only fires a small amount of times which is not sufficient to sustain the activity after the excitation period. Both gate interneurons coding $P_1 \rightarrow P_3$ (G_{13}) and $P_2 \rightarrow P_3$ (G_{23}) receive only the strong current, generate only two APs and are not able to retain the activity.

After the storage period, which in the above mentioned example lasted approximately 400 ms in total, the gate interneurons retain the information with a firing rate close to 12 Hz for a delay period which can be in the order of seconds. The recall process is initiated after reactivation of P_1. When P_1 is reactivated, G_{12} shows a match enhancement and its firing rate rises to more than 20 Hz producing a selective excitation to P_2 which leads to its depolarization and consequently to the generation of a small number of APs (the number depends on the activation of the inhibitory interneuron I_2 which inhibits P_2).

When larger networks are considered, each element in the memory sequence is no longer represented by a single neuron but instead by a group of neurons firing at the same time (not necessarily synchronized – a jitter on the order of tens of milliseconds is allowed). Every pattern in the sequence is composed by the same number of principal

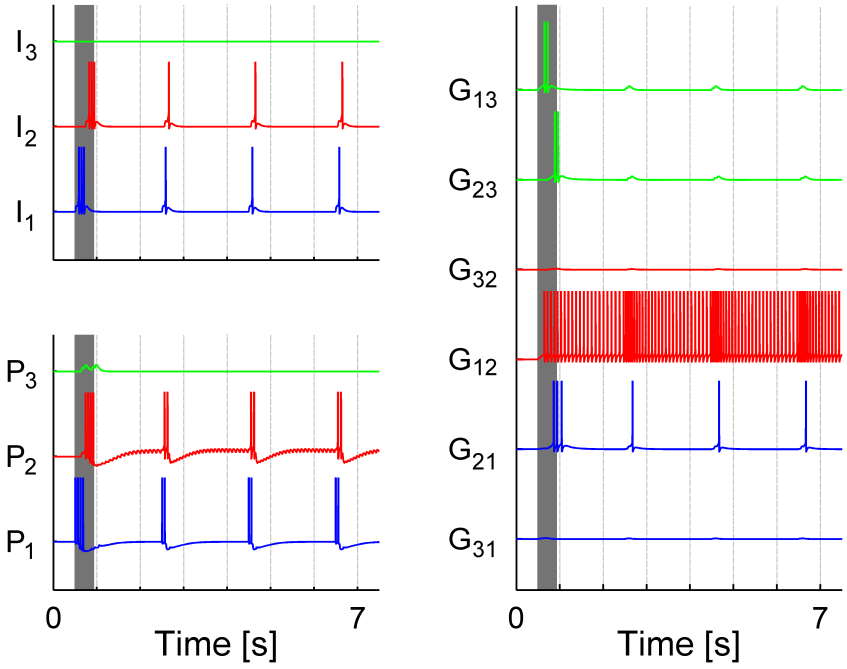

FIGURE 7.10. Working memory in a small network. In this example, the sequence $P_1 \rightarrow P_2$ is stored. The sequential activation of the principal neurons P_1 and P_2 excite consistently the gate interneuron responsible for coding the sequence $P_1 \rightarrow P_2$ (G_{12}), while exciting less the gate interneurons coding sequences $P_2 \rightarrow P_1$, $P_2 \rightarrow P_3$ and $P_1 \rightarrow P_3$. The storage interval is marked with a shaded bar. Only gate interneuron G_{12} self-sustains the activity during a delay period. After the storage period, every time P_1 fires there is a match enhancement in G_{12} leading to the activation of P_2.

neurons and the synaptic efficacies do not depend on the number of patterns, but rather on each pattern size. The model can consequently store sequences with different number of patterns, from one trial to the next, without any parameter change. Recall that this model does not have synapses linking principal neurons to each other: principal neuron P_i projects to principal neuron P_j if there is a gate interneuron encoding the sequence $i \rightarrow j$. It is worth mentioning that a recurrent network in the principal neurons population would further facilitate intra-pattern associations, but it is not required for the proper functional behavior of the model.

In larger networks it is not necessary to have an individual gate interneuron for each ordered pair of principal neurons. In this situation, principal neurons randomly establish

long-range connections with gate interneurons outside the local cluster according to a predefined fraction – named gate sampling fraction (γ). This fraction can be below 1.0 and represents the probability that, given an ordered pair of principal neurons, there is a gate interneuron establishing the connection between them. It is important to acknowledge that gate interneurons literally act as activity dependent gates routing the flow of activations in the principal neurons population.

Consider now a network with 100 principal neurons, with a high connectivity level at the gate interneurons (reflected in the gate sampling fraction $\gamma = 0.95$), leading to a total number of neurons close to $10,000$. These values are chosen to be well-matched with the properties of cortical columns. The number of neurons in a cortical minicolumn is in the order of 100 with an extremely high connectivity level (Buxhoeveden and Casanova, 2002); hypercolumns aggregate several minicolumns (again in the order of 100) to form another modular structure. Collectively, the highly connected hypercolumns combine on the order of $10,000$ neurons. We hypothesize that our working memory model for serial order is appropriate at this scale, where each principal neurons can be connected with a group of neighbor excitatory interneurons (in the order of 100) — the gate interneurons cluster — establishing the proposed network structure supporting one-shot short-term information storage. It is important to recall, that in our model, each principal neuron can represent a small ensemble of synchronized principal neurons. In terms of cortical columns this means that a principal neuron in the model may represent a small group of synchronized pyramidal cells.

To assess the performance of the model, a sequence of 5 activity patterns is stored in this network with 100 principal units, each pattern being represented by 17 P neurons. Evoked activity is induced in the neuronal sub-populations engaged in encoding the serial memory through generation of 4 spikes at a frequency of 17 Hz. Each sub-population is sequentially activated with a delay of 60 ms (measured between the end of one pattern and the beginning of the next). A jitter taken from a uniform distribution with 20 ms range is further added to the onset of the evoked activity in each neuron. Neurons that did not participate in the memory storage were subject to spontaneous stochastic activity with an average firing rate of 0.3 Hz. The results are shown in Figure 7.11.

A very interesting property that emerges at the network level is that the stored information is stable while it is being used: every reactivation of the sequence helps stabilizing

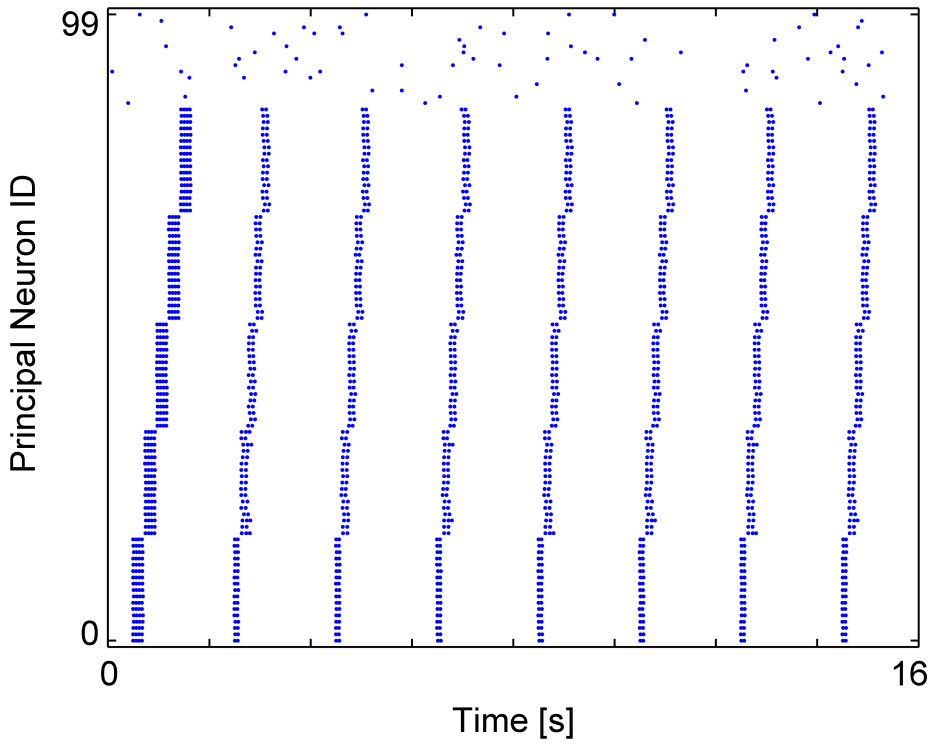

FIGURE 7.11. Working memory for serial order. In the storage phase the network stores the sequence of activity patterns in the gate interneurons, after a single exposure to the stimuli. In the recall phase, after activation of the first activity pattern, the network is capable of activating the remaining patterns in the appropriate order. Storage is accomplished exclusively through the modulation of intrinsic membrane excitability properties.

the gate interneurons activity; but if the stored information is not used (recalled) for a period of more than a few seconds the gate interneurons become silent and reset.

Simulations show that the model can store and recall successfully sequences with up to 6 patterns. If a seventh pattern is inserted, the recall process is corrupted: each pattern retains its individuality but the information of order is partially lost.

7.2.3.3. *Model's time constraints*

Temporal features are crucial elements on this model and it is important to quantify the robustness of the dynamics to the properties of the time windows associated with storage and recall. Important aspects include the amount of time needed to store a sequence of patterns, the time interval between the storage of one pattern and the next

one, the total amount of time during which the model can hold the information (if it is not being actively used), and mainly, the time required for the model to reset the information when it is not needed anymore. These points are now addressed.

Given the parameterization of the model, to activate the gate interneurons responsible for the inter-pattern codification is necessary that the principal neurons fire four spikes at firing rates between 16 and 20 Hz and the neurons in the next pattern fire another four spikes in the same frequency range. If the interval between the last spike in one constellation and the first spike in the next is too short, gate interneurons assume that all the neurons belong to one unique pattern and the sequence will be lost. On the other hand, if the interval between the last spike in one constellation and the first spike in the next is too long, when the weaker current arrives to the gate interneurons it is no longer able to elicit the remaining APs required for the activation to be considered as consistent. Depending on the firing rate of the activation, the storage of each pattern in the sequence takes roughly between 150 and 190 ms, while the interval between two consecutive patterns is within 40 and 100 ms.

In order to determine the holding time and resetting time, some tests were performed. The first test involves the storage of a sequence of three constellations, constellation 1 consisting of neurons P_0 to P_4, constellation 2 consisting of neurons P_5 to P_9, and constellation 3 consisting of neurons P_{10} to P_{14}. After the storage period, the reactivations of the first pattern were delayed from one trial to the next in 0.5 seconds. The first reactivation occurs after 2 seconds of the storage, the second reactivation after 2.5 seconds of the first and so on. It is possible to notice that the system can sustain the activity by itself for a period above 4.5 seconds (Figure 7.12A). In terms of resetting time, the system must remain unstimulated for a period close to six seconds before it completely forgets the previous information and be ready to store a new sequence (Figure 7.12B).

The six seconds interval reflects the time needed to naturally destabilize the gates self-sustained activity and deactivate the currents involved in the intrinsic excitability modulation. This interval can nevertheless be shortened if the action of inhibitory synapses is considered. The self-sustained activity can be interrupted with strong inhibitory synapses (or with the combined action of synapses with smaller conductances). These synapses have been modeled by alpha functions with 10 ms time constant, 2×10^{-2} μS peak conductance, and reversal potential of -75 mV (Figure 7.12C, D). So,

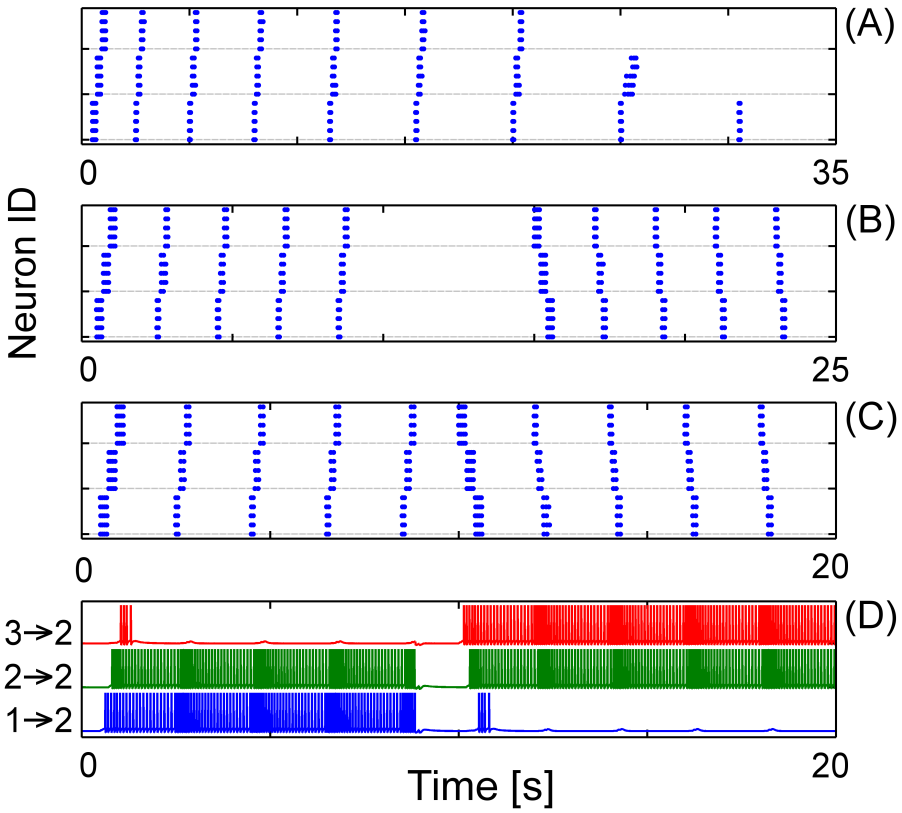

FIGURE 7.12. Storage and recall temporal constraints. (A) The system is able to retain the information up to the point where the reactivation interval becomes larger than 4.5 s. (B) Roughly 6 s are required to reset the system and allow it to store a different sequence. (C) If inhibitory synapses block the activity in all gate interneurons, the system can reset in less time. (D) The activity on the gate interneurons encodes the serial order information. Here is shown the membrane potential of three gate interneurons belonging to the cluster of principal neuron #6 (part of the 2^{nd} pattern): the sequential activation of neurons in pattern 1 and in pattern 2 ($1 \rightarrow 2$); the co-activation of two neurons in pattern 2 ($2 \rightarrow 2$); and the sequential activation of neurons in pattern 3 and in pattern 2 ($3 \rightarrow 2$).

in the presence of inhibitory control, after roughly one second, the system can be reset and allowed to store completely new sequences. In the example shown in Figure 7.12, a new sequence was constructed by reactivating the same patterns by the reverse order. However, any other sequence of patterns would be possible, even sequences comprising a

different number of patterns, or sequences where each individual pattern was formed by neurons that in the previous sequence belonged to different patterns.

Notice that the magnitude of the inhibition required for the model's reset is not too small (which would render the storage unreliable) nor too big (requiring very strong inhibition, for very long time to reset the system). This balance in the inhibition magnitude is not always present in other models where, in some cases, strong and long-lasting inhibition is necessary to reset the system (see for example Fransén et al. 2002).

7.2.3.4. *Robustness in parameter space*

Globally the dynamics of the full model are stable to small changes in the parameters. As expected, the parameters capturing the highest variability in the main features of the model are the ones associated with the CAN current. Changing the time constant and/or the kinetics of the CAN current produces modifications in the total time that gate interneurons are able to self-sustain activity. However it should be pointed that the gate interneurons electrophysiological model, despite its simplicity in the number of currents, is rich in compensatory mechanisms. Larger changes in the CAN current can be compensated, for example, with changes in the CaL current. We therefore argue that, while larger changes in isolated parameters can severely affect the performance of the model, if these changes are counteracted by other modifications under the assumption of regulatory homeostatic mechanisms (Grashow et al., 2010; Prinz et al., 2004), the model is robust at maintaining the same qualitative results. In other words, the parameter space of this model contains large regions capable of producing the same qualitative results. For example, the same qualitative results are obtained after an increase of 100% in $\overline{g}_{CAN}$ if this change is compensated with a combined decrease of 38% in $\overline{p}_{CaL}$ and 4.5% in g_L.

7.2.3.5. *Model scaling*

The size of this model (total number of neurons) grows quadratically with the size of the principal neurons population. Let N_P be the size of the population P and N_G the number of gate interneurons in each local cluster. If γ is the gate sampling fraction, each cluster contains $\gamma\,(N_P - 1) = N_G$ gate interneurons, and the total size of the model is $N_P \times (2 + N_G) = \gamma N_P^2 + (2 - \gamma)\,N_P$. For large P populations and high gate sampling fractions there is therefore a large discrepancy between the sizes of P population and G population. To ensure a small difference between the orders of magnitude of P and G

population sizes, while preserving high gate sampling fractions, the size of the principal population should fall within the scale of a couple hundred independent units. This is the scale compatible with cortical columns.

When the P population size is large, it is possible to reduce the gate sampling fraction. This reduction, while retaining a stable memory system behavior, can be attained as long as the following bounds are held: the input current to each principal neuron provided by the available gate interneurons must be i) strong enough to make sure the expected evoked responses are produced and ii) weak enough to avoid spurious activations. Given these bounds it is possible to assess, for a specific principal population size, the minimal number of gate interneurons per local cluster to ensure the proper functional behavior of the memory system. In other words, what is the minimal gate sampling fraction that guarantees correct storage/recall. Gate sampling connections are assumed to be purely random (i.e. no topographic connections).

Consider the principal neuron P_i, which is engaged in one of the sequence patterns (other than the first). If there are N_G gate interneurons projecting to P_i, after the storage period, only some will be active: the ones encoding the activity pattern where P_i is engaged and the ones encoding the activity of the previous pattern in the sequence. In total, if each pattern is composed of M neurons, there are $2 \times M - 1$ active gate interneurons projecting synapses to P_i, if the gates sampling fraction is 1. Each of these gate interneurons are firing continuously at a rate of about 12 Hz, except during the period in which the pattern is reactivated, where the rates exceed 20 Hz. So, in order to avoid that P_i reactivates due to its gate interneurons inputs (as they fire at 12 Hz), but force P_i to reactivate when its gate interneurons increase their firing rates (slightly above 20 Hz), the sum of all synaptic inputs arriving on a short time window (membrane's time constant) must be within a controlled interval. For our model parameters, this interval is between to 1.02×10^{-3} and $1.22 \times 10^{-3} \mu S$. This is the core constrain setting the memory system performance and capacity. Fixing the pattern size M in the beginning, the number of gate interneurons engaged in encoding the patterns sequence follows the hypergeometric distribution

$$X \equiv \text{HyperGeometric}(N_P - 1; 2 \times M - 1; N_G)$$

with mean value

$$E[X] = \frac{(2 \times M - 1) \times N_G}{N_P - 1}.$$

Therefore, to obtain a functional and robust working memory system, the synaptic strengths between gate interneurons and principal neurons must be weighted by $E[X]$ in order to obtain a total synaptic input that falls within the pre-established interval. For $\gamma < 1$, and as a result of the random connectivity, there is some variability in the number of input each principal neuron receives from active gate interneurons. While in larger P populations these fluctuations are less relevant, for the scale at which this model is intended, cortical columns, where the number of independent principal units is on the order of 100 – the gate sampling fraction should be above 0.9. This is accordance with cortical columns size and connectivity (Buxhoeveden and Casanova, 2002). This working memory model for serial order does not scale well for larger numbers of independent principal units because the network architecture is prepared to store every possible pattern (with a fixed number of active units). This provides high flexibility in encoding novel information, but leads to a high discrepancy between the sizes of P and G populations when the size of the former grows beyond a couple hundred independent units. There is consequently a balance between the flexibility to store more information (encoded in the complexity of the individual patterns of activity) and the discrepancy between the sizes of P and G populations.

The gate interneurons framework can nevertheless be extended to large networks, with better scaling properties, if the ability to encode novel information is reduced.

7.2.3.6. *Modified model with linear scaling properties*

A linear relation between total principal neurons and gate interneurons can be attained in a slightly modified architecture, but also relying on our gate interneurons hypothesis to create a short-term memory system capable of storing order. This modified architecture is less powerful in encoding information, but is adequate to larger principal populations where each independent principal unit is associated with a small number of excitatory interneurons (the gate interneurons cluster).

Consider, as before, a population of principal neurons P connected with a population of gate interneurons G, but where each gate interneuron cluster is composed by a small number n of gates, independent of the size of population P. On the limit, n can be

1. Each gate interneuron receives C^c long-range random connections from the principal population ($C^c \gg 1$), and establishes a connection with the local principal neuron. An external population controls directly the activity on the gate interneurons. As before, synaptic efficacies are parameterized so that activity can only be transferred between two principal neurons through a gate interneuron if that gate interneuron is activated.

Depending on the specific pattern of activity temporarily stored in the gate interneurons population, completely different sequences of activations will be formed in the principal population. The gate interneurons population is therefore used to temporarily store routing information, and drive different sequences of activations on the principal population. Different constellations of active gates mean different sequences. In Figure 7.13 we present the results of a simulation with 20 P neurons and 20 G neurons. This routing model only differs from the previous WM model for serial order in the above mentioned modifications in the connections with the gate interneuron cluster, and in the fact that the information is stored directly on the G population (as opposed as in the P population in the WM model). In this modified architecture, the positive feed-back which may lead to increasing levels of activity is solved with an inhibitory activity level control mechanism. While not part of this modified model, complementary plastic mechanisms can be used to modify the connections of the network, selecting and shaping the activation sequences in the P population which are associated with specific active constellations in the G population.

7.2.4. Final remarks

We have shown that the modulation of the intrinsic excitability properties of neurons can be effectively used for producing short-term memory systems capable of storing sequences of patterns. The membrane dynamics in our neuronal models are biologically plausible and use a reduced number of currents (two in the principal and inhibitory interneurons, four in the gate interneurons population).

Importantly, cells fitting the properties required by our gate interneurons hypothesis can be found in areas related with working memory. This is the case of spiny stellate cells which are excitatory interneurons involved in recurrent excitation in neocortical circuits (Feldmeyer et al., 1999; Thomson et al., 2002). The features of the network architecture assumed in this model are thus attuned with what can be found in cortical networks.

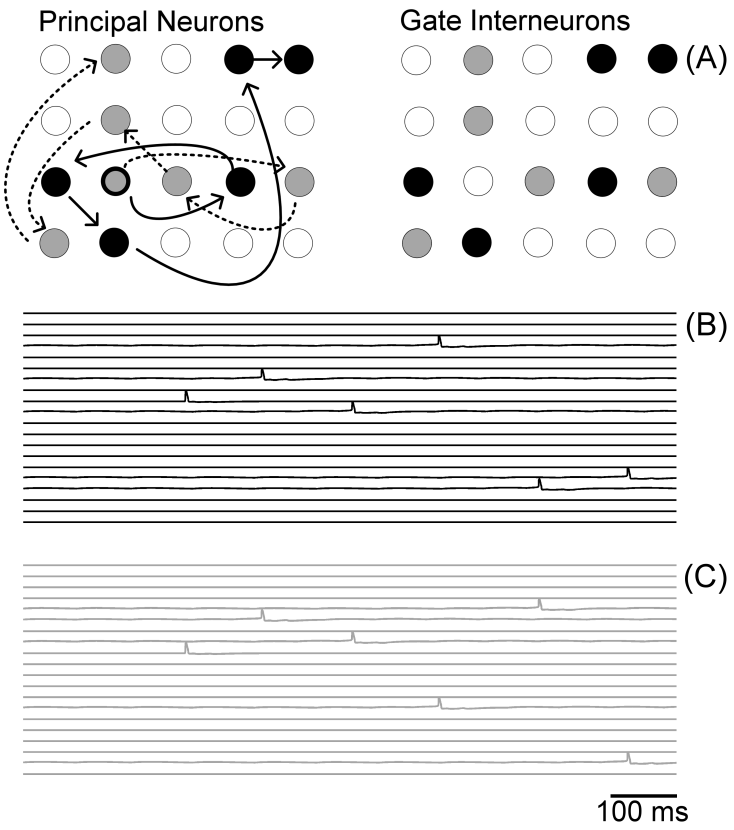

FIGURE 7.13. Gate interneurons can temporarily store different sequences of activations in the principal population. (A) Activation of the same principal neuron (#12, middle line second column) leads to different activation sequences (*black* or *gray*) depending on the constellation of gate interneurons that are presently active (*black* or *gray*, respectively). (B, C) Membrane potential of the P population neurons driven by the two different patterns of activity temporarily stored in the G population (*black*, *gray*). The first neuron in both sequences (neuron #12) is externally activated.

Moreover it is worth mentioning that gate-like excitatory interneurons can also be found in the hippocampal formation, a structure which is similarly involved in sequence learning and short-term memory mechanisms (Suh et al., 2011): bi-directional connectivity between principal neurons and excitatory interneurons are reported between granule cells and mossy cells in the dentate gyrus (Jackson and Scharfman, 1996). The existence of synergistic currents capable of prolonging self-sustained activity in these excitatory interneurons (e.g. CAN and CaL currents) remains however a hypothesis of our model (but see Nagy et al. 2013).

Our working memory model capable of storing sequences has important properties that are in agreement with known features of short-term memory for serial order. First, information can be stored upon a single exposure to the stimuli (stimulation period of hundreds of milliseconds), compatible with the notion of one-shot memory. Second, information can be retained for periods of many seconds and finally, memory reactivation/usage extends memory retention. The fact that gate interneurons are not bistable has important consequences, namely gate activity can be reset with short-duration inhibitory currents with biophysically reasonable amplitudes. The capability of our model to encode temporal sequences in the background activity of gate interneurons after a short (transient) exposure to the stimuli, is in agreement with recent results regarding memory retention in brain tissue in vitro (Hyde and Strowbridge, 2012).

A key element in our model is to establish a pathway between principal neurons which is mediated not by synapses but by a specific class of neurons – the gate interneurons – with the ability to control the flow of activations (routing) in the principal neurons population. The information temporarily stored in the gates specifies which sub-populations will be activated and in which order. The combination of gate interneuron and the assumed architecture allows a versatile serial order storage-recall mechanism. Considering two units A and B, the model shows that any configuration involving these two units is equally feasible: i) A followed by B; ii) B followed by A; iii) A and B co-activated; and iv) all other configurations where A and B are independent or do not activate sequentially.

With the gate interneurons we are, in some sense, replacing synaptic storage for neuronal storage. It should be noted that storing information in neuronal intrinsic membrane dynamics:

- provides a robust storage mechanism (synapses in the central nervous system are often highly probabilistic);
- makes information available in a non-local manner - changing a synapse only modulates a target neuron while a single gate interneuron can be used to modulate several neurons (gate interneurons can "broadcast" the stored information to more targets)
- works reliably, and is less affected by noise, on time scales of a few hundred milliseconds, compatible with fast storage mechanisms (one-shot learning)

- provides continuous access to the stored information (in the form of firing activity), while a synapse needs to be activated to readout the stored information

We therefore argue that, while penalizing scalability, there are many contexts and scales where storing information in interneuron's intrinsic membrane dynamics, instead of in synapses, can lead to important functional advantages.

Acknowledgments

Research funded by the European Regional Development Fund through the programme COMPETE and by the Portuguese Government through the FCT - Fundação para a Ciência e a Tecnologia under the project PEst-C/MAT/UI0144/2011. Eduardo Conde-Sousa was supported by the grant SFRH/BD/65633/2009 from FCT, co-financed by European Social Fund under the program POPH of the National Strategic Reference Framework.

7.3. Computational Tools for Assessing Synaptic Integration

This component of the work is part of larger collaborative project. At the time of the submission of this thesis, the complete manuscript is still in preparation for submission in peer-reviewed international journal.

In Section 7.3.1 the problem is contextualized, and in the following sections the mathematical/computational components that were developed under the scope of this thesis are addressed.

7.3.1. Introduction

Electrophysiological studies of the superficial dorsal horn of the spinal cord show a high prevalence of the so-called tonic neurons. This functional classification is the result of experiments where a constant current is injected into the soma leading to the generation of a periodic (tonic) train of action potentials. The frequency of this train is dependent on the injected current amplitude. Although generalized in the literature, this functional classification is quite limiting and artificial as neurons in real networks are unlikely to be stimulated by constant currents.

With the goal of better understanding the functional role of these neurons a multidisciplinary team involving researchers from the Neural Networks Group @ IBMC produced multi-compartment models from detailed reconstructions of the morphology (including spine locations) of 25 neurons. In order to obtain neuronal models which recreate the tonic properties of the recorded neurons, each model was then tuned to fit the electrophysiological traces obtained experimentally.

The collaboration with this team/project was focused of the construction of mathematical and computational tools to support an artifact free neuronal topology reconstruction, inclusion of synaptic locations in the dendritic tree using spines locations, and estimation of synaptic efficacies.

7.3.2. Materials and methods

An interdisciplinary team was involved in this work. First, several electrophysiologists have collected the data. The cells were intracellularly recorded and morphologically reconstructed in all the extension of the lamina I dorsal horn of the spinal cord plus the lateral

spinal nucleus of Wistar Rats. Electrophysiological analysis and morphometric characterization is already published by Luz et al. (2010, 2014) and Szucs et al. (2010, 2013). Then, the Neurolucida files (http://www.mbfbioscience.com/neurolucida), with neuronal reconstructions, were imported into the NEURON Simulation Environment (Hines and Carnevale, 1997).

7.3.2.1. *Spines location*

NEURON has not yet implemented any function capable of reading all the data that Neurolucida exports. Spines specified in Neurolucida files are automatically removed by NEURON. Therefore, the solution found to overcome this problem was to import the spines location into NEURON in a later step as .dat files.

To identify the segment of the dendritic tree to where each spine belongs to, a searching algorithm was created. For each neuron, the spatial position of each of the N spines are imported into a $N \times 3$ matrix and an exhaustive search is then made, by computing, for each spine, the euclidean distances between the 3D coordinates of all points of the neuron and the 3D coordinates of the spine. Then, the section and the segment where the closest point is located are stored.

Although this is an exhaustive search algorithm, it was not necessary to heavily optimize it since the amount of spines and 3D points of each neuron allows the process to run in a few seconds.

After the spines location, in each of the corresponding segments an artificial synapse is attached. Each synapse is modeled as a single exponential function with decay time constant of 5 ms. The activation time of each individual synapse or cluster of synapses as well as the synaptic efficacy can be easily adjusted.

7.3.2.2. *Artifacts handling*

As a consequence of slicing damage or shrinkage during histological preparation, neuronal reconstructions are often subject to the introduction of artifacts that modify morphological shape and size. 3D reconstructions are frequently impaired by the introduction of several bumps (see left panel of Figure 7.16) that may modify the synaptic propagation through the dendrites. An algorithm, which runs over all compartments, was developed in NEURON to remove these bumps without loss of the neuron main morphology (a schematic representation of the algorithm could be found in Figure 7.14).

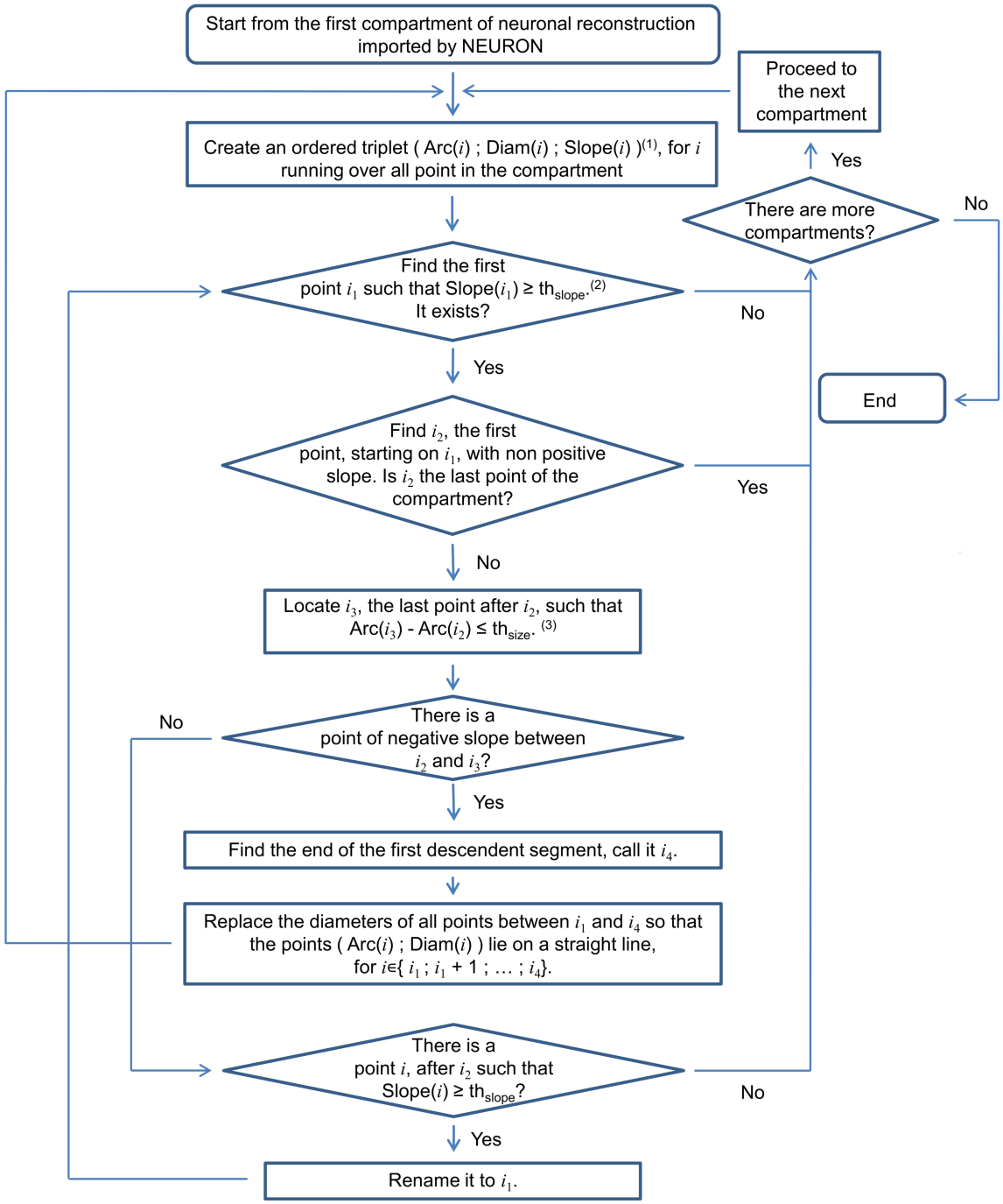

FIGURE 7.14. A schematic representation of the algorithm. (1) $Arc(i)$ is the distance, through the fiber, between the i^{th} point and the first point of its compartment; $Diam(i)$ is the diameter associated with the i^{th} point; and $Slope(i) = (Diam(i+1) - Diam(i))/(Arc(i+1) - Arc(i))$. For each compartment, $Slope(j) = 0$ if j is the last point. (2) th_{slope} is a given threshold value. (3) th_{size} is a given threshold value.

7.3.2.3. *Electrotonic distance*

The logarithm of voltage attenuation was proposed as a measure of electrotonic distance (Zador et al., 1991; Brown et al., 1992). In an infinite cylindrical cable, the electrotonic distance X is proportional to the physical distance x: $X = \frac{x}{\lambda}$. Nevertheless, real neurons have complex and irregular anatomies. Thus, in most of the real neurons the voltage attenuation can not be approximated by an exponential function of distance (see Section 2.6.3).

The Electrotonic Workbench of the NEURON simulation environment (Carnevale et al., 1995) was used to built a procedure that computes the logarithm of attenuation for voltage spreading toward (V_{in}) or away (V_{out}) from a reference point. Due to the membrane capacitance, attenuation (and so, the electrotonic distance) is function of frequency. As so, the built procedure takes as arguments:

(i) the direction of the voltage spreading (V_{in} or V_{out});
(ii) the reference point;
(iii) the frequency; and
(iv) the list of points of interest;

and computes the electrotonic distances between all points of interest (usually the locations of presynaptic terminals) and the reference point (usually the center of the soma compartment).

7.3.3. Results

The computational tools described in Sections 7.3.2.1 to 7.3.2.3 were tested in all the 25 neurons of the sample.

7.3.3.1. *Spines location*

As a result of the procedure described in Section 7.3.2.1 all spines identified at the morphological reconstructions were located and an artificial synapse was attached at the center of each of the corresponding compartments in the neuronal model (see Figure 7.15).

7.3.3.2. *Artifacts handling*

Some of the neuronal models had bumps resulting from shrinkage during histological preparation. Before proceeding to any simulation, it was necessary to fix them in order

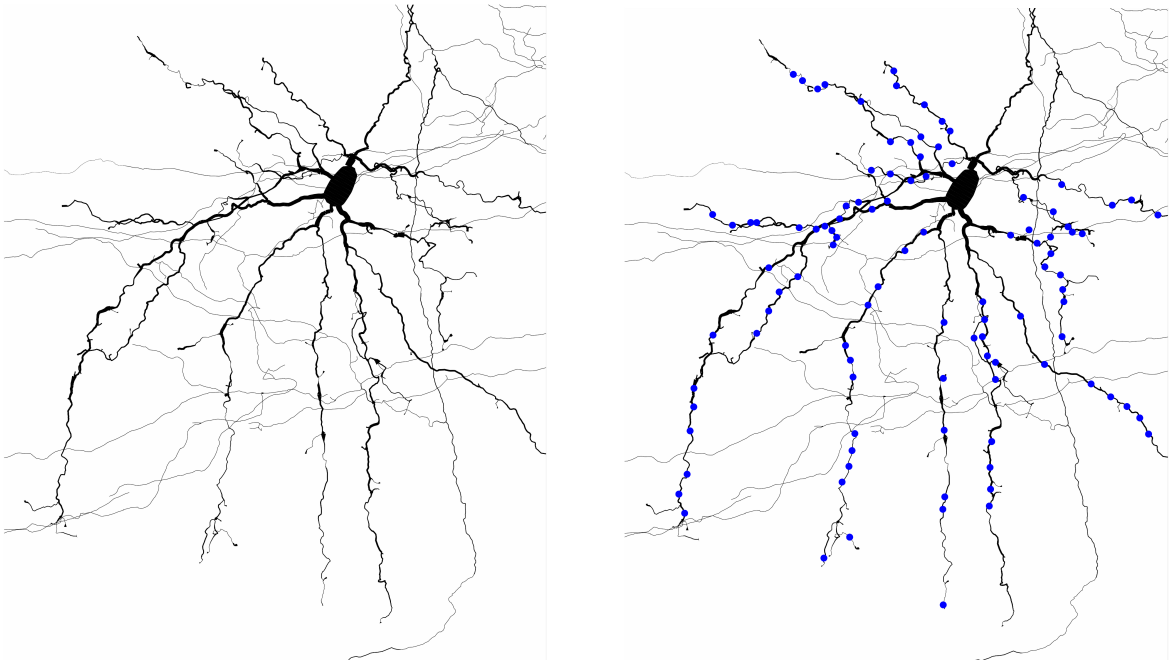

FIGURE 7.15. Spines location. On the left, part of the reconstruction of neuron L387_E2. On the right, the same neuron with synapses (represented by dots) attached to the compartments where the spines were located.

to prevent modifications in the signal propagation resulting from the existence of these bumps. In Figure 7.16 it is possible to visualize part of the reconstruction of one of the neurons (L395). On the left panel it is shown the neuron with several bumps and in the right panel the same neuron is shown after the smoothing process.

7.3.3.3. *Electrotonic distance*

In the work where these tools are being used, it is intended to assess how synaptic signals attached to different locations in the dendritic tree are integrated and processed by one neuron. A key point in the development of that work is to find a good synaptic efficacy predictor. Since synaptic inputs tend to act like a current source, the impact on membrane potential at the spike trigger zone is best described by normalized transfer impedance which is identical to attenuation for voltage spreading away form the spiking trigger zone (for more information see Jaffe and Carnevale, 1999).

Different configurations of synaptic efficacies can be observed in the neurons. Some neurons have highly effective synaptic clusters at distal regions of the dendrites, while other neurons show relatively "democratic" distributions. In Figure 7.17 the physical

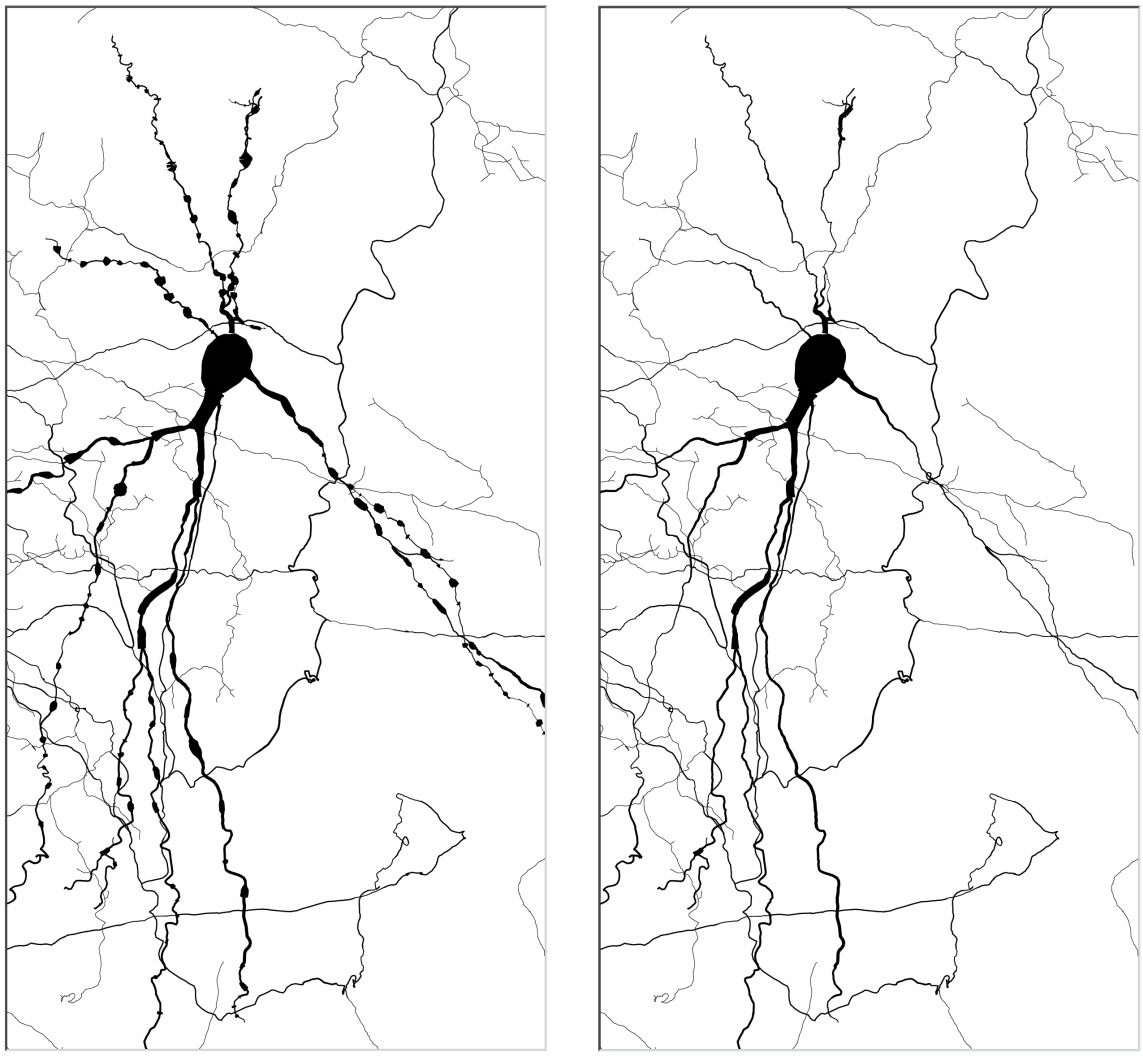

FIGURE 7.16. Shrinkage removal. Part of the same neuron (L395) is represented before (left panel) and after (right panel) the shrinkage removal with parameters $th_{slope} = 0.1$ and $th_{size} = 20\ \mu m$.

distance through the fiber is plotted versus the electrotonic distance, measured at 10 Hz, for two neurons of our sample (Zs158 on top and Zs074 on bottom). One of the neurons (Zs158), displays synapses at similar physical distances form the soma with very different electrotonic distances. Nevertheless, it is possible to observe an overall growth tendency of the electrotonic distance with the physical distance. In the second neuron (Zs074), it is possible to observe clusters of distal synapses (between 500 and 700 μm from the soma) with similar electrotonic distance as others at less than 150 μm.

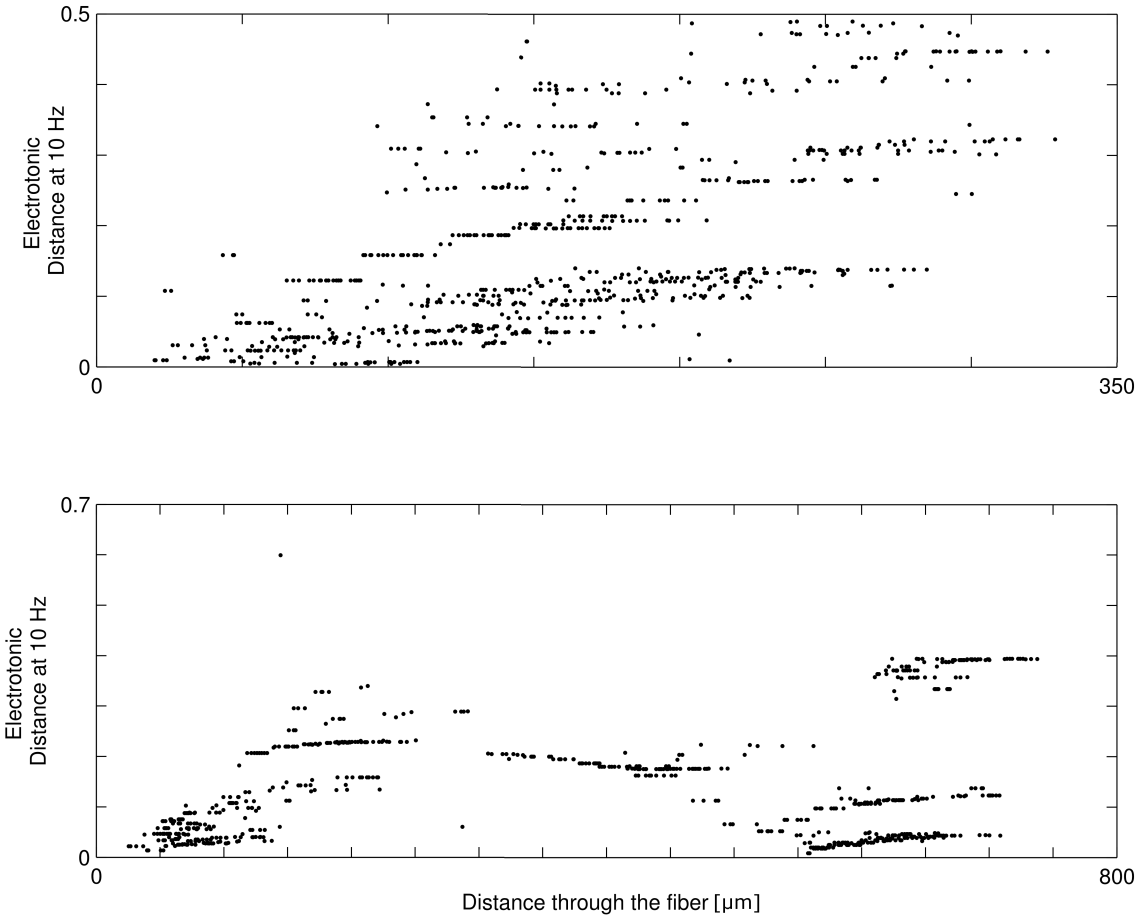

FIGURE 7.17. Physical distance through the fiber (in μm) versus the electrotonic distance, measured at 10 Hz. In neuron Zs158 (top panel) the electrotonic distance tends to grow with physical distance from the soma, while neuron Zs074 (bottom panel) shows highly effective synaptic clusters at distal regions.

8 Discussion

The work developed during this thesis focus on the application of mathematical/computational methodologies to better understand specific features of the brain.

Two self-contained articles are presented in Sections 7.1 and 7.2 focusing in the Working Memory field. In Section 7.3, the computational tools developed under the scope of a collaborative project with an experimental group working in electrophysiology (Neural Networks, IBMC) are presented.

In Articles I and II (Sections 7.1 and 7.2) we investigate non-synaptic mechanisms underlying a working memory system capable of storing novel information. A working memory system has to be able to store information in time windows of a few hundreds of milliseconds and sustain it for at least a few seconds. The interplay between different ion currents is proposed in these works as a possible mechanism underlying a working memory system which exhibits properties in close agreement with experimental results. This is an important and relevant alternative, supported by experimental data, to the dogma of synaptic plasticity (Mozzachiodi and Byrne, 2010).

The starting point in both these works is a single compartment conductance-based model with a reduced set of ion currents providing biological realism but also allowing the simulation of relatively large neural networks. A "minimal model" approach allows the identification of the core mechanisms giving rise to dynamics under study.

The coexistence between the high threshold calcium current and the non-specific cation current enables the *modulation of the intrinsic neuronal excitability* as a function of the neuron's recent activity. In other words, it is possible for a neuron with these two ion currents to give different responses to the same stimulus depending on the level of excitability induced by its past activity.

Considering this single cell model, which despite being conceptually simple shows a rich dynamic behavior, we show that the modulation of the intrinsic neuronal excitability is sufficient to support the fast storage of novel information and the activity during the

delay period. That is, in this work we provide evidence that a working memory system does not require synaptic plasticity. Also, the memory system described here is capable of encoding and storing new information in the form of patterns of activity, as opposed to other models which assume the preexistence of clusters of neurons strongly connected as a consequence of long-term learning mechanisms.

This model supports the possibility of learning new information not on the basis of cellular bistability, but by taking advantages of cellular mechanisms to build a network capable of storing any pattern of activity in a noise robust manner.

The network presented in Article I is also able of detecting the repetition of the previously stored pattern after the delay period and can "decide" whether a new pattern should only be classified as different from the first or should replace it.

In Article II we extend the model presented in Article I. Considering a similar neuronal model (using the same ion currents but with different parameters) and specifying the network architecture, we enlarge the model capabilities. The network model presented in Article II is capable of storing the serial order of a sequence of patterns of activity. In Article II we also present a powerful novel concept: gate interneurons. Given the state of its intrinsic excitability, such neurons are capable of routing the activity in a neuronal network in a synaptic independent manner.

Despite the results presented in this thesis succeed in justify several experimental results, some caution in the conclusions that can be drawn from any computational model in Biology is needed. Firstly, it is necessary to assess the appropriateness of the assumptions made. As mentioned in Articles I and II, there are sufficient evidence of the presence in several cortical neurons of the used ionic currents (Bal and McCormick, 1993; Haj-Dahmane and Andrade, 1999; Klink and Alonso, 1997) as well as the existence of excitatory interneurons in regions related to working memory (Feldmeyer et al., 1999; Thomson et al., 2002). One of the key points to take into account concerns to the chosen network topologies. If, by one hand, the topology chosen in Article I (random connections without any spatial constraints) is commonly used and accepted by the scientific community, the topology implemented in the model proposed in Article II requires some additional considerations. Neuronal populations in the proposed network are arranged in clusters. Each cluster is composed by a principal neuron (which may serve as a model

for a group of synchronized pyramidal cells), an inhibitory interneuron, and a large number of excitatory interneurons, the gate interneurons. Despite the precise architecture in cortical columns has not yet being known (to the best of our knowledge), the network implemented in this model suits the known dimensions of these cortical structures. Thus, the suitability of the proposed connectivity to the cortical columns is an assumption of our model that future experimental works must study. Although it should be noted that some of the results presented in Article II are dependent on the chosen connectivity, and therefore must be experimentally tested, gate interneurons are a powerful concept which is independent of that choice and can be applied to working memory systems with less storage capacity where gate interneurons are responsible for defining the order of activations in the principal neuron population allowing long-term storage and recall of multiple sequences with overlapping patterns.

It is also important to notice that the proposed single cell model use a reduced number of ion currents, and so, it is unlikely to find a real neuron in the cortex that can be fully described by this model. Nevertheless, it is our belief that adding different ion currents and/or other cellular or network mechanisms to the model will not disrupt most of the presented results.

A relevant mechanism that is ubiquitous in the cortex and that nevertheless was not implemented in neither of the proposed models is the synaptic plasticity. Although widespread in Neuroscience literature synaptic plasticity is not necessary to store information. In this work we chose not to include it in order to show that the storage of information in a working memory system is possible and some experimental results in the working memory field can be explained in the absence of synaptic plasticity.

Naturally, these models could be improved by adding other mechanisms with the goal of capturing more experimental data. One important limitation of the presented models is the small spike variability, as compared with experimental traces (Compte et al., 2003; Shafi et al., 2007). This can be explained, in part, as a consequence of the reduced amount of inhibition in both models, when compared to other models (Brunel and Wang, 2001; Rolls et al., 2013). Given the computational constraints, in both models, inhibition to each excitatory neuron is carried by a smaller number of connections: zero (for gate interneurons in Article II), one (for principal neurons in Article II) or two (for principal neurons in Article I). This reduction in the number of inhibitory connections allowed the

increase of the network size but at the same time increases the firing regularity in the excitatory population (Tsodyks and Sejnowski, 1995; van Vreeswijk and Sompolinsky, 1996; Vogels and Abbott, 2009).

In Section 7.3, we discuss the mathematical/computational tools developed in the framework of collaborative work with a team of electrophysiologists. The goal of this multidisciplinary team was to study and classify in terms of function neurons from the spinal cord. The participation in the work reveals the increasing relevance of quantitative approaches in neuroscience. More and more, the experimental work requires support from advanced mathematical and computational techniques, not only to analyze complex data but also to build and simulate models which can test hypothesis and cast new ideas. The tools developed in the context of this collaboration allowed the 3D reconstruction of neuronal topologies with a high level of detail, including the locations of spines (as markers of the potential location of synaptic terminals). Such ability to import this data and generate the appropriate synaptic locations was not available in the NEURON simulation environment.

9 Future Work

The models proposed in Articles I and II, if combined, could give rise to a more versatile memory system. If the encoding information requires just one pattern of activity, it is only necessary to activate neurons in the network proposed in Article I. However, if a sequence of patterns of activity is required the network proposed in Article II should be considered. Nevertheless it is worthwhile noting that the network proposed in Article II depends on the reactivation of the first pattern of activity to elicit the sequential activation of the remaining patterns. Therefore, the interconnection between both models can constitute a useful and more complete model for working memory.

The model proposed in Article I can explain some experimental results. Over the past decades, different protocols were performed in delayed match to sample (DMS) experiments (Fuster and Alexander, 1971; Miyashita, 1988). For example, Miller and Desimone (1994) proposed the so-called ABBA protocol (see Chapter 5). The model presented in Article I when subject to this protocol, produces results which are in agreement with experimental data. Nevertheless, other protocols were implemented whose results cannot be explained by our model. Yakovlev et al. (2005) proposed the ABCDEC protocol, where a sequence of stimuli (A–B–C–D–E) is presented and any of it could be the sample stimulus. In the presented sequence C is the sample (third stimulus) and the match (sixth stimulus) and A, B, D and E are distractors. The model presented in Article I alone cannot account for this protocol and so should be improved. The interconnection between both models can be a way to account for a sequence of stimuli from which is necessary to identify the first repetition.

Moreover, it should be noted that the model proposed in Article II can not store sequences with a repeated pattern (eg it can not store the sequence A B C A D E). An additional mechanism that allows the storage of sequences with repeated elements must be considered. Also, although the model proposed in Article II stores order, it does not

store the time intervals between sequence elements. How to properly store timings, in addition to order, is still an open question in computational neuroscience.

Relatively to the collaborative work presented in Section 7.3, it is our believe that the algorithm created to detect and fix artifacts resulting from shrinkage during histological preparation (Section 7.3.2.2) could became useful to neuroscientists working on detailed neuronal reconstructions. Nevertheless, it should became more user-friendly before making it available for the use by the scientific community.

References

Abbott, L. F. and Nelson, S. B. Synaptic plasticity: taming the beast. *Nat Neurosci*, 3 Suppl:1178–83, 2000.

Aguiar, P., Sousa, M., and Lima, D. NMDA channels together with L-type calcium currents and calcium-activated nonspecific cationic currents are sufficient to generate windup in WDR neurons. *J Neurophysiol*, 104(2):1155–66, 2010.

Alonso, A., De Curtis, M., and Llinás, R. Postsynaptic hebbian and non-hebbian long-term potentiation of synaptic efficacy in the entorhinal cortex in slices and in the isolated adult guinea pig brain. *Proceedings of the National Academy of Sciences*, 87 (23):9280–9284, 1990. URL http://www.pnas.org/content/87/23/9280.short.

Amari, S. Dynamics of pattern formation in lateral-inhibition type neural fields. *Biol Cybern*, 27(2):77–87, Aug 1977.

Amini, B., Clark, J. W., and Canavier, C. C. Calcium dynamics underlying pacemaker-like and burst firing oscillations in midbrain dopaminergic neurons: a computational study. *Journal of Neurophysiology*, 82(5):2249–2261, 1999. URL http://jn.physiology.org/content/82/5/2249.short.

Amit, D. J. and Brunel, N. Model of global spontaneous activity and local structured activity during delay periods in the cerebral cortex. *Cerebral Cortex*, 7(3):237–252, 1997. URL http://cercor.oxfordjournals.org/content/7/3/237.short.

Amit, D. J., Bernacchia, A., and Yakovlev, V. Multiple-object working memory–a model for behavioral performance. *Cereb Cortex*, 13(5):435–443, May 2003.

Anderson, D. J., Rose, J. E., Hind, J. E., and Brugge, J. F. Temporal position of discharges in single auditory nerve fibers within the cycle of a sine-wave stimulus: frequency and intensity effects. *The Journal of the Acoustical Society of America*, 49(4), April 1971. ISSN 0001-4966. URL http://view.ncbi.nlm.nih.gov/pubmed/4994692.

Artola, A., Bröcher, S., and Singer, W. Different voltage-dependent thresholds for inducing long-term depression and long-term potentiation in slices of rat visual cortex.

Nature, 347(6288):69–72, Sep 1990. doi: 10.1038/347069a0.

Baddeley, A. Working memory: looking back and looking forward. *Nat Rev Neurosci*, 4 (10):829–39, 2003.

Baddeley, A. and Hitch, G. J. Working memory. *Scholarpedia*, 5(2):3015, 2010.

Bal, T. and McCormick, D. A. Mechanisms of oscillatory activity in guinea-pig nucleus reticularis thalami in vitro: a mammalian pacemaker. *J Physiol*, 468:669–91, 1993.

Barak, O. and Tsodyks, M. Working models of working memory. *Current Opinion in Neurobiology*, 25:20–24, April 2014. doi: 10.1016/j.conb.2013.10.008.

Bi, G. and Poo, M. Synaptic modification by correlated activity: Hebb's postulate revisited. *Annu Rev Neurosci*, 24:139–166, 2001. doi: 10.1146/annurev.neuro.24.1.139. URL http://dx.doi.org/10.1146/annurev.neuro.24.1.139.

Bliss, T. V. and Lomo, T. Long-lasting potentiation of synaptic transmission in the dentate area of the anaesthetized rabbit following stimulation of the perforant path. *J Physiol*, 232(2):331–56, 1973.

Botvinick, M. M. and Plaut, D. C. Short-term memory for serial order: a recurrent neural network model. *Psychol Rev*, 113(2):201–33, 2006.

Brette, R. and Gerstner, W. Adaptive exponential integrate-and-fire model as an effective description of neuronal activity. *Journal of Neurophysiology*, 94(5):3637–3642, November 2005. ISSN 1522-1598. doi: 10.1152/jn.00686.2005. URL http://dx.doi.org/10.1152/jn.00686.2005.

Brown, T. H., Zador, A. M., Mainen, Z. F., and Claiborne, B. J. Hebbian computations in hippocampal dendrites and spines. In McKenna, T., Davis, J., and Zornetzer, S. F., editors, *Single Neuron Computation*, pages 81–116. Academic Press Professional, Inc., San Diego, CA, USA, 1992. ISBN 0-12-484815-X. URL http://dl.acm.org/citation.cfm?id=132435.132440.

Brunel, N. and Wang, X. J. Effects of neuromodulation in a cortical network model of object working memory dominated by recurrent inhibition. *Journal of computational neuroscience*, 11(1):63–85, 2001. URL http://www.springerlink.com/index/J45U215W525142UK.pdf.

Brunel, N. and van Rossum, M. C. W. Lapicque's 1907 paper: from frogs to integrate-and-fire. *Biol Cybern*, 97(5-6):337–339, Dec 2007. doi: 10.1007/s00422-007-0190-0. URL http://dx.doi.org/10.1007/s00422-007-0190-0.

Burnashev, N., Zhou, Z., Neher, E., and Sakmann, B. Fractional calcium currents through recombinant glur channels of the NMDA, AMPA and kainate receptor subtypes. *J Physiol*, 485 (Pt 2):403–418, Jun 1995.

Burrell, B. D., Sahley, C. L., and Muller, K. J. Non-associative learning and serotonin induce similar bi-directional changes in excitability of a neuron critical for learning in the medicinal leech. *The Journal of Neuroscience*, 21(4):1401–1412, 2001. URL http://www.jneurosci.org/content/21/4/1401.abstract.

Buxhoeveden, D. P. and Casanova, M. F. The minicolumn hypothesis in neuroscience. *Brain*, 125(Pt 5):935–51, 2002.

Campanac, E., Daoudal, G., Ankri, N., and Debanne, D. Downregulation of dendritic ih in CA1 pyramidal neurons after LTP. *J. Neurosci.*, 28(34):8635–8643, August 2008. doi: 10.1523/jneurosci.1411-08.2008.

Camperi, M. and Wang, X. J. A model of visuospatial working memory in prefrontal cortex: recurrent network and cellular bistability. *J Comput Neurosci*, 5(4):383–405, Dec 1998.

Carnevale, N. T. and Johnston, D. Electrophysiological characterization of remote chemical synapses. *J Neurophysiol*, 47(4):606–621, Apr 1982.

Carnevale, N. T., Tsai, K. Y., Claiborne, B. J., and Brown, T. H. The electrotonic transformation: a tool for relating neuronal form to function. In *Leen (Eds.), Advances in Neural Information Processing Systems*, pages 69–76. MIT Press, 1995.

Compte, A., Brunel, N., Goldman-Rakic, P. S., and Wang, X. J. Synaptic mechanisms and network dynamics underlying spatial working memory in a cortical network model. *Cerebral Cortex*, 10(9):910–923, September 2000. ISSN 1460-2199. doi: 10.1093/cercor/10.9.910. URL http://dx.doi.org/10.1093/cercor/10.9.910.

Compte, A., Constantinidis, C., Tegnér, J., Raghavachari, S., Chafee, M. V., Goldman-Rakic, P. S., and Wang, X.-J. Temporally irregular mnemonic persistent activity in prefrontal neurons of monkeys during a delayed response task. *Journal of neurophysiology*, 90(5):3441–3454, 2003. URL http://jn.physiology.org/content/90/5/3441.short.

Conde-Sousa, E. and Aguiar, P. A working memory model for serial order that stores information in the intrinsic excitability properties of neurons. *Journal of Computational Neuroscience*, Mar 2013. doi: 10.1007/s10827-013-0447-7. URL http://dx.doi.org/10.1007/s10827-013-0447-7.

Crasto, C. J., Marenco, L. N., Liu, N., Morse, T. M., Cheung, K.-H., Lai, P. C., Bahl, G., Masiar, P., Lam, H. Y. K., Lim, E., Chen, H., Nadkarni, P., Migliore, M., Miller, P. L., and Shepherd, G. M. Senselab: new developments in disseminating neuroscience information. *Brief Bioinform*, 8(3):150–162, May 2007. doi: 10.1093/bib/bbm018. URL http://dx.doi.org/10.1093/bib/bbm018.

Dayan, P. and Abbott, L. F. *Theoretical Neuroscience: Computational and Mathematical Modeling of Neural Systems (Computational Neuroscience)*. The MIT Press, 2005. ISBN 0262541858.

Dehaene, S., Changeux, J. P., and Nadal, J. P. Neural networks that learn temporal sequences by selection. *Proceedings of the National Academy of Sciences*, 84(9):2727–2731, 1987. URL http://www.pnas.org/content/84/9/2727.short.

Destexhe, A., Babloyantz, A., and Sejnowski, T. J. Ionic mechanisms for intrinsic slow oscillations in thalamic relay neurons. *Biophysical journal*, 65(4):1538–1552, 1993. URL http://www.sciencedirect.com/science/article/pii/S0006349593811901.

Destexhe, A., Contreras, D., Sejnowski, T. J., and Steriade, M. A model of spindle rhythmicity in the isolated thalamic reticular nucleus. *J Neurophysiol*, 72(2):803–18, 1994a.

Destexhe, A., Mainen, Z. F., and Sejnowski, T. J. Synthesis of models for excitable membranes, synaptic transmission and neuromodulation using a common kinetic formalism. *J Comput Neurosci*, 1(3):195–230, Aug 1994b.

Destexhe, A., Mainen, Z. F., and Sejnowski, T. J. Kinetic models of synaptic transmission. In Koch, C. and Segev, I., editors, *Methods in Neuronal Modeling: From Synapse to Networks*, pages 1–25. MIT press, 1998. ISBN 978-0-262-11231-4.

Dudai, Y. *Memory from A to Z: Keywords, Concepts, and Beyond*. Oxford University Press, USA, 2002.

Durstewitz, D., Seamans, J. K., and Sejnowski, T. J. Neurocomputational models of working memory. *Nat Neurosci*, 3 Suppl:1184–91, 2000.

Durstewitz, D. Self-organizing neural integrator predicts interval times through climbing activity. *The Journal of neuroscience*, 23(12):5342–5353, 2003. URL http://www.jneurosci.org/content/23/12/5342.short.

Egorov, A. V., Hamam, B. N., Fransén, E., Hasselmo, M. E., and Alonso, A. A. Graded persistent activity in entorhinal cortex neurons. *Nature*, 420(6912):173–178, Nov 2002.

doi: 10.1038/nature01171. URL http://dx.doi.org/10.1038/nature01171.

Elman, J. L. Finding structure in time. *Cognitive Science*, 14(2):179–211, 1990. URL http://citeseerx.ist.psu.edu/viewdoc/summary?doi=10.1.1.28.9476.

Fall, C. P. and Rinzel, J. An intracellular Ca2+ subsystem as a biologically plausible source of intrinsic conditional bistability in a network model of working memory. *J Comput Neurosci*, 20(1):97–107, 2006.

Fan, Y., Fricker, D., Brager, D. H., Chen, X., Lu, H.-C., Chitwood, R. A., and Johnston, D. Activity-dependent decrease of excitability in rat hippocampal neurons through increases in I(h). *Nat Neurosci*, 8(11):1542–1551, Nov 2005. doi: 10.1038/nn1568. URL http://dx.doi.org/10.1038/nn1568.

Feldmeyer, D., Egger, V., Lubke, J., and Sakmann, B. Reliable synaptic connections between pairs of excitatory layer 4 neurones within a single 'barrel' of developing rat somatosensory cortex. *J Physiol*, 521 Pt 1:169–90, 1999.

FitzHugh, R. Impulses and physiological states in theoretical models of nerve membrane. *Biophys J*, 1(6):445–466, Jul 1961.

Fransén, E., Alonso, A. A., and Hasselmo, M. E. Simulations of the role of the muscarinic-activated calcium-sensitive nonspecific cation current INCM in entorhinal neuronal activity during delayed matching tasks. *J Neurosci*, 22(3):1081–97, 2002.

Fransén, E., Tahvildari, B., Egorov, A. V., Hasselmo, M. E., and Alonso, A. A. Mechanism of graded persistent cellular activity of entorhinal cortex layer V neurons. *Neuron*, 49 (5):735–46, 2006.

Fuhrmann, G., Segev, I., Markram, H., and Tsodyks, M. Coding of temporal information by activity-dependent synapses. *J Neurophysiol*, 87(1):140–148, Jan 2002.

Funahashi, S. and Kubota, K. Working memory and prefrontal cortex. *Neurosci Res*, 21 (1):1–11, Nov 1994.

Funahashi, S., Bruce, C. J., and Goldman-Rakic, P. S. Mnemonic coding of visual space in the monkey's dorsolateral prefrontal cortex. *J Neurophysiol*, 61(2):331–349, Feb 1989.

Fuster, J. M. and Alexander, G. E. Neuron activity related to short-term memory. *Science*, 173(3997):652–654, Aug 1971.

Ganguly, K., Kiss, L., and Poo, M. Enhancement of presynaptic neuronal excitability by correlated presynaptic and postsynaptic spiking. *Nat Neurosci*, 3(10):1018–1026, Oct 2000. doi: 10.1038/79838.

Gibson, W. and Robinson, J. Statistical analysis of the dynamics of a sparse associative memory. *Neural Networks*, 5(4):645–661, 1992. URL http://www.sciencedirect.com/science/article/pii/S0893608005800425.

Grashow, R., Brookings, T., and Marder, E. Compensation for variable intrinsic neuronal excitability by circuit-synaptic interactions. *J Neurosci*, 30(27):9145–56, 2010.

Hahn, T. T., McFarland, J. M., Berberich, S., Sakmann, B., and Mehta, M. R. Spontaneous persistent activity in entorhinal cortex modulates cortico-hippocampal interaction in vivo. *Nat Neurosci*, 15(11):1531–8, 2012.

Haj-Dahmane, S. and Andrade, R. Muscarinic receptors regulate two different calcium-dependent non-selective cation currents in rat prefrontal cortex. *Eur J Neurosci*, 11(6): 1973–80, 1999.

Hansel, D. and Sompolinsky, H. Modeling feature selectivity in local cortical circuits. In Koch, C. and Segev, I., editors, *Methods in Neuronal Modeling: From Synapse to Networks*. MIT Press, Cambridge, MA, second edition edition, 1998.

Hasselmo, M. E. and Stern, C. E. Mechanisms underlying working memory for novel information. *Trends Cogn Sci*, 10(11):487–493, Nov 2006. doi: 10.1016/j.tics.2006.09.005. URL http://dx.doi.org/10.1016/j.tics.2006.09.005.

Hebb, D. O. *The Organization of Behavior*. New York: Wiley, 1949.

Henson, R. N. Short-term memory for serial order: the start-end model. *Cogn Psychol*, 36(2):73–137, Jul 1998. doi: 10.1006/cogp.1998.0685. URL http://dx.doi.org/10.1006/cogp.1998.0685.

Herz, A., Li, Z., and Van Hemmen, J. Statistical mechanics of temporal association in neural networks with transmission delays. *Physical review letters*, 66(10):1370–1373, 1991. URL http://link.aps.org/doi/10.1103/PhysRevLett.66.1370.

Hines, M. L. and Carnevale, N. T. The neuron simulation environment. *Neural Comput*, 9(6):1179–209, 1997.

Hines, M. L., Morse, T., Migliore, M., Carnevale, N. T., and Shepherd, G. M. Modeldb: A database to support computational neuroscience. *J Comput Neurosci*, 17(1):7–11, 2004. doi: 10.1023/B:JCNS.0000023869.22017.2e. URL http://dx.doi.org/10.1023/B:JCNS.0000023869.22017.2e.

Hodgkin, A. L. and Huxley, A. F. A quantitative description of membrane current and its application to conduction and excitation in nerve. *The Journal of physiology*, 117

(4):500, 1952a. URL http://www.ncbi.nlm.nih.gov/pmc/articles/PMC1392413/.

Hodgkin, A. L. and Huxley, A. F. Currents carried by sodium and potassium ions through the membrane of the giant axon of loligo. *The Journal of physiology*, 116(4):449–472, 1952b. ISSN 0022-3751.

Hodgkin, A. L. and Huxley, A. F. The components of membrane conductance in the giant axon of loligo. *The Journal of physiology*, 116(4):473–496, 1952c. ISSN 0022-3751.

Hodgkin, A. L. and Huxley, A. F. The dual effect of membrane potential on sodium conductance in the giant axon of loligo. *The Journal of physiology*, 116(4):497–506, 1952d. ISSN 0022-3751.

Hodgkin, A. L., Huxley, A. F., and Katz, B. Measurement of current-voltage relations in the membrane of the giant axon of loligo. *The Journal of physiology*, 116(4):424–448, April 1952. ISSN 0022-3751.

Hopfield, J. J. Neural networks and physical systems with emergent collective computational abilities. *Proceedings of the national academy of sciences*, 79(8):2554–2558, 1982. URL http://www.pnas.org/content/79/8/2554.short.

Hyde, R. A. and Strowbridge, B. W. Mnemonic representations of transient stimuli and temporal sequences in the rodent hippocampus in vitro. *Nat Neurosci*, 15(10):1430–1438, Oct 2012. doi: 10.1038/nn.3208. URL http://dx.doi.org/10.1038/nn.3208.

Izhikevich, E. M. Simple model of spiking neurons. *Neural Networks, IEEE Transactions on*, 14(6):1569–1572, Nov 2003. ISSN 1045-9227. doi: 10.1109/TNN.2003.820440.

Izhikevich, E. M. Which model to use for cortical spiking neurons? *IEEE Transactions on Neural Networks*, 15(5):1063–1070, Sept 2004. ISSN 1045-9227. doi: 10.1109/TNN.2004.832719.

Izhikevich, E. M. and FitzHugh, R. FitzHugh-Nagumo model. *Scholarpedia*, 1(9):1349, 2006.

Izhikevich, E. M. Resonate-and-fire neurons. *Neural Networks*, 14(6–7):883 – 894, 2001. ISSN 0893-6080. doi: http://dx.doi.org/10.1016/S0893-6080(01)00078-8. URL http://www.sciencedirect.com/science/article/pii/S0893608001000788.

Jackson, M. B. and Scharfman, H. E. Positive feedback from hilar mossy cells to granule cells in the dentate gyrus revealed by voltage-sensitive dye and microelectrode recording. *Journal of neurophysiology*, 76(1):601–616, 1996. URL http://jn.physiology.org/content/76/1/601.short.

Jaffe, D. B. and Carnevale, N. T. Passive normalization of synaptic integration influenced by dendritic architecture. *J Neurophysiol*, 82(6):3268–3285, Dec 1999.

Jahr, C. E. and Stevens, C. F. Voltage dependence of NMDA-activated macroscopic conductances predicted by single-channel kinetics. *J Neurosci*, 10(9):3178–3182, Sep 1990.

Jensen, O., Idiart, M. A., and Lisman, J. E. Physiologically realistic formation of autoassociative memory in networks with theta/gamma oscillations: role of fast NMDA channels. *Learn Mem*, 3(2-3):243–56, 1996.

Kandel, E. R. The molecular biology of memory storage: a dialogue between genes and synapses. *Science*, 294(5544):1030–8, 2001.

Klink, R. and Alonso, A. Morphological characteristics of layer II projection neurons in the rat medial entorhinal cortex. *Hippocampus*, 7(5):571–83, 1997.

Klintsova, A. Y. and Greenough, W. T. Synaptic plasticity in cortical systems. *Current Opinion in Neurobiology*, 9(2):203 – 208, 1999. ISSN 0959-4388. doi: http://dx.doi.org/10.1016/S0959-4388(99)80028-2. URL http://www.sciencedirect.com/science/article/pii/S0959438899800282.

Koene, R. A. and Hasselmo, M. E. First-in-first-out item replacement in a model of short-term memory based on persistent spiking. *Cereb Cortex*, 17(8):1766–81, 2007.

Koene, R. A. and Hasselmo, M. E. Consequences of parameter differences in a model of short-term persistent spiking buffers provided by pyramidal cells in entorhinal cortex. *Brain Res*, 1202:54–67, 2008.

Laing, C. R. and Longtin, A. Noise-induced stabilization of bumps in systems with long-range spatial coupling. *Physica D: Nonlinear Phenomena*, 160(3–4):149 – 172, 2001. ISSN 0167-2789. doi: http://dx.doi.org/10.1016/S0167-2789(01)00351-7. URL http://www.sciencedirect.com/science/article/pii/S0167278901003517.

Lapicque, L. Recherches quantitatives sur l'excitation électrique des nerfs traitée comme une polarisation. *J. Physiol. Pathol. Gen.*, 9:620–635, 1907.

Latham, P. E., Richmond, B. J., Nelson, P. G., and Nirenberg, S. Intrinsic dynamics in neuronal networks. i. theory. *Journal of Neurophysiology*, 83(2):808–827, 2000. URL http://jn.physiology.org/content/83/2/808.

Laurent, G. Dynamical representation of odors by oscillating and evolving neural assemblies. *Trends Neurosci*, 19(11):489–496, Nov 1996. doi: 10.1016/S0166-2236(96)10054-0.

URL http://dx.doi.org/10.1016/S0166-2236(96)10054-0.

Lee, K. S., Schottler, F., Oliver, M., and Lynch, G. Brief bursts of high-frequency stimulation produce two types of structural change in rat hippocampus. *Journal of Neurophysiology*, 44(2):247–258, 1980. URL http://jn.physiology.org/content/44/2/247.

Lisman, J. E. and Idiart, M. A. Storage of 7 +/- 2 short-term memories in oscillatory subcycles. *Science*, 267(5203):1512–5, 1995.

Luz, L. L., Szucs, P., Pinho, R., and Safronov, B. V. Monosynaptic excitatory inputs to spinal lamina I anterolateral-tract-projecting neurons from neighbouring lamina I neurons. *J Physiol*, 588(Pt 22):4489–4505, Nov 2010. doi: 10.1113/jphysiol.2010.197012. URL http://dx.doi.org/10.1113/jphysiol.2010.197012.

Luz, L. L., Szucs, P., and Safronov, B. V. Peripherally driven low-threshold inhibitory inputs to lamina I local-circuit and projection neurones: a new circuit for gating pain responses. *J Physiol*, 592(Pt 7):1519–1534, Apr 2014. doi: 10.1113/jphysiol.2013.269472. URL http://dx.doi.org/10.1113/jphysiol.2013.269472.

Marder, E., Abbott, L. F., Turrigiano, G. G., Liu, Z., and Golowasch, J. Memory from the dynamics of intrinsic membrane currents. *Proc Natl Acad Sci U S A*, 93(24):13481–6, 1996.

Marom, S. and Abbott, L. F. Modeling state-dependent inactivation of membrane currents. *Biophys J*, 67(2):515–520, Aug 1994. doi: 10.1016/S0006-3495(94)80518-1. URL http://dx.doi.org/10.1016/S0006-3495(94)80518-1.

McCormick, D. A. and Huguenard, J. R. A model of the electrophysiological properties of thalamocortical relay neurons. *J Neurophysiol*, 68(4):1384–1400, Oct 1992.

Migliore, M., Cannia, C., Lytton, W. W., Markram, H., and Hines, M. L. Parallel network simulations with NEURON. *Journal of computational neuroscience*, 21(2): 119–129, October 2006. ISSN 0929-5313. doi: 10.1007/s10827-006-7949-5. URL http://dx.doi.org/10.1007/s10827-006-7949-5.

Miller, E. K. and Desimone, R. Parallel neuronal mechanisms for short-term memory. *Science*, 263(5146):520–522, Jan 1994.

Miller, E. K., Li, L., and Desimone, R. A neural mechanism for working and recognition memory in inferior temporal cortex. *Science*, 254(5036):1377–1379, Nov 1991.

Miller, G. A. The magical number seven plus or minus two: some limits on our capacity for processing information. *Psychol Rev*, 63(2):81–97, Mar 1956.

Miller, G. A., Galanter, E., and Pribram, K. H. *Plans and the Structure of Behaviour*. Holt,Rinehart & Winston, 1960.

Miyashita, Y. Neuronal correlate of visual associative long-term memory in the primate temporal cortex. *Nature*, 335(6193):817–820, October 1988. ISSN 0028-0836. doi: 10.1038/335817a0. URL http://dx.doi.org/10.1038/335817a0.

Mongillo, G., Barak, O., and Tsodyks, M. Synaptic theory of working memory. *Science Signalling*, 319(5869):1543, 2008. URL http://stke.sciencemag.org/cgi/content/abstract/sci;319/5869/1543.

Morris, C. and Lecar, H. Voltage oscillations in the barnacle giant muscle fiber. *Biophys J*, 35(1):193–213, Jul 1981.

Mozzachiodi, R. and Byrne, J. H. More than synaptic plasticity: role of nonsynaptic plasticity in learning and memory. *Trends Neurosci*, 33(1):17–26, 2010.

Murdock, B. B. Developing todam: three models for serial-order information. *Mem Cognit*, 23(5):631–645, Sep 1995.

Nagumo, J., Arimoto, S., and Yoshizawa, S. An active pulse transmission line simulating nerve axon. *Proceedings of the IRE*, 50(10):2061–2070, October 1962. ISSN 0096-8390. doi: 10.1109/jrproc.1962.288235. URL http://dx.doi.org/10.1109/jrproc.1962.288235.

Nagy, G. A., Botond, G., Borhegyi, Z., Plummer, N. W., Freund, T. F., and Hájos, N. DAG-sensitive and Ca(2+) permeable TRPC6 channels are expressed in dentate granule cells and interneurons in the hippocampal formation. *Hippocampus*, 23(3):221–232, Mar 2013. doi: 10.1002/hipo.22081. URL http://dx.doi.org/10.1002/hipo.22081.

Otis, T. S., De Koninck, Y., and Mody, I. Characterization of synaptically elicited gabab responses using patch-clamp recordings in rat hippocampal slices. *J Physiol*, 463:391–407, Apr 1993.

Patneau, D. K. and Mayer, M. L. Kinetic analysis of interactions between kainate and AMPA: evidence for activation of a single receptor in mouse hippocampal neurons. *Neuron*, 6(5):785–798, May 1991.

Prinz, A. A., Bucher, D., and Marder, E. Similar network activity from disparate circuit parameters. *Nat Neurosci*, 7(12):1345–52, 2004.

Rieke, F., Warland, D., de de Ruyter van Steveninck, R., and Bialek, W. *Spikes: Exploring the Neural Code (Computational Neuroscience)*. A Bradford Book, 1999. ISBN 0262681080.

Rolls, E. T., Dempere-Marco, L., and Deco, G. Holding multiple items in short term memory: a neural mechanism. *PLoS One*, 8(4):e61078, 2013. doi: 10.1371/journal.pone.0061078. URL http://dx.doi.org/10.1371/journal.pone.0061078.

Sahley, C. L., Modney, B. K., Boulis, N. M., and Muller, K. J. The S cell: an interneuron essential for sensitization and full dishabituation of leech shortening. *The Journal of Neuroscience*, 14(11):6715–6721, 1994. URL http://www.jneurosci.org/content/14/11/6715.abstract.

Schreurs, B. G., Gusev, P. A., Tomsic, D., Alkon, D. L., and Shi, T. Intracellular correlates of acquisition and long-term memory of classical conditioning in purkinje cell dendrites in slices of rabbit cerebellar lobule hvi. *J Neurosci*, 18(14):5498–5507, Jul 1998.

Shafi, M., Zhou, Y., Quintana, J., Chow, C., Fuster, J., and Bodner, M. Variability in neuronal activity in primate cortex during working memory tasks. *Neuroscience*, 146(3):1082–1108, 2007. URL http://www.sciencedirect.com/science/article/pii/S0306452206017593.

Sjöström, J. and Gerstner, W. Spike-timing dependent plasticity. *Scholarpedia*, 5(2):1362, 2010.

Sjöström, P. J., Turrigiano, G. G., and Nelson, S. B. Endocannabinoid-dependent neocortical layer-5 LTD in the absence of postsynaptic spiking. *J Neurophysiol*, 92(6):3338–3343, Dec 2004. doi: 10.1152/jn.00376.2004.

Smith, G. D., Cox, C. L., Sherman, S. M., and Rinzel, J. Fourier analysis of sinusoidally driven thalamocortical relay neurons and a minimal integrate-and-fire-or-burst model. *Journal of Neurophysiology*, 83(1):588–610, 2000. URL http://jn.physiology.org/content/83/1/588.

Sterratt, D., Graham, B., Gillies, D. A., and Willshaw, D. *Principles of Computational Modelling in Neuroscience*. Cambridge University Press, 2011. ISBN 0521877954.

Stevens, C. F. and Wang, Y. Facilitation and depression at single central synapses. *Neuron*, 14(4):795–802, Apr 1995.

Suh, J., Rivest, A. J., Nakashiba, T., Tominaga, T., and Tonegawa, S. Entorhinal cortex layer III input to the hippocampus is crucial for temporal association memory. *Science*, 334(6061):1415–20, 2011.

Szucs, P., Luz, L. L., Lima, D., and Safronov, B. V. Local axon collaterals of lamina I projection neurons in the spinal cord of young rats. *J Comp Neurol*, 518(14):2645–2665,

Jul 2010. doi: 10.1002/cne.22391. URL http://dx.doi.org/10.1002/cne.22391.

Szucs, P., Luz, L. L., Pinho, R., Aguiar, P., Antal, Z., Tiong, S. Y. X., Todd, A. J., and Safronov, B. V. Axon diversity of lamina I local-circuit neurons in the lumbar spinal cord. *J Comp Neurol*, 521(12):2719–2741, Aug 2013. doi: 10.1002/cne.23311. URL http://dx.doi.org/10.1002/cne.23311.

Thomson, A. M., West, D. C., Wang, Y., and Bannister, A. P. Synaptic connections and small circuits involving excitatory and inhibitory neurons in layers 2-5 of adult rat and cat neocortex: triple intracellular recordings and biocytin labelling in vitro. *Cereb Cortex*, 12(9):936–53, 2002.

Traub, R. D. and Miles, R. *Neuronal networks of the hippocampus*, volume 777. Cambridge University Press, 1991.

Traub, R. D., Wong, R., Miles, R., and Michelson, H. A model of a CA3 hippocampal pyramidal neuron incorporating voltage-clamp data on intrinsic conductances. *Journal of Neurophysiology*, 66(2):635–650, 1991. URL http://jn.physiology.org/content/66/2/635.short.

Tsodyks, M. and Wu, S. Short-term synaptic plasticity. *Scholarpedia*, 8(10):3153, 2013.

Tsodyks, M. V. and Sejnowski, T. Rapid state switching in balanced cortical network models. *Network: Computation in Neural Systems*, 6(2):111–124, 1995. URL http://informahealthcare.com/doi/abs/10.1088/0954-898X_6_2_001.

Turrigiano, G. G., Marder, E., and Abbott, L. F. Cellular short-term memory from a slow potassium conductance. *J Neurophysiol*, 75(2):963–966, Feb 1996.

van Vreeswijk, C. and Sompolinsky, H. Chaos in neuronal networks with balanced excitatory and inhibitory activity. *Science*, 274(5293):1724–1726, 1996. URL http://www.sciencemag.org/content/274/5293/1724.short.

Versace, M. and Zorzi, M. The role of dopamine in the maintenance of working memory in prefrontal cortex neurons: Input-driven versus internally-driven networks. *International journal of neural systems*, 20(04):249–265, 2010. URL http://www.worldscientific.com/doi/abs/10.1142/S0129065710002401.

Vogels, T. P. and Abbott, L. F. Gating multiple signals through detailed balance of excitation and inhibition in spiking networks. *Nature neuroscience*, 12(4):483–491, 2009. URL http://www.nature.com/neuro/journal/vaop/ncurrent/full/nn.2276.html.

Wang, X. J. Synaptic basis of cortical persistent activity: the importance of NMDA receptors to working memory. *J Neurosci*, 19(21):9587–9603, Nov 1999.

Wang, X. J. Synaptic reverberation underlying mnemonic persistent activity. *Trends Neurosci*, 24(8):455–463, Aug 2001.

Wang, X. J., Tegnér, J., Constantinidis, C., and Goldman-Rakic, P. S. Division of labor among distinct subtypes of inhibitory neurons in a cortical microcircuit of working memory. *Proceedings of the National Academy of Sciences of the United States of America*, 101(5):1368–1373, February 2004. ISSN 0027-8424. doi: 10.1073/pnas.0305337101. URL http://dx.doi.org/10.1073/pnas.0305337101.

White, O. L., Lee, D. D., and Sompolinsky, H. Short-term memory in orthogonal neural networks. *Phys Rev Lett*, 92(14):148102, Apr 2004.

Xu, J., Kang, N., Jiang, L., Nedergaard, M., and Kang, J. Activity-dependent long-term potentiation of intrinsic excitability in hippocampal CA1 pyramidal neurons. *J Neurosci*, 25(7):1750–60, 2005.

Yakovlev, V., Bernacchia, A., Orlov, T., Hochstein, S., and Amit, D. Multi-item working memory – a behavioral study. *Cereb Cortex*, 15(5):602–615, May 2005. doi: 10.1093/cercor/bhh161.

Zador, A., Koch, C., and Brown, T. H. Biophysical model of a hebbian synapse. *Proc Natl Acad Sci U S A*, 87(17):6718–6722, Sep 1990.

Zador, A. M., Claiborne, B. J., and Brown, T. H. Electrotonic transforms of hippocampal neurons. *Soc. Neurosci. Abst.*, 17:1515, 1991.

Zucker, R. S. and Regehr, W. G. Short-term synaptic plasticity. *Annu Rev Physiol*, 64: 355–405, 2002. doi: 10.1146/annurev.physiol.64.092501.114547.